MODELING AND DESIGNING CONTROL CHART FOR MONITORING TIME-BETWEEN-EVENTS DATA

ZHANG HAIYUN

(B.Sc., Huazhong University of Science and Technology)

A THESIS SUBMITTED

FOR THE DEGREE OF DOCTOR OF PHILOSOPHY

DEPARTMENT OF INDUSTRIAL & SYSTEMS ENGINEERING

NATIONAL UNIVERSITY OF SINGAPORE

2009

ACKNOWLEDGEMENTS

The PhD study in National University of Singapore is a fruitful journey for me. Not only I have learnt much professional knowledge, but also I have met a lot of new friends. At the end of the PhD study, I would like to show my gratitude to all the people who have generously offered their help, encouragement and care to me.

First, I would like to express my deepest gratitude and appreciation to my two supervisors, Prof. Goh Thong Ngee and Prof. Xie Min, for their invaluable advice, guidance, patience and encouragement. Without them, this thesis would not be possible.

Besides, I would like to thank National University of Singapore for offering me the research scholarship. I would also like to thank all the faculty members in the Industrial & Systems Engineering Department, from whom I have leant both knowledge and teaching skills. My thanks also extend to all my friends Liu Jiying, Pan Jie, Hendry, Long Quan, Jiang Hong, Wu Yanping, Zhu Zhecheng, Yao Zhishuang, Yuan Le, Qu Huizhong, Wei Wei, Shen Yan, Li Yanfu, Xiong Chengjie, Zhu Xiaoying, Fu Yinghui, Xie Yujuan, Li Xiang, Wu Jun, Peng Rui, Jiang Jun, Ye Zhisheng for their help and accompany.

Last, but not the least, my special thanks go to my parents, my sister and Mr. Han Dongling. Their love, support and understanding are the major motivation for me to pursue my PhD.

Table of Contents

Summary

This thesis aims to improve the existing time-between-events chart by making it more practical, enhance the effectiveness of the time-between-events chart by integrating it with other techniques and at the same time increase the average profit per unit time or reduce the average cost per unit time.

Chapter 1 gives a brief introduction of the basic principles of control chart and introduces the time-between-events chart. Chapter 2 reviews the existing time-between-events charts according to the classification of time-between-events charts.

Chapter 3 and chapter 4 focus on improving a single time-between-events chart. In chapter 3 an economic model of the time-between-events chart under the random process shift is developed. Design of the proposed control chart scheme has been demonstrated and properties have been compared with those of the time-between-events chart under the fixed process shift. In chapter 4 an integrated model of time-between-events chart and preventive maintenance is developed. The implementing cost of time-between-events chart and preventive maintenance is considered and the cost minimization criterion is used to find optimal values for decision variables. Then the performance of the integrated model is compared with the pure time-between-events chart model and pure preventive maintenance model.

Chapters 5 and 6 develop a control chart system consisting of several time-between-events charts, each of which is used to monitor the time between successive events at different process stages in a multistage manufacturing system. Chapter 5 focuses on the

statistical properties of time-between-events chart system. Out-of-control average time to signal is used as the optimization objective and in-control average time to signal is used as the constraint. Chapter 6 focuses on the economical properties of time-between-events chart system. Minimization of average profit per unit time is used as the optimization objective and in-control average time to signal is used as the constraint.

Chapter 7 concludes this thesis and some possible future research directions are suggested according to the limitations of this thesis.

This thesis focuses not only on theoretical study but also on the practical application. Results from each chapter show that approaches proposed here do make the time-between-events chart more practical, improve the effectiveness of the time-between-events chart and increase the profit or reduce the cost per unit time.

List of Tables

List of Figures

NOMENCLATURE

B_0	Average profit per unit time when the system is in-control
B_1	Average profit per unit time when the system is out-of-control
D_0	Average cost per unit when the system is in-control
D_1	Average cost per unit when the system is out-of-control
A_0	Average cost associated with one false alarm
A_i	Average cost for locating and removing the assignable cause from the *i*th stage
C	Average cost for observing and plotting an event
L	Expected length of an operating cycle
P	Average profit from an operating cycle
O	Average profit per unit of time during an operating cycle
SPC	Statistical process control
SQC	Statistical quality control
DOE	Design of experiment
UCL	Upper control limit
CL	Central control limit
LCL	Lower control limit
ARL	Average run length

ARL_0 Average run length when the process is in-control

ARL_1 Average run length when the process is out-of-control

ATS Average time to signal

ATS_0 Average time to signal when the process is in-control

ATS_1 Average time to signal when the process is out-of-control

α Type I error

β Type II error

λ_0 Rate of occurrence of the event when the system is in-control

λ_1 Rate of occurrence of the event when the system is out-of-control

λ_a Rate of occurrence of the assignable cause

FNR Fractional nonconforming rate

CCC Cumulative count of conforming

CQC Cumulative quantity of conforming

CPC Cumulative probability control

CUSUM Cumulative sum

EWMA Exponentially weighted moving average

C^4	Cumulative chain-conforming count
VSI	Variable sampling interval
OC	Operating characteristic
CRL	Conforming run length
SPRT	Sequential probability ratio test
TBE	Time-between-events

Chapter 1 Introduction

The history of quality control can be traced back to the origin of industry. From the time people began to manufacture, there has been an interest in the quality of the product. But statistical quality control (SQC) is new because the history of statistics itself is only two to three centuries and the greatest development of statistics was in the early 20th century. It was not until the 1920s that statistical theory began to be applied effectively to quality control. A good summary of historical background of SQC can be found in Duncan (1986).

SQC is a branch of industrial statistics which includes, primarily, the areas of acceptance sampling, statistical process control (SPC), design of experiment (DOE), and capability analysis. Briefly speaking, acceptance sampling methods are used in industry to make decisions regarding the disposition of "lots"; SPC techniques are employed to monitor production processes over time to detect changes in the process performance; DOE is applied to identify specific levels of important factors that lead to optimum (or near-

optimum) performance; capability analysis is to assess whether or not a process is capable of meeting specification limits on key quality characteristics (Woodall and Montgomery, 1999).

As an important branch of SQC, SPC has been adopted and widely used in many areas, such as manufacturing industry (Wu and Tian, 2005; Zantek, 2006; Wu and Wang, 2007; Zantek *et al*. 2007; Marcellus, 2008), health care (Grigg *et al*., 2003; Woodall, 2006; Coory *et al*., 2008; Biswas and Kalbfleisch, 2008), service management (Herbert *et al*., 2003 and Pettersson, 2004) and finance (Shin and Sohn, 2007). It is a powerful collection of problem-solving tools useful in achieving process stability and improving capability through the reduction of variability (Montgomery, 2005). Its seven major tools, often called "the magnificent seven" are:

- Histogram or stem-and-leaf plot: a graphical display of tabulated frequencies.
- Check sheet: a simple document used to collect operating data.
- Pareto chart: a special type of bar chart used to separate the significant aspects of a problem from the trivial ones.
- Cause-and-effect diagram: a diagram shows the causes of a certain event and identifies desirable factors leading to an overall effect.

- Defect concentration diagram: a plot to show the location of errors or defects.
- Scatter diagram: a plot for identifying a potential relationship between two variables.
- Control chart: a tool for detecting the occurrence of assignable causes of process shift.

Of these seven tools, control chart is probably the most technically sophisticated. The rest of this chapter will focus on principles of control chart, problems with traditional control chart, the newly developed control chart and the motivation of this research.

1.1 Control Chart

Control chart was first invented by Walter A. Shewhart while working for Bell Labs in the 1920s. It is a graphical display of a quality characteristic that has been measured or computed from a sample versus the sample number or time (Montgomery, 2005). The chart usually consists of a center line (CL) which represents the average value of the quality characteristic, upper control limit (UCL) and lower control limit (LCL). In the recent years, researchers propose adding warning limits to the control chart, which will increase the efficiency of the control chart (De Magalhaes and Moura Neto, 2005; De

Magalhaes *et al*., 2006; Lin and Chou, 2007; Costa and Machado, 2008). A general model for a control chart can be given as below:

$$\begin{aligned} UCL &= \mu_w + k\sigma_w \\ CL &= \mu_w \\ LCL &= \mu_w - k\sigma_w \end{aligned} \tag{1.1}$$

w is a sample statistic that measures some quality characteristic of interest. μ_w and σ_w are mean and standard deviation of *w*. *k* is the distance of the control limits from the center line expressed in standard deviation units.

Specifying control limits (choosing value for *k*) is an important decision for designing a control chart. Before explaining how to specify control limits, two types of error should be introduced first:

- Type I error: the risk of a point falling beyond control limits when the process is in control.
- Type II error: the risk of a point falling between control limits when the process is out of control.

When control limits are far from the centre line, Type I error is small but Type II error is large. When control limits are near to the centre line, Type II error is small but Type I error is large. As a result, optimal control limits are determined based on the tradeoff

between Type I error and Type II error. In practice, *k* is set to be three so that 99.73% of the data will be within control limits when the process is in control and data is normally distributed.

Analyzing patterns on control charts can help us to identify problems for the process. The Western Electric Handbook (1956) suggests a set of decision rules for detecting nonrandom patterns on control charts. If control charts show any of the patterns listed below, it suggests the process is out of control.

- One point plots outside the three-sigma control limits;
- Two out of three consecutive points plot beyond the two-sigma warning limits;
- Four out of five consecutive points plot at a distance of one-sigma or beyond from the center line;
- Eight consecutive points plot on one side of the center line.

The above rules apply to one side of the center line at a time. They can enhance the sensitivity of control charts. But they will also increase the Type I error if several rules are applied simultaneously.

Measuring the efficiency of control charts can help us to better design control charts. There are two criterions for measuring the efficiency of control charts. One is the average run length (ARL). ARL is the average number of points that must be plotted before a point indicates an out-of-control condition. If the process observations are uncorrelated, the ARL for any Shewhart control chart is:

$$ARL = \frac{1}{P} \tag{1.2}$$

where P is the probability for any point beyond control limits. Then, the in-control ARL (ARL_0) and out-of-control ARL (ARL_1) are expressed as:

$$\begin{aligned} ARL_0 &= \frac{1}{\alpha} \\ ARL_1 &= \frac{1}{1-\beta} \end{aligned} \tag{1.3}$$

where α is the Type I error and β is the Type II error. When designing control charts, we should try our best to maximize ARL_0 while at the same time to minimize ARL_1 . The other one is average time to signal (ATS). The relationship between ARL and ATS can be expressed in the following equation:

$$ATS = ARL \cdot h \tag{1.4}$$

The condition for this equation is that samples must be collected at a fixed interval of time that are *h* hours apart.

Since Dr. Shewhart invented control charts in the 1920s, control charts have been widely used in industry. The classification of Shewhart control charts is summarized in Figure 1.1. Because of using control charts for more than 80 years, quality of processes has been improved significantly. Nowadays, many processes' fraction nonconforming rate (FNR) can achieve parts per million or parts per billion levels. This kind of process is called high yield process. For high yield processes, traditional Shewhart control charts face a lot of problems. In the next part, these problems will be discussed in detail.

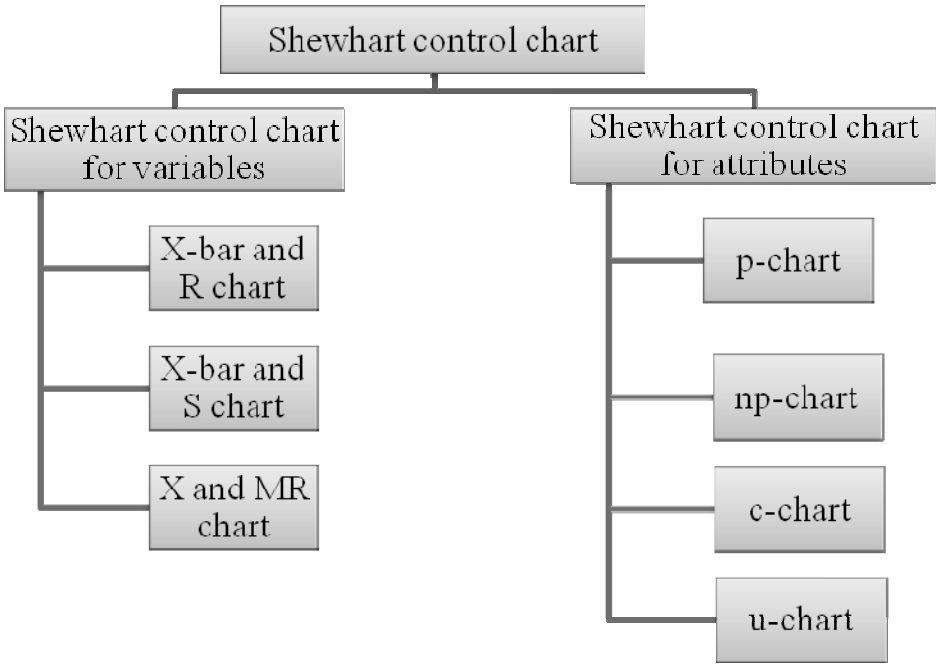

Figure 1.1 Classification of Shewhart control chart

1.2 Inadequacies of traditional Shewhart control charts

For high yield processes, many traditional Shewhart control charts would face a lot of practical problems and the situation is more serious with attribute control charts (Xie *et al*. 2002a). There are three main problems for attribute control charts.

- High false alarm rate

  Traditional attribute control charts are based on normal approximation. But for high yield processes, normal approximation to binomial (for *p* and *np*-charts) and poisson

(for *c* and *u*-charts) does not work well because *p* and *c* are quite small. Let's take *np*-chart for example. Control limits for *np*-chart are as below:

$$\begin{aligned} UCL &= np + 3\sqrt{np(1-p)} \\ CL &= np \\ LCL &= np - 3\sqrt{np(1-p)} \end{aligned} \tag{1.5}$$

The equation for calculating false alarm rate is listed below:

$$P(False\ alarm) = 1 - P(LCL \le X \le UCL) \tag{1.6}$$

X follows binominal distribution with parameters *n* and *p*. Table 1.1 shows the exact false alarm probability for *np*-chart with different *n* and *p*. From Table 1.1, we can see the exact false alarm probability is much higher than 0.0027 when n is less than 50.

Table 1.1 Exact false alarm rate for *np*-chart with 3-sigma limits

p	n=5	n=10	n=20	n=50	n=100
0.01	0.9520	0.9086	0.8189	0.6066	0.3695
0.02	0.9078	0.8179	0.6747	0.3674	0.1367
0.03	0.8672	0.7402	0.5465	0.2218	0.0508
0.04	0.8160	0.6710	0.4494	0.1335	0.0191
0.05	0.7749	0.5998	0.3611	0.0801	0.0074
0.06	0.7359	0.5406	0.2957	0.0480	0.0047
0.07	0.6988	0.4876	0.2362	0.0287	0.0023
0.08	0.6636	0.4402	0.1925	0.0171	0.0026
0.09	0.6304	0.3904	0.1529	0.0103	0.0015
0.10	0.5910	0.3503	0.1240	0.0084	0.0023

- Meaningless control limits

For high yield processes, *LCL* may always be negative. For negative *LCL*, it will be replaced by zero. In this case, process improvement cannot be detected unless some run rules are used. *UCL* may be smaller than one for *np*-chart and *c*-chart, which means the chart will signal whenever there is one nonconforming item in the sample. It is obviously an over-reaction to noises. Let's take *c*-chart for example. The equations for calculating control limits for *c*-chart are as below:

$$\begin{aligned} UCL &= c + 3\sqrt{c} \\ CL &= c \\ LCL &= c - 3\sqrt{c} \end{aligned} \tag{1.7}$$

When the in-control *c* equals 0.05, the calculated upper control limit and lower control limit equal 0.072082 and -0.62082. Since the calculated LCL is negative, it is replaced by zero. 100 simulated data with *c*=0.05 is plotted in Figure 1.2. Because the upper control limit is less than 1, there are many false alarms as shown in Figure 1.2.

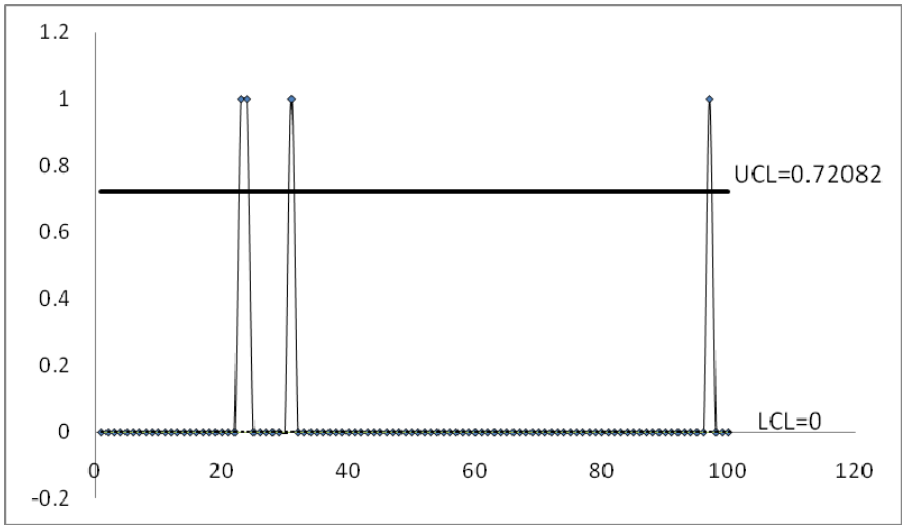

Figure 1.2 c-chart with c=0.05

- Depend on sample size

With the same dataset, the frequency of signaling out of control depends heavily on the choice of sample size. For a certain value of sample size, there may be very frequent signals for out of control; while for a slightly larger value of sample size, there may be very infrequent or no signal for out of control. Let's take an example from Chan *et al.* (2003) to illustrate this point. Suppose a total of 8160 items are inspected and the items at the following 48 positions in sequence are found to be nonconforming: 113, 218, 282, 505, 664, 792, 963, 1110, 1184, 1341, 1547, 1733, 1808, 1861, 2030, 2186, 2337, 2569, 2704, 2889, 3063, 3263, 3373, 3433, 3559, 3809,

4021, 4206, 4472, 4517, 4833, 5032, 5325, 5375, 5553, 5729, 5988, 6338, 6424, 6692, 6996, 7201, 7227, 7314, 7578, 7703, 7879, 7963. The fraction of nonconforming items for this process is estimated as p=48/8160=0.00588. When the sample size equals 15, *UCL* for the *np*-chart according to Equation (1.5) is 0.979<1, which means all these 48 items will trigger out of control signal. But when the sample size equals 16, *UCL* is 1.014>1, which means the *np*-chart will signal if there are two or more nonconforming items in a sample size of 16. In this case, none of the above 48 items will signal out of control.

In order to overcome the above problems, there are two methods. The first method is to transform the non-normally distributed data into normally distributed data. Many transformation methods have been proposed by researchers, such as power transformation method (McCool and Joyner-Motley, 1998; Batson *et al*. 2006), fourth root transformation method (Kittlitz, JR., 1999), minimizing the sum of the absolute difference transformation method (Kao *et al*. 2006) and minimizing the sum of the squared difference transformation method (Kao and Ho, 2007). But transformation methods have been subjected to much criticism because of their difficulty in interpreting

data. The second method is to introduce a new type of control chart called time-between-events chart which will be discussed in the next section in detail.

1.3 Time-between-events chart

In order to solve the inefficiency of traditional Shewhart control charts for monitoring high yield processes, Calvin (1983) proposed monitoring the cumulative number of conforming items between two nonconforming items. This is the origin of time-between-events chart. The words ‘time’ and ‘event’ can have different meanings in different situations. In the manufacturing industry, ‘event’ means the occurrence of a nonconforming item and ‘time’ means the time between two nonconforming items or the cumulative number of conforming items between two nonconforming items. In the service industry, ‘event’ means the arrival of a customer and ‘time’ means the time between the arrival of customers. In the reliability area, ‘event’ means the failure of the system and ‘time’ means the time between the failures of the system.

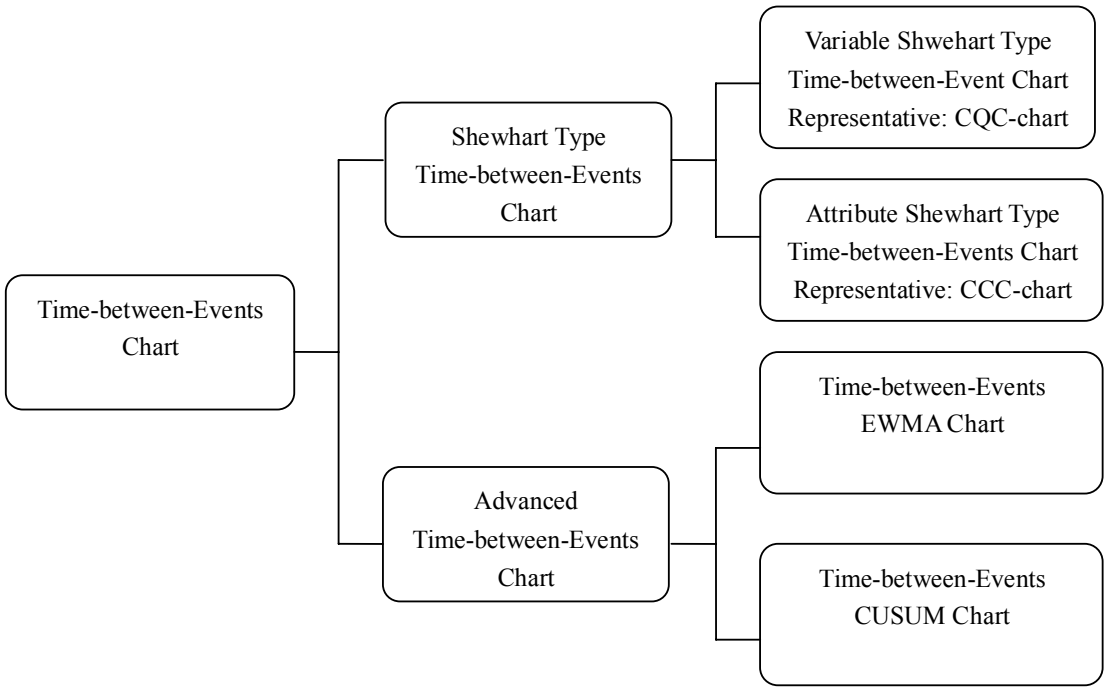

Figure 1.3 Classification of Time-between-Events Chart

Figure 1.3 gives a broad classification of time-between-events chart. In the next chapter, each kind of time-between-events chart (CCC, CQC, time-between-events CUSUM chart and time-between-events EWMA chart) will be reviewed in detail.

1.4 Objective and structure of the study

Time-between-events chart has been studied by many researchers after its introduction in the 1980s. Although time-between-events chart has solved a lot of inefficiencies of

traditional Shewhart control charts for monitoring high yield processes, it still has some problems. First the existing time-between-events chart is designed under an unrealistic assumption that process shift is fixed all the time. Second, the design of time-between-events chart doesn't consider the effect of preventive maintenance although time-between-events chart and preventive maintenance exist at the same time quite often. Third, although time-between-events charts are used to monitor multistage manufacturing system, they are designed independently without considering the quality dependence between them. These problems are the motivation for this these. The major objective of the study is to solve these problems and improve the existing time-between-events chart by making it more practical and to enhance the effectiveness of the time-between-events chart by integrating it with other techniques. This thesis will focus on the following topics regarding time-between-events chart to fulfill the stated objective.

- Random process shift idea is taken into consideration, which makes the time-between-events chart more practical.

- Preventive maintenance technique is integrated with time-between-events chart, which makes the monitoring system more effective and more economical.

- Algorithm for designing time-between-events chart for monitoring multistage problem is developed, which greatly improves the effectiveness of the time-between-events chart system.

The remainder of this thesis is organized as follows. Chapter 2 reviews the existing time-between-events chart.

Chapter 3 and chapter 4 focus on designing and improving a single time-between-events chart. In chapter 3, the economic model of time-between-events chart under random process shift is constructed. In chapter 4, the economic design of the integrated model of time-between-events chart and preventive maintenance is developed.

Chapters 5 and 6 focus on designing a control chart system which consists of several individual time-between-events charts. Each time-between-events chart is used to monitor one process stage in a multistage manufacturing system. Chapter 5 focuses on the statistical properties of the time-between-event charts system while chapter 6 focuses on the economical properties of the time-between-events chart system.

Finally, chapter 7 concludes this thesis and suggests some possible future research directions according to the limitations of this thesis.

Chapter 2 Literature Review

Each of the four kinds of time-between-events chart (CCC, CQC, time-between-events CUSUM chart and time-between-events EWMA chart) will be reviewed in detail in this chapter, with each section focusing on one kind.

2.1 Cumulative count of conformance chart and its extensions

In this part, the review will be classified into two sub parts: the cumulative count of conformance chart and the extensions to cumulative count of conformance chart.

2.1.1 Cumulative count of conformance chart

The cumulative count of conformance chart (CCC-chart) was first proposed by Calvin (1983) to monitor zero-defects processes. Then, it was further studied by Goh (1987) who gave it the name CCC-chart. The usefulness of CCC-chart was pointed out in Woodall (1997) and Woodall and Montgomery (1999). Although CCC-chart was designed for zero-defects processes in manufacturing industry, the application of CCC-chart is not

limited to the manufacturing industry. Benneyan (2001a, 2001b) applied CCC-chart in the healthcare area. The application of CCC-chart is also not limited to zero-defects processes. Schwertman (2005) showed the effectiveness of CCC-chart for monitoring processes with lesser quality. The basic idea of a CCC-chart is that the cumulative count of conformance should be plotted instead of the number of nonconforming items for high yield processes.

Suppose a production process is operating in a stable condition, the probability for the occurrence of an item to be nonconforming is p_0. The successive items produced are assumed to be independent. Then each item produced is a realization of a Bernoulli random variable with parameter p_0. The cumulative count of conforming items between two nonconforming items N is geometric distributed, with

$$P[N = n] = p_0(1 - p_0)^n, \text{ for } n = 0,1,2,... \tag{2.1}$$

The method for setting up CCC-chart is similar to the method for common Shewhart control chart. Kaminsky *et al*. (1992) proposed using three sigma limits for CCC-chart. But there are some serious problems for this method, such as higher false alarm rate than expected and meaningless lower control limit (Xie and Goh, 1997). In order to overcome these problems, Xie and Goh (1997) proposed using probability limits for CCC-chart. If

the acceptable false alarm rate is α, control limits for CCC-chart based on probability limits method are as below:

$$\begin{aligned} UCL &= \frac{\ln(\alpha/2)}{\ln(1-p_0)} \\ CL &= \frac{1}{p_0} \\ LCL &= \frac{\ln(1-\alpha/2)}{\ln(1-p_0)} \end{aligned} \tag{2.2}$$

Based on this set of control limits, the average run length (*ARL*) for CCC-chart is calculated as below:

$$ARL = \frac{1}{1-\beta} = \frac{1}{1-(1-p)^{LCL-1}-(1-p)^{UCL}} \tag{2.3}$$

where β is the Type II error or the probability of no alarm when the process is out of control. By studying the properties of this equation, we find that the ARL may initially increase when the process has deteriorated. As a result, it will take a longer time to trigger an alarm when the process has deteriorated than it is in control. Xie *et al*. (2000) proposed a method to eliminate this undesirable property for ARL. By multiplying an adjustment factor γ_α to the previous control limits, ARL will be maximized when the process is in control. As a result ARL will always decrease when the process has shifted. The new optimal control limits for CCC-chart are:

$$UCL = \gamma_\alpha \frac{\ln(\alpha/2)}{\ln(1-p_0)} = \frac{\ln[\frac{\ln(1-\alpha/2)}{\ln(\alpha/2)}]}{\ln[\frac{(\alpha/2)}{(1-\alpha/2)}]} \frac{\ln(\alpha/2)}{\ln(1-p_0)}$$

$$CL = \frac{1}{p_0} \tag{2.4}$$

$$LCL = \gamma_\alpha \frac{\ln(1-\alpha/2)}{\ln(1-p_0)} = \frac{\ln[\frac{\ln(1-\alpha/2)}{\ln(\alpha/2)}]}{\ln[\frac{(\alpha/2)}{(1-\alpha/2)}]} \frac{\ln(1-\alpha/2)}{\ln(1-p_0)}$$

Before the above equation for calculating control limits of CCC-chart can be used, the value of p_0 should be given or estimated. The usual estimator is

$$\hat{p}_0 = \frac{m}{M} \tag{2.5}$$

where *m* is the number of nonconforming items among a total of *M* items sampled. Yang *et al.* (2002) investigated the sample size *M* effect on the false alarm rate and ARL when p_0 is estimated by Eq. (2.5). Yang *et al*. (2002) showed that the actual false alarm rate can deviate significantly from its desired value of 0.0027, especially when p_0 is very small. But the influence on average run length is milder than on false alarm rate.

The estimator in Eq. (2.5) has one problem that the estimate is biased under sequential sampling (Girshick *et al*. 1946), and the problem becomes more serious for small *M*. Tang and Cheong (2004) suggested using the unbiased estimator given by Haldane (1945):

$$\hat{p}_0 = \frac{m-1}{M-1} \tag{2.6}$$

Further, it is suggested that the estimate and control limits are sequentially updated according to the number of nonconforming items observed. Their results showed that the performance of CCC-chart with sequentially updated parameters is comparable with that of the known value CCC-chart.

Until now, the procedures and techniques on how to set up and measure the efficiency of CCC-chart have been covered. However, studies on CCC-chart are not limited to these scopes. Extensive studies on CCC-chart have extended to the following four aspects.

The first aspect is the study of serial correlation on CCC-chart. When the production process exhibits a serial correlation, the false alarm rate will be much higher than the false alarm rate calculated under the independent assumption. Lai *et al*. (1998) used Madsen (1993)'s correlation binomial model to solve the correlation problem for CCC-chart. Lai *et al*. (2000) applied the Markov model which was studied by Broadbent (1958), Sampath Kumar & Rajarshi (1987) and McShane & Turnbull (1991) to investigate the correlation problem. Tang and Cheong (2006) proposed a new chart called the cumulative chain-conforming count (C^4) chart to solve the correlation problem within each inspection group. An inspection group is categorized as a chain-conforming

group when it contains zero nonconforming item or one nonconforming item and there were no non-conforming items in the previous i groups. Then C^4 chart plots the cumulative number of chain-conforming groups before a non-chain-conforming group surfaces. Chen and Cheng (2007) studied CCC-chart for monitoring Markov dependent processes. In their paper, the variable sampling procedure is applied to CCC-chart.

The second aspect is the study of variable sampling interval (VSI) for CCC-chart. VSI scheme has been studied extensively by many researchers (Lee and Bai, 2000; Bai and Lee, 2002; Carot *et al*. 2002; Wu and Luo, 2004; Chen, 2004; Lin and Chou, 2005; Villalobos *et al*. 2005). The reason for applying VSI is that the cost of sampling can be reduced and the sensitivity of the chart can be increased with proper design parameters. Considering the successful application of VSI in other charts, Liu *et al*. (2006a) applied VSI scheme in CCC-chart. Her results showed that VSI scheme was also effective in CCC-chart.

The third aspect is the study of random shift mode of CCC-chart. The random shift mode means the occurrence of process shift can occur at any point between two nonconforming items. The fixed shift mode means the occurrence of process shift can only occur immediately after a nonconforming item. Wu and Spedding (1999) studied the properties

of ATS for both fixed and random shift mode. Their results told us that ATS under fixed shift mode may produce notable error while ATS under random shift mode is more accurate.

The fourth aspect is economic design of CCC-chart. Duncan (1956) was the pioneer work in economic design of control chart. Later, Lorenzen and Vance (1986) gave a more general model for economic design of control chart. Xie *et al*. (2001) applied Lorenzen and Vance's model to CCC-chart and used Chung (1991)'s simplified procedure to derive the optimal solution. Zhang *et al*. (2008) developed an economic model of CCC-chart when the original production order is not preserved. Instead of monitoring the cumulative number of conforming items, the CCC-chart in Zhang *et al*. (2008) monitors the cumulative number of conforming samples, which a sample is considered conforming if it contains no nonconforming item.

2.1.2 Extensions to cumulative count of conformance chart

Although the cumulative count of conformance chart is much more efficient than the traditional Shewhart chart for monitoring high yield processes, this does not mean that it cannot be further improved. In order to increase the efficiency and sensitivity of the

CCC-chart, researchers have proposed many extensions to CCC-chart. These extensions can be generally classified into the following four kinds.

The first kind of extension is to use CCC-r chart which monitors the cumulative count of conforming items produced before *r* nonconforming ones are observed. CCC-r chart was first proposed by Xie *et al*. (1999) to detect further process improvement and avoid excessive false alarms. If the occurrence probability of a nonconforming item is p_0 and the successive items produced are assumed to be independent, each item produced is a realization of a Bernoulli random variable with parameter p_0. The cumulative count of conforming items *N* until *r* nonconforming items is negative binomial distributed, with

$$P[N = n] = \binom{n-1}{r-1} {p_0}^r (1-p_0)^{n-r}, \text{ for } n = r, r+1, \ldots \tag{2.7}$$

The cumulative distribution function can be derived as:

$$F(n, r, p_0) = \sum_{i=r}^{n} P(N = i) = \sum_{i=r}^{n} \binom{i-1}{r-1} {p_0}^r (1-p_0)^{i-r} \tag{2.8}$$

If the acceptable false alarm rate is α, the exact probability control limits for CCC-r chart are the solutions of the following equations:

$$F(UCL_r, r, p_0) = \sum_{i=r}^{UCL_r} \binom{i-1}{r-1} {p_0}^r (1-p_0)^r = 1-\alpha/2$$
$$F(CL_r, r, p_0) = \sum_{i=r}^{CL_r} \binom{i-1}{r-1} {p_0}^r (1-p_0)^r = 0.5 \quad (2.9)$$
$$F(LCL_r, r, p_0) = \sum_{i=r}^{LCL_r} \binom{i-1}{r-1} {p_0}^r (1-p_0)^r = \alpha/2$$

But Chen (2009) pointed out that control limits calculated from Eq. (2.9) may cause non-optimal or biased in control ARL. In Chen (2009) a new approach to set control limits with near optimal and near unbiased ARL is proposed.

Ohta *et al*. (2001) developed the economic model of CCC-r chart and proposed a simplified method to determine the optimal design variables. Wu *et al*. (2001) and Zhang *et al*. (2007) studied the average time to signal (*ATS*) properties of CCC-r chart under random shift mode. The random shift mode means process shift is not restricted to occur immediately after a sample is collected, but can occur at any time. Bucchianico *et al*. (2005) studied the implementation aspects of CCC-r in the real situation.

The second kind of extension is to use a conditional decision procedure for CCC-chart. Since the conventional CCC-chart only uses a single count to make a decision about the process, Kuralmani *et al*. (2002) suggested that incorporating a certain number of previous runs or observations in the decision procedure can increase the sensitivity of the

CCC-chart. In this case, the process is considered to be in control if the count of conforming items between two nonconforming items is within control limits or *s* previous runs were in control although the current count is not within the control limits. The comparison of the OC curve and ARL between the conventional CCC-chart and the CCC-chart under conditional decision procedure in Kuralmani *et al*. (2002) proved that the CCC-chart under conditional decision procedure is more sensitive. Noorossana *et al*. (2007) pointed out the implicit assumption in Kuralmani *et al*. (2002) that run lengths are independent and geometric distributed. But actually this assumption does not hold for the CCC-chart under conditional decision procedure because it considers a certain number of the previous observations. Noorossana *et al*. (2007) derived the formula for calculating exact ARL. Comparing the ARL derived in Kuralmani *et al*. (2002) with the exact ARL, it is found that procedures in Kuralmani *et al*. (2002) always underestimate ARL values.

The third kind of extension is to combine conforming run length (CRL) chart which is equivalent to CCC-chart with *np*-chart. Wu *et al*. (2001) proposed this idea and called it a synthetic control chart. Actually the synthetic control chart functions the same way as CRL chart except that each item in the CRL chart is replaced by a sample. The *np*-chart is used to identify whether the sample is conforming or nonconforming. Then CRL chart is

used to plot the cumulative number of conforming samples between two nonconforming samples. The results of Wu *et al*. (2001) showed that by using the synthetic control chart, the out of control ATS can be reduced by 50% or greater. But Bourke (2008) pointed out that "the good performance of the synthetic chart was due to the implicit inclusion of a 'head-start' feature when computing the reported values of ATS. Without the head-start feature, the performance of the synthetic chart is not much better than that of the *np*-chart." In Bourke (2008), the ATS of synthetic chart was compared with *np*-chart, RL_2 chart and RL-CUSUM chart.

The fourth kind of extension is to use a two-stage decision procedure for CCC-chart. The CCC-r chart (r>=2) which cumulates *r* counts is more reliable than CCC-chart which only uses a single count to make the decision of the process. But it requires inspection of a large number of items before a decision can be made. Facing this dilemma, Chan *et al*. (2003) proposed a $CCC_{1+\gamma}$ chart which was inspired by double sampling. A $CCC_{1+\gamma}$ chart is a two-stage CCC-chart with false alarm rate $(1-\gamma)\alpha$ for the first stage and $\gamma\alpha$ for the second stage. Let *n* be the number of items inspected and N(r, p_0) be the number of items inspected until *r* nonconforming items occur. There are two LCLs for a $CCC_{1+\gamma}$ chart for

detecting upward shift: n_1 for the first stage and n_2 for the second stage. The process is considered to be out of control either when $N(1, p_0) \le n_1$ or $n_1 < N(1, p_0) < N(2, p_0) \le n_2$.

2.2 Cumulative quantity control chart and its extensions

In this part, the review will also be classified into two sub parts: the cumulative quantity control chart and the extensions to cumulative quantity control chart.

2.2.1 Cumulative quantity control chart

Cumulative quantity control chart (CQC-chart) which is the counterpart of CCC-chart, was proposed by Chan *et al*. (2000).

Supposing nonconformities in a process occur according to a Poisson process with mean occurrence rate λ per unit quantity of product. The number of units Q between two nonconformities is exponentially distributed with probability density function, cumulative distribution function and mean as below:

$$\begin{aligned} f(Q) &= \lambda e^{-\lambda Q} \\ F(Q) &= 1 - e^{-\lambda Q} \\ E(Q) &= 1/\lambda \end{aligned} \tag{2.10}$$

If the false alarm rate is set at α, the probability control limits for CQC-chart are as below:

$$
\begin{aligned}
1-e^{-\lambda Q_{LCL}} &= \alpha/2 \Rightarrow Q_{LCL} = -\frac{\ln(1-\alpha/2)}{\lambda} \\
1-e^{-\lambda Q_{CL}} &= 0.5 \Rightarrow Q_{CL} = -\frac{\ln(0.5)}{\lambda} \\
1-e^{-\lambda Q_{UCL}} &= 1-\alpha/2 \Rightarrow Q_{UCL} = -\frac{\ln(\alpha/2)}{\lambda}
\end{aligned}
\tag{2.11}
$$

Before control limits can be calculated according to Eq. (2.11), the value of λ needs to be estimated, which is called Phase-I stage of CQC-chart. There are two estimation methods. The first method is to collect a certain size of preliminary samples to estimate the parameter value (Jones and Champ, 2002). The equation is as below:

$$\hat{\lambda} = \frac{m}{M} \tag{2.12}$$

where M is the number of units inspected until m nonconformities are observed. This method requires the determination of an appropriate number of preliminary samples to be collected. Usually it will take a long time to collect samples before control limits can be set up, and this estimator is biased. The second method is to sequentially update the estimator and control limits each time a new nonconformity is observed. The sequentially updating method is first proposed by Tang and Cheong (2004) and then applied to Phase I CQC-chart by Zhang *et al*. (2006). In Zhang *et al*. (2006), the unbiased estimator $\bar{\lambda}$ was used:

$$\bar{\lambda} = \frac{m-1}{M} \tag{2.13}$$

Before Eq. (2.13) can be used, at least two nonconformities should be collected.

The ARL of CQC-chart for a given λ is calculated as below:

$$ARL = \frac{1}{1-\beta} = \frac{1}{1-\exp(-\lambda Q_{LCL}) + \exp(-\lambda Q_{UCL})} \tag{2.14}$$

But ARL calculated in this manner will first increase and then decrease as λ increases, which is the same as the ARL for CCC-chart. Following the same suggestion of Xie *et al*. (2000) for ARL of CCC-chart, Zhang *et al*. (2006) developed a factor to adjust the control limits for CQC-chart so that the ARL won't be biased.

Following the model of Duncan (1956), Zhang *et al*. (2005) developed an economic model of CQC-chart (which was called exponential chart in their paper). The statistical design, economic design and statistical-economic design were compared in Zhang *et al*. (2005). The results showed that the statistical-economic design identifies an optimal tradeoff the between statistical objective and the economic objective.

One common problem for both CCC-chart and CQC-chart is that *n* or *Q* will grow larger and larger, and eventually exceed the boundary of the plot as the process continues. In order to solve this problem, Xie *et al*. (1995) proposed using the logarithmic scale, which means log n or log Q is plotted. But plotting log n or log Q distorts the shape of the chart and it is hard to interpret the data. To overcome this problem, Chan *et al*. (2002) proposed

a new chart called cumulative probability control charts (CPC-chart). In the CPC-chart, the cumulative probability is plotted against the sample number, and so the vertical axis is scaled to [0, 1].

2.2.2 Extensions to cumulative quantity control chart

How to improve the sensitivity of CQC-chart attracts a lot of researchers. The extensions to CQC-chart can be classified into the following three kinds.

The first kind of extension is to use CQC-r chart which monitors the cumulative number of units inspected until *r* nonconformities occur. CQC-r chart was proposed by Xie *et al*. (2002b). But it was called T_r-chart in his paper because the chart was used for reliability monitoring. Instead of monitoring the cumulative number of units inspected until *r* nonconformities, the cumulative time till *r* failures was monitored.

If process failure is modeled by a Poisson process, the time between failures will be exponential. It is well known that the sum of *r* exponentially distributed random variables follows the Erlang distribution, so the cumulative time until *r* failures, T_r, follows Erlang distribution with probability density function and cumulative density function as below:

$$f(t_r, r, \lambda) = \frac{\lambda^r t_r^{\,r-1}}{(r-1)!}\exp(-\lambda t_r)$$
$$F(t_r, r, \lambda) = 1 - \sum_{k=0}^{r-1}\frac{(\lambda t_r)^k}{k!}\exp(-\lambda t_r) \tag{2.15}$$

If the false alarm rate is α, control limits for T_r-chart are as below:

$$F(UCL_{t_r}, r, \lambda) = 1 - \sum_{k=0}^{r-1} e^{-\lambda UCL_{t_r}}\frac{(\lambda UCL_{t_r})^k}{k!} = 1 - \alpha/2$$
$$F(CL_{t_r}, r, \lambda) = 1 - \sum_{k=0}^{r-1} e^{-\lambda CL_{t_r}}\frac{(\lambda CL_{t_r})^k}{k!} = 0.5 \tag{2.16}$$
$$F(LCL_{t_r}, r, \lambda) = 1 - \sum_{k=0}^{r-1} e^{-\lambda LCL_{t_r}}\frac{(\lambda LCL_{t_r})^k}{k!} = \alpha/2$$

Xie *et al*. (2002b) also derived the equation for calculating ARL for T_r-chart:

$$ARL_{t_r} = \frac{r}{\lambda[1 + \sum_{k=0}^{r-1} e^{-\lambda UCL_{t_r}}\frac{(\lambda UCL_{t_r})^k}{k!} - \sum_{k=0}^{r-1} e^{-\lambda LCL_{t_r}}\frac{(\lambda LCL_{t_r})^k}{k!}]} \tag{2.17}$$

Surucu and Sazak (2009) extend the T_r-chart by assuming that the time between failures follows a three-parameter Weibull distribution. Since the distribution of the sum of independent Weibull random variables is not known, the moment approximation method is used. Although it is more appropriate to model the time between events by a Weibull distribution, Khoo and Xie (2008) showed that the failure time distribution can be approximated by the exponential distribution for the regularly maintained system.

The second extension is to use a two-stage decision procedure for CQC-chart, which is called CQC_{1+r} -chart. Similar to CCC_{1+r} -chart, the false alarm rate is divided into two parts: $(1-\gamma)\alpha$ for the first stage and $\gamma\alpha$ for the second stage. Then the lower control limit for the first stage LCL_1 and the lower control limit for the second stage LCL_2 should satisfy the following equation:

$$\begin{aligned} 1-e^{-\lambda_0 LCL_1} &= (1-\gamma)\alpha \\ 1-e^{-\lambda_0 LCL_2}(1+\lambda_0 LCL_2) &= \gamma\alpha \end{aligned} \tag{2.18}$$

The process will be considered to be out of control if $Q_1 < LCL_1$ or $LCL_1 \le Q_1 < Q_2 < LCL_2$, where Q_i is the cumulative number of units inspected until i nonconformities occurred. Lai *et al*. (2001) studied the distribution for ARL and AQI (average quantity inspected). Chan *et al*. (2007) compared the properties of ARL and AQI between CQC_1, CQC_2 and CQC_{1+r}.

The third extension is to combine a CQC-chart with x-chart. When CQC-chart is used to monitor the time between the occurrences of the events, it is called t-chart. Wu *et al*. (2008) proposed combining a CQC-chart with x-chart and called it a t&x chart. The t-chart is used to plot the time between the occurrences of the events, while the x-chart is used to plot the magnitude of the event. The results of Wu *et al*. (2008) showed that t&x

chart is more effective in detecting process shift compared with t-chart or individual x-chart, particularly for detecting downward shifts. When the magnitude of the event is an attribute data, t&c chart can be constructed similarly. But Liu *et al*. (2009) showed that t&c chart is not as effective as the ratio chart, which plots the ratio of c/t.

2.3 Time-between-events EWMA Chart

EWMA chart, which was introduced by Roberts (1959), is viewed as a compromise between the Shewhart chart and the CUSUM chart by Hunter (1986). The reason is that the classical Shewhart chart only uses the last point plotted and the ordinary CUSUM chart gives equal weight to all historical data while the EWMA chart uses all historical data but giving different weights to different data.

Let $x_1, x_2, \ldots$ be a series of sequential time-between-events data. Then the statistic of EWMA chart is:

$$Z_i = \lambda x_i + (1-\lambda) Z_{i-1} \tag{2.19}$$

where λ is a constant, $0 < \lambda \leq 1$. The initial value of Z_i should be Z_1 and is taken as the mean of *x*. It is easy to obtain the mean and variance of the EWMA chart statistic:

$$\begin{aligned} \mu_{EWMA} &= E(X) \\ \sigma^2{}_{EWMA} &= [\lambda/(2-\lambda)]V(X) \end{aligned} \tag{2.20}$$

According to the distribution of time-between-events data, time-between-events EWMA chart can be classified into geometric EWMA chart, negative binomial EWMA chart, exponential EWMA chart, gamma EWMA chart and Weibull EWMA chart. Gan (1999) developed one and two-sided exponential EWMA chart. Gan and Chang (2000) published a computer program for computing ARL of the exponential EWMA chart. Liu *et al*. (2007) suggested transforming exponentially distributed time-between-events data into normally distributed data and then using the ordinary EWMA chart to monitor it. Sun and Zhang (2000) set up the geometric EWMA chart and compared it with the two-stage CCC-chart. Results showed that the geometric EWMA chart is more efficient than the two-stage CCC-chart. Kotani *et al*. (2005) designed an $EWMA_{CCC\text{-}r}$ chart which the cumulative count of conforming items between *r* nonconforming items is plotted in the EWMA chart. A Markov chain approach is used to calculate the average number of observations to signal. Zhang and Chen (2004) used EWMA chart to monitor the censored Weibull time-between-events data. The method of Steiner and Mackay (2000, 2001) that replaces censored data with conditional expected values is used in Zhang and Chen (2004). But the EWMA chart in Zhang and Chen (2004) can only detect one-side shift at a time. Lu and Tsai (2008) improved the EWMA chart proposed by Zhang and

Chen (2004) so that only a single EWMA chart can detect a two-side shift. The improved EWMA chart was used to monitor the censored gamma distributed data.

2.4 Time-between-events CUSUM Chart

Cumulative sum (CUSUM) control chart was first proposed by Page (1954). Monitoring time-between-events data by CUSUM chart was first proposed by Lucas (1985). But Lucas (1985) only focused on attribute time-between-events data. The typical attribute time-between-events CUSUM is a geometric CUSUM chart which was first proposed by Bourke (1991) for the case of 100% inspection. Bourke (2001a) extended geometric CUSUM chart to the sampling inspection. Geometric CUSUM chart was proposed to monitor the fraction defective of a process. Binomial CUSUM chart (Gan, 1993; Reynolds and Stoumbos, 1998, 1999; Bourke, 2001b) can also be used to monitor the fraction defective of a process by forming a CUSUM chart of the number of defectives found in successive samples of size n. But many researchers, such as Gan (1993), Reynolds and Stoumbos (1998), Bourke (2001b), recommended the sample size n to be 1. In this case, the Binomial CUSUM chart becomes the Bernoulli CUSUM chart.

Let $Y_1, Y_2, \ldots$ be a sequence of independent and identically geometrically distributed random variables. The geometric CUSUM chart for detecting an upward shift in the fraction defective can be formed as follows:

$$G_i = Max[0, (G_{i-1} + k_G - Y_i)], \text{ for } i = 1,2,\ldots \tag{2.21}$$

where k_G is the reference value of the geometric CUSUM chart and G_0 is the initial value. According to SPRT analysis, k_G can be calculated as below:

$$k_G = \frac{\ln(p_1 / p_0)}{\ln[(1-p_0)/(1-p_1)]} \tag{2.22}$$

where p_0 is the in control defective rate and p_1 is the out of control defective rate.

The sensitivities of geometric CUSUM chart, Bernoulli CUSUM chart and Binomial CUSUM chart are compared in Chang and Gan (2001). Wu *et al*. (2000) compared geometric CUSUM chart (called CRL-CUSUM chart in the paper) with CCC_r-chart (called SCRL chart in the paper). Their results showed that geometric CUSUM chart outperforms CCC_r-chart in detecting downward shift and large-scale upward shift, while CCC_r-chart is superior in detecting the small and moderate scale upward shift.

The typical variable time-between-events CUSUM chart was exponential CUSUM which was first studied by Vardeman and Ray (1985). Let $X_1, X_2, \ldots$ be a sequence of

independent and identically exponentially distributed random variables. The lower-sided and upper-sided exponential CUSUM chart can be formulated as below:

$$\begin{aligned} T_0 &= v,\ \ T_t = \min\{0, T_{t-1} + (X_t - k)\}, t = 1,2,... \\ S_0 &= u,\ \ S_t = \max\{0, S_{t-1} + (X_t - k)\}, t = 1,2,... \end{aligned} \tag{2.23}$$

where k is a positive constant and h is the control limit, $-h < v \le 0, 0 \le u < h$. The lower-sided exponential CUSUM chart is used to detect the downward shift and it will signal if $T_t \le -h$. The upper-sided exponential CUSUM chart is used to detect the upward shift and it will signal if $S_t \ge h$. The exact run length distribution for exponential CUSUM chart is given by Gan (1992). The robustness of exponential CUSUM chart was studied by Borror *et al*. (2003). It was found that exponential CUSUM chart is very robust, so there is no need to worry about departures from exponential distribution.

Liu *et al*. (2006b) proposed another method to monitor the exponentially distributed random variable by CUSUM chart. It was suggested that exponentially distributed random variable be transformed to normally distributed random variable by SQRT transformation method proposed by Kittlitz (1999). Then the ordinary CUSUM chart is used to monitor the data after transformation. The results showed that CUSUM chart with transformed exponential data has comparable performance with exponential CUSUM chart.

2.5 Design of Control Chart

Designing a control chart means choosing values for control chart parameters, like sample size, sampling interval and control limits. Usually, there are two methods to design the control chart, statistical design and economic design. For the statistical design, control chart parameters are determined based on requirement Type I or Type II error or their requirement on ARL or ATS. Many authors have used statistical design method to design control chart. Saniga (1984) used statistical design to determine the optimal parameters for X-bar and R-charts. Woodall and Adams (1993) applied statistical design to CUSUM chart. Aparisi and Garcia-Diaz (2007) used statistical design method to design EWMA chart. Although statistical design can help us to achieve good results in the ARL or ATS, it is criticized for not taking cost into consideration. As a result, economic design is proposed. For the economic design, different cost is taken into considering when designing control charts, like sampling cost, cost of removing assignable cause and cost of producing nonconforming products. Control chart parameters are chosen either to minimize the average cost per unit time or to maximize the average profit per unit time. Duncan (1956) was the first to develop the economic model of X-bar chart. Then Lorenzen and Vance (1986) proposed a unified approach to model the economic control chart design. Economic design has been used to design many

different types of control chart. Xie *et al*. (2001) followed Lorenzen and Vance's model and constructed the economic model of CCC-chart. Zhang *et al*. (2005) used economic design method to find the optimal control limits for exponential chart. Although economic design can help us to minimize the cost or maximize the profit, it is at the cost of scarifying statistical properties, like ARL or ATS. In order to have a balance between statistical properties and economic properties, Saniga (1989) proposed an economic-statistical model. This model has also been used by many researchers, like Chou *et al*. (2002), Chen and Cheng (2007).

2.6 Preventive Maintenance

Equipment used in the production of goods and delivery of services are usually subject to deterioration with usage and age. If the equipment breaks down suddenly, it will increase the production cost due to the down time and increased nonconforming product. As a result, preventive maintenance is a very important topic. Until now, many researchers have done a lot of studies on preventive maintenance. The existing research on preventive maintenance can be classified into three groups: inspection models, minimal repair models and shock models.

Inspection models are models help to determine the optimal inspection intervals because it is not feasible to observe the condition of the equipment all the time. For the inspection model, usually it is assumed that the status of the equipment is completely unknown until an inspection is done and every inspection is assumed to be perfect. There are two decision variables for the inspection models. One is what maintenance action to be taken, replace, repair, or do nothing. The other is when the next inspection is. Many researchers have provided different methods to solve inspection models. Barlow *et al*. (1963) provided a basic pure inspection model. Beichelt (1981) provided a model to determine the optimal inspection times when the equipment can only be replaced or be left as it is. Luss (1976) introduced a degree of deterioration which made the model more practical.

Ciriaco and Richard (1989) defined minimal repair as: if a repair or replacement of the failed component restores function to the entire system but the proneness of system failure remains as it was just before failure, then the repair is called minimal repair. Barlow and Hunter (1960) was the first to study minimal repair using a periodic replacement model. Sheu *et al*. (2001) and Juang and Anderson (2004) used a Bayesian method to find an optimal adaptive preventive maintenance policy with minimum repair.

The typical scenario for a shock model is the equipment is subject to the shocks randomly. The shocks will cause certain damage to the equipment. The damage will accumulate until repair or replacement. Taylor (1975) gave a general shock model which assumed that shocks occur according to a Poisson process and the damages caused by shocks are independent and identically exponentially distributed. Zuckerman (1977) extended Taylor's model by not restricting the damage to be exponentially distributed. Most of the existing research in the shock models assumes that the equipment is new and operates successively like new after replacement. Qian *et al*. (2005) released this assumption and developed a shock model with a pre-defined damage level.

Summarizing the literature review in this chapter, it can be seen that a lot of research has been done on time-between-events chart. But there is still some research gap needed to be filled. First, all existing time-between-events charts assume process shift size is fixed, which is not true in the real life. Second, when designing the existing time-between-events charts, nobody considers the impact of preventive maintenance on time-between-events charts. In the practice, control charts and preventive maintenance are used at the same time. Third, research on time-between-events chart focuses on designing single time-between-events chart. No research has been done on designing time-between-events

chart system, which includes several time-between-events charts. All these problems will be solved one by one in the following chapters.

Chapter 3 Economic Design of Exponential Chart for Monitoring Time-between-Events Data under Random Process Shift

From the literature review in Chapter 2, it can be seen that there is one common assumption for control charts monitoring time-between-events data. The assumption is that process shift is fixed in all papers, which means the process characteristic will shift to a fixed value after the assignable cause happens (e.g. λ_0 shift to λ_1).

There are some problems with this assumption. Firstly, the value of the out of control characteristic is usually determined subjectively. As a result, the design procedure may not reflect practical process conditions. Secondly, the control chart designed under this assumption may achieve optimal performance under the predetermined value of process shift, but may not work satisfactorily for other process shifts.

In order to solve the above problems, random process shift which means the out of control process characteristic is a random variable following a certain probability distribution should be introduced. A few researchers have considered random process shift in their papers. Wu *et al*. (2002) incorporated random process shift when designing X-bar & S charts for monitoring process capability. In Wu *et al*. (2002), random process shift means there is an infinite number of pairs of $(\delta_\mu, \delta_\sigma)$ for a fixed process capability. Wu *et al*. (2004a) considered random process shifts when designing X-bar chart based on Taguchi's loss function, where process shift follows a Rayleigh distribution. Jiao and Helo (2008) applied random process shift to CUSUM control chart. Zeifman and Ingman (2005) used a continuous-state Markov chain to model the unexpected shift in SPC. All these papers show great improvement after introducing random process shift.

In this chapter, random process shift is applied to control chart for monitoring time-between-events data. The economic model of time-between-events chart under random process shift is constructed and optimal control limits for different shift sizes are given. The effectiveness of time-between-events chart under random process shift is compared with time-between-events chart under fixed process shift. Finally the sensitivity of the input cost parameters is studied.

3.1 Model formulation

In this chapter, it is assumed that there is only one assignable cause, the occurrence of which is modeled by a homogenous Poisson process. The occurrence of the event is assumed to follow Poisson distribution, so time between events follows exponential distribution. The control chart for monitoring exponentially distributed time-between-events data is called exponential chart here.

The optimization design is carried out using the following optimization model:

$$\text{Maximize: } O = P/L \tag{3.1}$$

$$\text{Design variable: } LCL \tag{3.2}$$

O is the expected profit per unit time when the process is operating. It equals the expected profit from an operating cycle divided by the expected operating cycle length. Since control limits are designed to monitor the time between two events, usually the larger the time, the better it is. Furthermore, producers are more concerned with the deterioration of the product quality than its improvement. Therefore, for simplicity, only the lower control limit LCL is considered in this chapter. The lower control limit LCL is given by

$$LCL = -\frac{\ln(1-\alpha)}{\lambda_0} \tag{3.3}$$

The probability density function $f(\lambda_1)$ of the random process shift λ_1 can be obtained from Rayleigh distribution (Wu *et al*. 2004a).

$$f(\lambda_1) = \frac{\pi\lambda_1}{2\bar{\lambda}_1^2}\exp(-\frac{\pi\lambda_1^2}{4\bar{\lambda}_1^2}) \tag{3.4}$$

The characteristics of the Rayleigh distribution is determined by the single parameter $\bar{\lambda}_1$, mean of the process shift λ_1. Figure.3.1 illustrates the density function of a Rayleigh distribution with $\bar{\lambda}_1$ equals one.

The mean of the process shift, $\bar{\lambda}_1$ can be estimated easily. Assuming that an out-of-control signal is detected at the *k*2th point on the control chart, and after searching, it is found that the assignable cause happened between the (*k*1-1)th point and *k*1th point. Taking the arithmetic average of these (*k*2 - *k*1) *T*s (random time *T* denotes the occurrence time of the assignable cause),

$$\lambda_{1,i} = \frac{1}{\sum_{j=k1+1}^{k2} T_j /(k2-k1)} \tag{3.5}$$

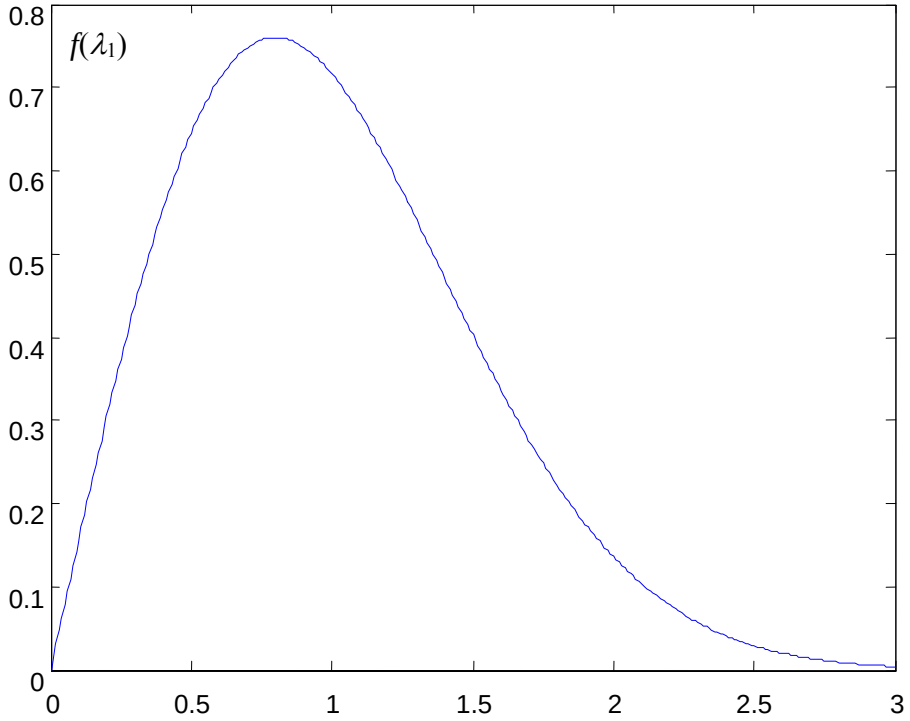

Figure 3.1 Density function of a Rayleigh distribution

By cumulating x such cases, $\overline{\lambda_1}$ can be estimated by the arithmetic average of these $\lambda_{1,i}\,(i=1,2,...,x)$ values,

$$\overline{\lambda_1} = \frac{\sum_{i=1}^{m} \lambda_{1,i}}{x} \tag{3.6}$$

The equation for calculating the expected profit per unit time, *O* is formulated below. Duncan (1956) first introduced the concept of economic design of a control chart which means considering the costs of sampling and testing, costs of investigating out of control signals and correcting assignable causes and costs of the occurrence of nonconforming items when choosing the control chart parameters. The same concept has been followed and applied in the proposed model. An operational cycle is composed of several parts of time as shown in the following figure (Figure 3.2).

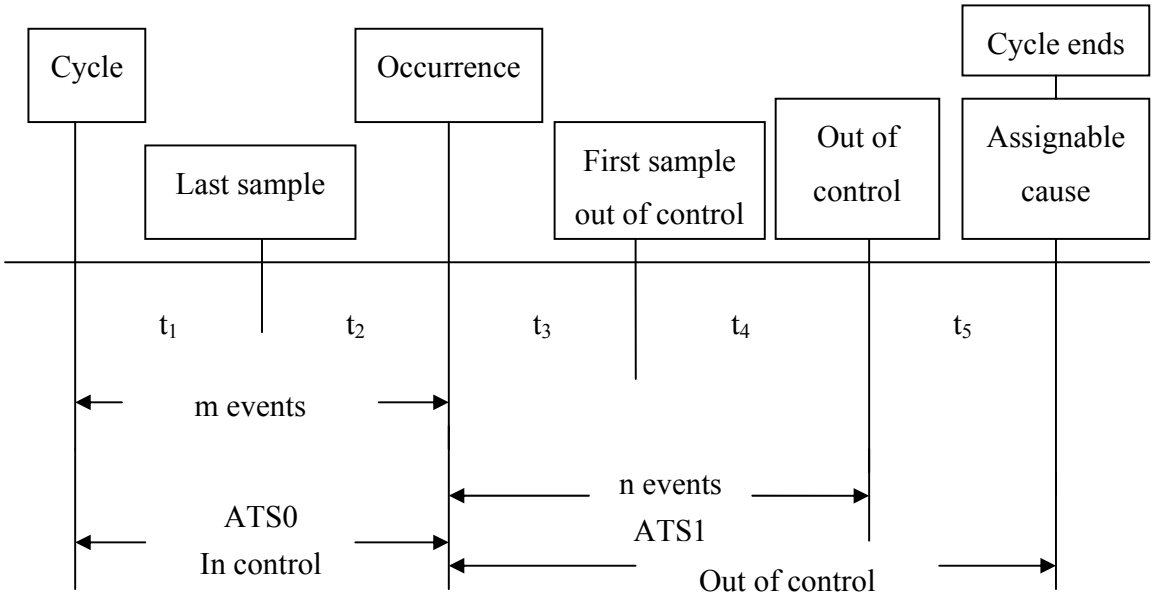

Figure 3.2 Diagram of an operational cycle

The meaning of the five time components of an operational cycle t_1, t_2, t_3, t_4 and t_5 are self-explanatory as shown in Figure 3.2. It is noted that all of these five parameters are random variables and thus we can only get the expected values for them.

Since the occurrence of the assignable cause can be modeled by a homogenous Poisson process, the time between the occurrences of the assignable causes follows an exponential distribution. According to the properties of the exponential distribution, the mean time between the occurrences of the assignable cause is $1/\lambda_a$, hence

$$t_1 + t_2 = 1/\lambda_a \tag{3.7}$$

The in-control mean time between events is $1/\lambda_0$ and the expected number of events occurred when the process is in-control is m, therefore,

$$t_1 = m/\lambda_0 \tag{3.8}$$

According to Duncan (1956), if the assignable cause occurs between the jth and (j +1)th event, then the expected time t_2 is given by

$$t_2 \approx \frac{\int_{j/\lambda_0}^{(j+1)/\lambda_0} \lambda_a e^{-\lambda_a y}(y - j/\lambda_0)dy}{\int_{j/\lambda_0}^{(j+1)/\lambda_0} \lambda_a e^{-\lambda_a y} dy} = \frac{1}{\lambda_a} - \frac{1}{\lambda_0(e^{\lambda_a/\lambda_0} - 1)} \tag{3.9}$$

which is independent of j.

Thus,

$$t_1 + t_2 = m/\lambda_0 + \frac{1}{\lambda_a} - \frac{1}{\lambda_0(e^{\lambda_a/\lambda_0} - 1)} = \frac{1}{\lambda_a} \tag{3.10}$$

or

$$\mathrm{m} = \frac{1}{e^{\lambda_a/\lambda_0} - 1} \tag{3.11}$$

If M is the expected number of false alarms, then,

$$\mathrm{M} = \alpha\mathrm{m} = \frac{\alpha}{e^{\lambda_a/\lambda_0} - 1} = \frac{1 - e^{-\lambda_0 LCL}}{e^{\lambda_a/\lambda_0} - 1} \tag{3.12}$$

where $\alpha = 1 - e^{-\lambda_0 LCL}$.

When the process is in-control, the probability that an event is a false alarm is α, which means for every $1/\alpha$ events, one would be a false alarm. Hence, the in-control ATS_0 of the chart is,

$$ATS_0 = \frac{1}{\alpha}\mathrm{E}(T) = \frac{1}{\alpha\lambda_0} \tag{3.13}$$

After the assignable cause occurs, the occurrence rate of the event will be randomly shifted to a certain value λ_1 other than λ_0, where λ_1 follows a Rayleigh distribution. Then, according to the memoryless property of the exponential distribution,

$$t_3 = \int_0^{\infty} \frac{1}{\lambda_1} f(\lambda_1) d\lambda_1 = \int_0^{\infty} \left(\frac{1}{\lambda_1} \right) \cdot \left(\frac{\pi \lambda_1}{2\bar{\lambda}_1^2} \exp\left(-\frac{\pi \lambda_1^2}{4\bar{\lambda}_1^2} \right) \right) d\lambda_1 = \frac{\pi}{2\bar{\lambda}_1} \tag{3.14}$$

The expected time t_4 can be obtained by,

$$t_4 = \int_0^{\infty} \frac{n-1}{\lambda_1} f(\lambda_1) d\lambda_1 = \int_0^{\infty} \left(\frac{n-1}{\lambda_1} \right) \cdot \left(\frac{\pi \lambda_1}{2\bar{\lambda}_1^2} \exp\left(-\frac{\pi \lambda_1^2}{4\bar{\lambda}_1^2} \right) \right) d\lambda_1 = \frac{(\mathrm{n}-1) \cdot \pi}{2\bar{\lambda}_1} \tag{3.15}$$

The equation for calculating *n* will be explained shortly.

In this study, it is assumed that the expected time t_5 to locate and remove the assignable cause is a known parameter. The process continues operating during searching for the assignable cause.

The expected number of observed events *n*, when the process is out-of-control, can be obtained by Zhang *et al*. (2005),

$$n = p_x + (1 - p_x) \cdot [2 \cdot \mathrm{E}(1-\beta) + 3 \cdot \mathrm{E}(1-\beta) \cdot \mathrm{E}(\beta) + 4 \cdot \mathrm{E}(1-\beta)\mathrm{E}(\beta^2) + \ldots] \tag{3.16}$$

where, p_x is the power of the first sample and (1 - β) is the power of each of the subsequent samples (β is the type II error probability). The expected power E(1 - β) can be obtained by,

$$\begin{aligned}
\mathrm{E}(1-\beta) &= \int_0^\infty (1-\beta) f(\lambda_1) d\lambda_1 \\
&= \int_0^\infty \left(1 - \mathrm{e}^{-\lambda_1 LCL}\right) \cdot \left(\frac{\pi \lambda_1}{2\bar{\lambda}_1^{\,2}} \exp\left(-\frac{\pi \lambda_1^{\,2}}{4\bar{\lambda}_1^{\,2}} \right) \right) d\lambda_1 \\
&= \int_0^\infty \left(\frac{\pi \lambda_1}{2\bar{\lambda}_1^{\,2}} \exp\left(-\frac{\pi \lambda_1^{\,2}}{4\bar{\lambda}_1^{\,2}} \right) \right) d\lambda_1 - \int_0^\infty \mathrm{e}^{-\lambda_1 LCL} \left(\frac{\pi \lambda_1}{2\bar{\lambda}_1^{\,2}} \exp\left(-\frac{\pi \lambda_1^{\,2}}{4\bar{\lambda}_1^{\,2}}\right) \right) d\lambda_1 \\
&= \frac{\bar{\lambda}_1 LCL}{\sqrt{\pi}} \exp\left(\frac{\bar{\lambda}_1^{\,2} LCL^2}{\pi} \right) \left[\Gamma\left(\frac{1}{2}\right) - \Gamma\left(\frac{1}{2}, \frac{\bar{\lambda}_1^{\,2}}{\pi} LCL^2 \right) \right]
\end{aligned} \tag{3.17}$$

The power p_x of the first sample T_x of time between events after the occurrence of the assignable cause can be obtained by,

$$p_x = \int_0^\infty \Pr\{T_x \le LCL\} f(\lambda_1) d\lambda_1 \tag{3.18}$$

To determine the power p_x, it is assumed that the random variable T_a denotes the occurrence time of the assignable cause, which follows exponential distribution with parameter λ_a. It is also assumed that the random variable T_2 denotes the time from the occurrence of the last event before the assignable cause to the occurrence of the

assignable cause, and random variable T_3 denotes the time from the occurrence of the assignable cause to the observation of the first event after the assignable cause (see Figure 3.2). Then, due to the memoryless property of the exponential distribution, T_3 follows an exponential distribution with parameter λ_1. Since, T_x is the first sample of time between events, then, $T_x = T_2 + T_3$. It is difficult to determine the distributions of T_x and T_2, as T_2 is a randomly truncated exponential random variable. However, they are determined approximately as follows.

$$\begin{aligned}
\Pr\{T_x \le LCL\} &= \Pr\{T_2 + T_3 \le LCL\} \\
&= \int_0^{LCL} \Pr\{T_2 + T_3 \le LCL \mid T_3 = T\}\lambda_1 e^{-\lambda_1 T} dT \\
&= \int_0^{LCL} \Pr\{T_2 \le (LCL - T)\}\lambda_1 e^{-\lambda_1 T} dT \\
&\approx \int_0^{LCL} \frac{1 - e^{-\lambda_a (LCL-T)}}{1 - e^{-\lambda_a / \lambda_0}} \lambda_1 e^{-\lambda_1 T} dT = \frac{\lambda_a (1 - e^{-\lambda_1 LCL}) - \lambda_1 (1 - e^{-\lambda_a LCL})}{(\lambda_a - \lambda_1)(1 - e^{-\lambda_a / \lambda_0})}
\end{aligned} \tag{3.19}$$

where,

$$\begin{aligned}
\Pr\{T_2 \le (LCL - T)\} &= \sum_{j=0}^{\infty} \Pr\{T_2 \le (LCL - T), \frac{j}{\lambda_0} \le T_a \le \frac{j+1}{\lambda_0}\} \\
&\approx \sum_{j=0}^{\infty} \Pr\{\frac{j}{\lambda_0} \le T_a \le (\frac{j}{\lambda_0} + (LCL - T))\} \\
&= \sum_{j=0}^{\infty} (e^{-j\lambda_a / \lambda_0} - e^{-j\lambda_a / \lambda_0 - \lambda_a (LCL-T)}) \\
&= \frac{1 - e^{-\lambda_a (LCL-T)}}{1 - e^{-\lambda_a / \lambda_0}}
\end{aligned} \tag{3.20}$$

The out-of-control average time to signal, ATS_1 is then given by,

$$ATS_1 = t_3 + t_4 = \frac{\pi \cdot \mathrm{n}}{2\bar{\lambda}_1} \tag{3.21}$$

The equation for calculating the expected length of an operational cycle L can now be obtained by summing up all the parts t_1, t_2, t_3, t_4 and t_5 together.

$$L = \frac{1}{\lambda_a} + t_3 + t_4 + t_5 = \frac{1}{\lambda_a} + \frac{\pi \cdot n}{2\bar{\lambda}_1} + t_5 \tag{3.22}$$

Thus, the expected profit from an operational cycle P is,

$$\mathrm{P} = \frac{\mathrm{B}_0}{\lambda_a} + B_1 \cdot \left(\frac{\pi \cdot n}{2\bar{\lambda}_1} + t_5 \right) - A_0 \cdot \frac{1 - e^{-\lambda_0 LCL}}{e^{\lambda_a / \lambda_0} - 1} - A_1 - C \cdot \left(\frac{1}{e^{\lambda_a / \lambda_0} - 1} + n \right) \tag{3.23}$$

According to Ross (1970), this is a renewal reward process, so the expected profit per unit time O during an operational cycle is equal to the ratio of the expected profit P to the expected length L during the cycle, $O = P/L$ (Eq.3.1).

3.2 Numerical studies

This section includes three parts. Firstly, a comparison between statistical design of exponential chart under random process shift and economic design of exponential chart under random process shift is conducted. Then, an example is given to show the

exponential chart under random process shift is more realistic than the exponential chart under fixed process shift. Finally, the sensitivities of the input parameters on average profit per unit time are studied.

Before moving on to the next part, let's first specify the values of some parameters,

$$\lambda_a = 0.0001,\ B_0 = 150,\ B_1 = 50,\ C = 0.5,\ A_0 = 10,\ A_1 = 30,\ t_5 = 0.3$$

These values are chosen for the illustrative purpose. Xie *et al.* (1997) used the same set of values to illustrate the similar problem.

3.2.1 Comparison between statistical design and economic design

The comparison between statistical design and economic design under random process shift is conducted in this part. The expected profit per unit time O is compared between statistical design and economic design. The percentage of increase in O from using statistical design to economic design is calculated. Since there is only one decision variable for this economic model (Eq. 3.2), it can be easily solved by Matlab. For the statistical design, the false alarm rate α is set to 0.0027 as the usual case. Results of the comparison are shown in Table 3.1.

Table 3.1 A comparison between statistical design and economic design

		Statistical Design					Economic Design					Increase
λ_0	λ_1	α	LCL	ATS_0	ATS_1	O	α	LCL	ATS_0	ATS_1	O	In O (%)
0.01	0.02	0.0027	0.27	37037	14653	90.55	0.7907	156.40	126.47	78.57	149.13	64.69
0.01	0.03	0.0027	0.27	37037	6541.1	110.45	0.7557	140.94	132.33	52.36	149.39	35.26
0.01	0.05	0.0027	0.27	37037	2375.4	130.79	0.7182	126.66	139.24	31.42	149.60	14.38
0.01	0.07	0.0027	0.27	37037	1222.4	139.10	0.6983	119.83	143.20	22.44	149.70	7.62
0.01	0.1	0.0027	0.27	37037	606.71	144.27	0.6499	104.95	153.87	16.36	149.76	3.81
0.01	0.2	0.0027	0.27	37037	158.13	148.43	0.4083	52.48	244.92	9.79	149.85	0.96
0.01	0.3	0.0027	0.27	37037	73.15	149.26	0.2952	34.98	338.75	6.88	149.89	0.42
0.01	0.4	0.0027	0.27	37037	42.77	149.56	0.2307	26.23	433.46	5.34	149.91	0.23

Table 3.1 shows that the average profit per unit time *O* for economic design is larger than the statistical design. The increase in *O* from statistical design to economic design as shown in the last column of Table 3.1 decreases as λ_1 / λ_0 increases. When λ_1 / λ_0 is less than 10, the increase in *O* is quite significant from statistical design to economic design. When λ_1 / λ_0 is larger than 10, the increase in *O* is very minor and can be ignored.

3.2.2 A numerical example

In this part, a numerical example is given to show that the exponential chart under the random process shift design is more realistic than the exponential chart under fixed shift design.

A complex system is adopted by a manufacturing company. The time between the breaking down of the system can be well approximated by an exponential distribution. The in control failure rate of the exponential distribution λ_0 is estimated to be 0.01. An exponential chart with only lower control limit and false alarm rate set at 0.0027 is used to monitor the time between the breaking down of the system. During the operation of this exponential chart, 20 out of control cases have been observed. The increased failure rate d_i (in terms of λ_0) and its corresponding out of control failure rate λ_1 ($\lambda_1 = (1+d_i)\lambda_0$) have been listed in Table 3.2. The data are taken from Jiao *et al.* 2006. For each of the 20 out of control cases, simulation method is used to get the time to signal. Summarizing the 20 times to signal and dividing it by 20, it is considered to be the 'practical' *ATS* when the process is out of control. In this problem the simulated result is *ATS*=8139.9.

Table 3.2 Increased failure rate and corresponding out of control failure rate

No.	d_i	λ_1	No.	d_i	λ_1
1	1.845	0.02845	11	1.549	0.02549
2	0.588	0.01588	12	1.929	0.02929
3	1.722	0.02722	13	1.940	0.02940
4	0.642	0.01642	14	1.102	0.02102
5	0.622	0.01622	15	0.449	0.01449
6	1.756	0.02756	16	0.418	0.01418
7	2.958	0.03958	17	1.444	0.02444
8	2.208	0.03208	18	0.597	0.01597
9	3.623	0.04623	19	1.320	0.02320
10	1.950	0.02950	20	1.370	0.02370

From Table 3.2, the average out of control failure rate can be calculated, $\overline{\lambda_1}$ =0.025. The theoretical *ATS* when the system is out of control for the exponential chart under fixed shift design is *ATS*=5977.9. (The equations for calculating *ATS* can be found in Zhang *et al.* 2005) The theoretical *ATS* when the system is out of control for the exponential chart under random shift design is *ATS*=9398.7 (Eq. 3.21).

Comparing the theoretical *ATS* for the fixed shift design and random shift design with the 'practical' *ATS*, it is found that the theoretical *ATS* for the random shift design is much closer to the 'practical' *ATS* than the fixed shift design. This finding shows that random process shift model is more realistic than the fixed process shift model. Also the random process shift model underestimates the detection power of the TBE chart a little while the fixed process shift model overestimates the detection power of the TBE chart a lot because the theoretical ATS under the random process shift is slightly larger than the 'practical' ATS and the theoretical ATS under the fixed process shift is significantly smaller than the 'practical' ATS.

3.2.3 Sensitivity analysis

In reality it is really hard to estimate the values for the cost parameters because of the complexity involved, and so errors would always exist in calculating *O*. But how large these errors would be and whether they are acceptable or not are unknown. This is why a sensitivity study is needed here. In this part, we will investigate the sensitivity of the input parameters (λ_a , B_0 , B_1 , C, A_0 , A_1 , t_5) on O by using "one-factor-at-a-time" method. The fixed parameters are $\lambda_0 = 0.01$ and $\overline{\lambda_1} = 0.1$. Each time only one parameter is chosen to vary around its reference value given at the beginning of this section, while

other parameters are kept constant at the reference value. The high value is chosen as two times of the reference value while the low value is chosen as half of the reference value. The results are shown in Table 3.3. Only B_0 has a significant effect on *O*. When B_0 changes from 75 to 300, *O* changes from 74.89 to 299.51. λ_a, B_1, A_0 have little effect on *O*. When λ_a changes from 0.00005 to 0.0002, *O* only changes from 149.85 to 149.59. When B_1 changes from 25 to 100, *O* only changes from 149.72 to 149.84. When A_0 changes from 5 to 20, *O* only changes from 149.79 to 149.70. C, A_1 and t_5 don't have effects on *O*. O keeps constant at 149.76 no matter how these parameters change.

Table 3.3 Sensitivity analysis

Input Parameters							Economic Design				
λ_a	B_0	B_1	C	A_0	A_1	t_5	α	LCL	ATS_0	ATS_1	O
0.00005	150	50	0.5	10	30	0.3	0.6499	104.95	153.87	16.36	149.85
0.0001	150	50	0.5	10	30	0.3	0.6499	104.95	153.87	16.36	149.76
0.0002	150	50	0.5	10	30	0.3	0.6499	104.95	153.87	16.36	149.59
0.0001	**75**	50	0.5	10	30	0.3	0.2262	25.64	442.08	31.43	**74.89**
0.0001	**150**	50	0.5	10	30	0.3	0.6499	104.95	153.87	16.36	**149.76**
0.0001	**300**	50	0.5	10	30	0.3	0.6499	104.95	153.87	16.36	**299.51**
0.0001	150	**25**	0.5	10	30	0.3	0.6499	104.95	153.87	16.36	149.72
0.0001	150	**50**	0.5	10	30	0.3	0.6499	104.95	153.87	16.36	149.76
0.0001	300	**100**	0.5	10	30	0.3	0.6499	104.95	153.87	16.36	149.84
0.0001	150	50	**0.25**	10	30	0.3	0.6499	104.95	153.87	16.36	149.76
0.0001	150	50	**0.5**	10	30	0.3	0.6499	104.95	153.87	16.36	149.76
0.0001	150	50	**1**	10	30	0.3	0.6499	104.95	153.87	16.36	149.76
0.0001	150	50	0.25	**5**	30	0.3	0.6499	104.95	153.87	16.36	149.79
0.0001	150	50	0.5	**10**	30	0.3	0.6499	104.95	153.87	16.36	149.76
0.0001	150	50	1	**20**	30	0.3	0.6499	104.95	153.87	16.36	149.70
0.0001	150	50	0.5	5	**15**	0.3	0.6499	104.95	153.87	16.36	149.76
0.0001	150	50	0.5	10	**30**	0.3	0.6499	104.95	153.87	16.36	149.76
0.0001	150	50	0.5	20	**60**	0.3	0.6499	104.95	153.87	16.36	149.76
0.0001	150	50	0.5	10	15	**0.15**	0.6499	104.95	153.87	16.36	149.76
0.0001	150	50	0.5	10	30	**0.3**	0.6499	104.95	153.87	16.36	149.76
0.0001	150	50	0.5	10	60	**0.6**	0.6499	104.95	153.87	16.36	149.76

3.3 Summary

In this chapter, the idea of random process shift is applied to the exponential chart. The economic model of the exponential chart under random process shift is constructed. The effectiveness of economic design is compared with statistical design. Results show that when λ_1 / λ_0 is less than 10, the increase in average profit per unit time is quite significant from statistical design to economic design. However when λ_1 / λ_0 is larger than 10, the increase is very minor. A comparison of exponential chart between random process shift and fixed process shift is also conducted. The results of comparison show that the exponential chart under random process shift is more realistic than the chart under fixed process shift. Finally, the sensitivity of the input parameters is evaluated. It is shown that only B_0 has a significant influence on O (the average profit per unit time).

Chapter 4 Economic Design of the Integrated Model of Time-between-Events Chart and Preventive Maintenance

In Chapter 3, the introduction of random process shift idea does improve the time-between-events chart to be more effective and more practical. In this chapter, the objective is still to improve the effectiveness of time-between-events chart. The difference is that chapter 3 only focuses on optimizing time-between-events chart itself while this chapter will combine time-between-events chart with preventive maintenance.

4.1 Introduction of integrated model of control chart and preventive maintenance

Integrated model of control chart and preventive maintenance is a model which considers both control chart and preventive maintenance. But control chart and preventive maintenance have always been treated as two independent topics. Although in some cases it is justifiable to separate them, in most cases it is advisable to integrate them. Tagaras (1988) said “Information obtained in the course of control chart determines possible

restoration actions to be taken and thus affects the preventive maintenance schedule. Similarly, maintenance activities interfere with the deterioration pattern of the production process, thus changing the control chart requirements." As the relationship between control chart and preventive maintenance is gradually realized by people, some researchers begin to integrate control chart and maintenance. To the best of the author's knowledge, Tagaras (1988) was the first to give the integrated model of process control and maintenance for X-bar chart. Wu and Makis (2008) extended the integration of control chart and maintenance to multivariate process and designed a chi-square chart under condition-based maintenance. Panagiotidou and Nenes (2008) further studied the integration of control chart and maintenance on the adaptive Shewhart chart. One common assumption for the above papers is that the time to shift to the out of control state and the time to failure are all exponentially distributed. Although failure rates are different when the process is in the in-control state and out-of-control state, such an assumption neither reflects the characteristic that the process usually deteriorates with time nor justifies the motivation of introducing preventive maintenance to quality control (Tagaras 1988).

A few more papers which integrate control chart and maintenance can be found. Cassady *et al*. (2000) used an X-bar chart in conjunction with age-based preventive maintenance to reduce the operating cost. The simulation method is used to demonstrate the cost reduction. Yeung *et al*. (2008) modified Cassady *et al* (2000)'s model and developed a solution algorithm to find the optimal solution instead of using simulation. Ben-Daya and Rahim (2000) studied the effect of maintenance levels on the economic design of X-bar chart. Linderman *et al*. (2005) constructed a model to show the significant cost reduction by integrating the control chart and preventive maintenance. However, all these papers assume that the process is not subject to failures which result in stoppage of the process. Wu and Makis (2008) said "For quality control problems, it is reasonable and usually sufficient to consider a simple two-state model (in-control and out-of-control) because system failure of preventive replacement is not considered. However, for maintenance optimization, the main issue is to effectively plan maintenance activities and avoid costly system failure, which means the system failure cannot be ignored".

Summarizing the above references and the literature review in Chapter 2, some research gap can be found. First, for the single variable model, the integration of control chart and preventive maintenance is restricted to the X-bar chart. But as it is pointed out in Chapter

1, X-bar chart has subjected to much criticism for its inefficiency in monitoring high yield processes. Second, process failure in the integrated model is either not considered or considered but exponentially distributed.

This chapter aims to fill the above gap by providing a more general and practical integrated model of control chart and preventive maintenance. There are three main contributions of this chapter. Firstly, a time-between-events (TBE) chart, instead of X-bar chart, is used in the integrated model. The reason why we use a TBE chart is used in this chapter is that the TBE chart is effective whether the defect rate of the process is low or not, although it is designed to monitor high yield processes (Chan *et al*. 2000). Secondly, both the assignable cause and process failure are considered in the integrated model. The occurrences of assignable cause and failure are modeled by the versatile Weibull distribution which can generate decreasing, constant and increasing failure rate by adjusting the values of shape parameters. Thirdly, the cost aspect of control chart and preventive maintenance is considered. The economic model is developed based on the pioneer work of Duncan (1956) and the cost minimization criterion is used to find the optimal values for decision variables.

4.2 Assumptions and problem statement

Additional nomenclature

T_p Scheduled time to perform preventive maintenance

T_a Occurrence time of assignable cause

T_f Failure time of the process

T_F Expected time spent on investigating a false alarm

T_R Expected time to perform reactive maintenance after process failure

T_A Expected time to perform reactive maintenance after quality shift

T_{PM} Expected time to perform preventive maintenance

C_R Expected cost to perform reactive maintenance after process failure

C_A Expected cost to perform reactive maintenance after quality shift

C_P Expected cost to perform preventive maintenance

γ_1 Indicator variable (1 if production ceases when investigating the false alarm, 0 otherwise)

4.2.1 Assumptions

1. Time to the occurrence of the assignable cause follows a Weibull distribution $f(t_a) = \lambda_a{}^{va} va t_a{}^{va-1} e^{-(\lambda_a t_a)^{va}}$ with mean $\theta_a = \Gamma(1+1/va)/\lambda_a$.

2. Time to the occurrence of the failure also follows a Weibull distribution $f(t) = \lambda^v v t^{v-1} e^{-(\lambda t)^v}$ with mean $\theta = \Gamma(1+1/v)/\lambda$.

3. Time between occurrences of defects follows an exponential distribution with the occurrence rate λ_0 when process is in control and λ_1 when process is out of control.

4. It is assumed process failure is independent of quality shift, which means the mean time to failure remains constant whether the shift occurs or not. Makis and Fung (1995, 1998) had made the same assumption.

5. Both preventive maintenance and reactive maintenance can restore the process to an "as-good-as-new" condition.

4.2.2 Problem statement

Suppose a production process is subjected to quality shift and process failure. There are three states for the process, "in-control state", "out-of-control state" and "failure state". The process is assumed to be in the in-control state at startup. When the process is in the

in-control state, the occurrence of defects can be modeled by a homogenous Poisson process with the occurrence rate λ_0. However, after a period of time, the process may shift to the out-of-control state because of the occurrence of the assignable cause. When the process is in the out-of-control state, the occurrence of defects can still be modeled by a homogenous Poisson process but with a larger occurrence rate λ_1. Since out-of-control state is not observable, a time-between-events (TBE) chart is used to detect the quality shift. If the TBE chart signals, a search for the assignable cause takes place. If the signal is found to be a true signal, a reactive maintenance is taken to restore the process to the in-control state. The process may break down after a period of time. The failure state is observable because the process stops working in the failure state. Once failure happens, a reactive maintenance is taken to restore the process to the in-control state. Reactive maintenance after quality shift and process failure costs different time and money respectively. If neither process failure nor signal from the TBE chart occurs before time T_p, preventive maintenance occurs at T_p. When the time for preventive maintenance comes, the process can be in the in-control state or in the out-of-control state. Cost for preventive maintenance in the out-of-control state is assumed to be the same as cost for reactive maintenance after quality shift.

Since either the reactive maintenance after quality shift, reactive maintenance after process failure or preventive maintenance restores the process to an "as-good-as-new" condition, a production cycle is defined as the time period from the startup or reinstatement of the process until the completion of maintenance. In the next part, different forms of production cycle are illustrated. The expected cycle time and cycle cost corresponding to each form are calculated. Since this is a renewal-reward process in which a renewal occurs at the completion of maintenance, the long-run average cost per unit time is expressed as the expected cost per cycle divided by the expected cycle length (Ross, 1996).

4.3 Model formulation

There are five possible scenarios for an operating cycle. The operating cycle is repeated again and again within the production process. The expected cycle time and cycle cost for each of the five scenarios are derived clearly as below:

Scenario 1: Process fails before the quality shift and preventive maintenance

Expected cycle time for scenario 1(S1) consists of mean time to failure, average time spent on investigating false alarms and reactive maintenance time. First, let's calculate mean time to failure:

$$\begin{aligned} E[\text{time to failure}\,|\,\text{S1}] &= E[T_f \,|\, T_f < T_p, T_f < T_a] \\ &= \int t_f \cdot f(t_f \,|\, T_f < T_p, T_f < T_a)\, dt_f \\ &= \int t_f \cdot \frac{f(t_f, T_f < T_p, T_f < T_a)}{P(T_f < T_p, T_f < T_a)} dt_f \\ &= \frac{\int_0^{T_p} t_f \cdot \lambda^v \cdot v \cdot {t_f}^{v-1} \cdot e^{-(\lambda \cdot t_f)^v} \cdot \int_{t_f}^{\infty} {\lambda_a}^{va} \cdot va \cdot {t_a}^{va-1} \cdot e^{-(\lambda_a \cdot t_a)^{va}} dt_a dt_f}{\int_0^{T_p} \lambda^v \cdot v \cdot {t_f}^{v-1} \cdot e^{-(\lambda \cdot t_f)^v} \cdot \int_{t_f}^{\infty} {\lambda_a}^{va} \cdot va \cdot {t_a}^{va-1} \cdot e^{-(\lambda_a \cdot t_a)^{va}} dt_a dt_f} \end{aligned} \tag{4.1}$$

Then the expression for expected cycle time is:

$$\text{E[cycle time}\,|\,\text{S1]} = \text{E[time to failure}\,|\,\text{S1]} + \gamma_1 \cdot \alpha \cdot \lambda_0 \cdot \text{E[time to failure}\,|\,\text{S1]} \cdot T_F + T_R \tag{4.2}$$

Expected cycle cost for scenario 1(S1) includes: cost of quality loss during production, cost of observing defects, cost of investigating false alarms and cost of reactive maintenance. In this scenario, production time equals mean time to failure. Moreover, since failure happens before quality shift, mean time to failure equals in-control time. Then the expression for expected cycle cost is:

$$\begin{aligned} \text{E[cycle cost}\,|\,\text{S1]} = {} & D_0 \cdot \text{E[time to failure}\,|\,\text{S1]} + C \cdot \lambda_0 \cdot \text{E[time to failure}\,|\,\text{S1]} \\ & + A_0 \cdot \alpha \cdot \lambda_0 \cdot \text{E[time to failure}\,|\,\text{S1]} + C_R \end{aligned} \tag{4.3}$$

The probability for the occurrence of scenario 1(P1) equals:

$$P1 = P(T_f < T_{p,} T_f < T_a) = \int_0^{T_p} \int_{t_f}^{\infty} {\lambda_a}^{va} \cdot va \cdot {t_a}^{va-1} \cdot e^{-(\lambda_a t_a)^{va}} \cdot \lambda^v v {t_f}^{v-1} e^{-(\lambda t_f)^v} dt_a dt_f \tag{4.4}$$

Scenario 2: Process fails in the out of control state but before the chart signals and preventive maintenance

Expected cycle time for scenario 2(S2) consists of mean time to failure, average time spent on investigating false alarms and reactive maintenance time. Since process fails after quality shift, mean time to failure equals sum of in-control time and out-of-control time. First let's calculate the in-control time:

$$\begin{aligned} \mathrm{E}[\text{ in - control time} \mid \mathrm{S2}] &= E[T_a \mid T_a < T_f < T_p] \\ &= \frac{\int t_a \cdot f(t_a \mid T_a < T_f < T_p) dt_a}{P(T_a < T_f < T_p)} \\ &= \frac{\int_0^{T_p} \int_0^{t_f} {\lambda_a}^{va} \cdot va \cdot {t_a}^{va} \cdot e^{-(\lambda_a t_a)^{va}} \cdot \lambda^v \cdot v \cdot {t_f}^{(v-1)} \cdot e^{-(\lambda \cdot t_f)^v} dt_a dt_f}{\int_0^{T_p} \int_0^{t_f} {\lambda_a}^{va} \cdot va \cdot {t_a}^{(va-1)} \cdot e^{-(\lambda_a t_a)^{va}} \cdot \lambda^v \cdot v \cdot {t_f}^{(v-1)} \cdot e^{-(\lambda \cdot t_f)^v} dt_a dt_f} \end{aligned} \tag{4.5}$$

Then mean time to failure equals:

$$\begin{aligned} \mathrm{E}[\text{time to failure} \mid \mathrm{S2}] &= E[T_f \mid T_a < T_f < T_p] \\ &= \frac{\int t_f \cdot f(t_f \mid T_a < T_f < T_p) dt_f}{P(T_a < T_f < T_p)} \\ &= \frac{\int_0^{T_p} \int_{t_a}^{T_p} \lambda^v \cdot v \cdot {t_f}^{v} \cdot e^{-(\lambda \cdot t_f)^v} \cdot {\lambda_a}^{va} \cdot va \cdot {t_a}^{(va-1)} \cdot e^{-(\lambda_a t_a)^{va}} dt_f dt_a}{\int_0^{T_p} \int_0^{t_f} {\lambda_a}^{va} \cdot va \cdot {t_a}^{(va-1)} \cdot e^{-(\lambda_a t_a)^{va}} \cdot \lambda^v \cdot v \cdot {t_f}^{(v-1)} \cdot e^{-(\lambda \cdot t_f)^v} dt_a dt_f} \end{aligned} \tag{4.6}$$

So, average out-of-control time is:

$$\text{E[out-of-control time|S1]=E[time to failure|S2]-E[in-control time|S2]} \quad (4.7)$$

Finally, the expression for expected cycle time is:

$$\text{E[cycle time}\,|\,\text{S2]} = \text{E[time to failure}\,|\,\text{S2]} + \gamma_1 \cdot \alpha \cdot \lambda_0 \cdot \text{E[in - control time}\,|\,\text{S2]} \cdot \text{T}_\text{F} + T_R \quad (4.8)$$

Expected cycle cost for scenario 2 (S2) includes: cost of quality loss while production is in-control, cost of quality loss while production is out-of-control, cost of observing defects, cost of investigating false alarms and cost of reactive maintenance.

$$\begin{aligned}\text{E[cycle cost}\,|\,\text{S2]} = {} & D_0 \cdot \text{E[in - control time}\,|\,\text{S2]} + D_1 \cdot \text{E[out - of - control time}\,|\,\text{S2]} \\ & + C \cdot \{\lambda_0 \cdot \text{E[in - control time}\,|\,\text{S2]} + \lambda_1 \cdot \text{E[out - of - control time}\,|\,\text{S2]}\} \\ & + A_0 \cdot \alpha \cdot \lambda_0 \cdot \text{E[in - control time}\,|\,\text{S2]} + C_R\end{aligned} \quad (4.9)$$

The probability for the occurrence of scenarios 2 equals:

$$\begin{aligned}P2 &= P(0 < T_a < T_f < T_p) \cdot P(\text{not signal}\,|\,\text{out of control}) \\ &= \int_0^{T_p}\int_0^{t_f} \lambda_a{}^{va} \cdot va \cdot t_a{}^{(va-1)} \cdot e^{-(\lambda_a t_a)^{va}} \cdot \lambda^v \cdot v \cdot t_f{}^{(v-1)} \cdot e^{-(\lambda \cdot t_f)^v} dt_a dt_f \cdot \beta^{\lfloor \lambda_1 E[\text{out-of-control time|S2}] \rfloor}\end{aligned} \quad (4.10)$$

($\lfloor\ \rfloor$ is the largest integer.)

Scenario 3: Quality shifts and the TBE chart signals before the process fails and preventive maintenance

Expected cycle time for scenarios 3(S3) consists of expected in-control time, expected out-of-control time, average time spent on investigating false alarms and reactive

maintenance time. In this scenario, the TBE chart signals so expected out-of-control time equals average time to signal (ATS). The equations for calculating each part are provided below:

$$\begin{aligned} E[\text{in control time} \mid \text{S3}] &= E[\text{in control time} \mid T_a < T_f, T_a < T_p] \\ &= E[\text{in control time} \mid T_a < T_p < T_f] \cdot \frac{P(T_a < T_p < T_f)}{P(T_a < T_f, T_a < T_p)} \\ &\quad + E[\text{in control time} \mid T_a < T_f < T_p] \cdot \frac{P(T_a < T_f < T_p)}{P(T_a < T_f, T_a < T_p)} \end{aligned} \tag{4.11}$$

$$\begin{aligned} E[\text{in control time} \mid T_a < T_p < T_f] &= \int t_a \cdot f(t_a \mid T_a < T_p < T_f) dt_a = \frac{\int_0^{T_p} t_a \cdot f(t_a) dt_a \int_{T_p}^{\infty} f(t_f) dt_f}{\int_0^{T_p} f(t_a) dt_a \cdot \int_{T_p}^{\infty} f(t_f) dt_f} \\ &= \frac{\int_0^{T_p} t_a \cdot f(t_a) dt_a}{\int_0^{T_p} f(t_a) dt_a} = \frac{\int_0^{T_p} {\lambda_a}^{va} \cdot va \cdot {t_a}^{va} \cdot e^{-(\lambda_a t_a)^{va}} dt_a}{\int_0^{T_p} {\lambda_a}^{va} \cdot va \cdot {t_a}^{va-1} \cdot e^{-(\lambda_a t_a)^{va}} dt_a} \end{aligned} \tag{4.12}$$

$$\begin{aligned} E[\text{in control time} \mid T_a < T_f < T_p] &= \int t_a \cdot f(t_a \mid T_a < T_f < T_p) dt_a = \frac{\int_0^{T_p} \int_0^{T_f} t_a \cdot f(t_a) \cdot f(t_f) dt_a dt_f}{\int_0^{T_p} \int_0^{T_f} f(t_a) \cdot f(t_f) dt_a dt_f} \\ &= \frac{\int_0^{T_p} \int_0^{T_f} {\lambda_a}^{va} \cdot va \cdot {t_a}^{va} \cdot e^{-(\lambda_a t_a)^{va}} \cdot \lambda^{v} \cdot v \cdot {t_f}^{v-1} \cdot e^{-(\lambda \cdot t_f)^{v}} dt_a dt_f}{\int_0^{T_p} \int_0^{T_f} {\lambda_a}^{va} \cdot va \cdot {t_a}^{va-1} \cdot e^{-(\lambda_a t_a)^{va}} \cdot \lambda^{v} \cdot v \cdot {t_f}^{v-1} \cdot e^{-(\lambda \cdot t_f)^{v}} dt_a dt_f} \end{aligned} \tag{4.13}$$

Let $M = \lfloor \lambda_1 (T_p - E[\text{in control time} \mid T_a < T_p < T_f]) \rfloor$, M is the maximum number of defects which can be seen when the occurrence order of quality shift, failure and preventive maintenance follows $T_a < T_p < T_f$.

$$E[\text{time to signal} \mid T_a < T_p < T_f] = \sum_{i=1}^{M} \frac{i}{\lambda_1} (1-\beta)\beta^{i-1} \tag{4.14}$$

where $\frac{i}{\lambda_1}$ is mean time to see the ith defect when process is out-of-control and $(1-\beta)\beta^{i-1}$ is the probability for the ith defect signaling (Since occurrences of defects follow Poisson distribution with λ_1, time between occurrences of defects follows exponential distribution with mean $\frac{1}{\lambda_1}$).

When the occurrence order of quality shift, failure and preventive maintenance follows $T_a < T_f < T_p$, mean time to failure should be calculated before we can calculate average time to signal.

$$E[\text{time to failure} \mid T_a < T_f < T_p] = \int t_f \cdot f(t_f \mid T_a < T_f < T_p) dt_f = \frac{\int_0^{T_p}\int_{T_a}^{T_p} t_f \cdot f(t_f)\cdot f(t_a) dt_f dt_a}{\int_0^{T_p}\int_{T_a}^{T_p} f(t_f)\cdot f(t_a) dt_f dt_a}$$
$$= \frac{\int_0^{T_p}\int_{T_a}^{T_p} {\lambda_a}^{va} \cdot va \cdot {t_a}^{va-1} \cdot e^{-(\lambda_a t_a)^{va}} \cdot \lambda^v \cdot v \cdot {t_f}^{v} \cdot e^{-(\lambda \cdot t_f)^v} dt_f dt_a}{\int_0^{T_p}\int_0^{T_f} {\lambda_a}^{va} \cdot va \cdot {t_a}^{va-1} \cdot e^{-(\lambda_a t_a)^{va}} \cdot \lambda^v \cdot v \cdot {t_f}^{v-1} \cdot e^{-(\lambda \cdot t_f)^v} dt_a dt_f} \quad (4.15)$$

Let $N = \left\lfloor \lambda_1 (E[\text{time to failure}|T_a < T_f < T_p] - E[\text{in control time}|T_a < T_f < T_p]) \right\rfloor$, N is the maximum number of defects which can be seen when the occurrence order of quality shift, failure and preventive maintenance follows $T_a < T_f < T_p$.

$$E[\text{time to signal} \mid T_a < T_f < T_p] = \sum_{i=1}^{N} \frac{i}{\lambda_1}(1-\beta)\beta^{i-1} \quad (4.16)$$

$$
\begin{aligned}
E[\text{out - of - control time} \mid \text{S3}] &= E[\text{time to signal} \mid \text{S3}] = E[\text{time to signal} \mid T_a < T_f, T_a < T_p] \\
&= E[\text{time to signal} \mid T_a < T_p < T_f] \cdot \frac{P(T_a < T_p < T_f)}{P(T_a < T_f, T_a < T_p)} \\
&+ E[\text{time to signal} \mid T_a < T_f < T_p] \cdot \frac{P(T_a < T_f < T_p)}{P(T_a < T_f, T_a < T_p)}
\end{aligned} \tag{4.17}
$$

Then the expression for expected cycle time is:

$$
\begin{aligned}
\mathrm{E}[\text{cycle time} \mid \mathrm{S3}] = \mathrm{E}[\text{in - control time} \mid \mathrm{S3}] + \mathrm{E}[\text{out - of - control time} \mid \mathrm{S3}] \\
+ \gamma_1 \cdot \alpha \cdot \lambda_0 \cdot \mathrm{E}[\text{in - control time} \mid \mathrm{S3}] \cdot \mathrm{T_F} + T_A
\end{aligned} \tag{4.18}
$$

Expected cycle cost for scenario 3(S3) includes: cost of quality loss while production is in-control, cost of quality loss while production is out-of-control, cost of observing defects, cost of investigating false alarms and cost of reactive maintenance.

$$
\begin{aligned}
\mathrm{E}[\text{cycle cost} \mid \mathrm{S3}] = D_0 \cdot \mathrm{E}[\text{in - control time} \mid \mathrm{S3}] + D_1 \cdot \mathrm{E}[\text{out - of - control time} \mid \mathrm{S3}] \\
+ C \cdot (\lambda_0 \cdot \mathrm{E}[\text{in - control time} \mid \mathrm{S3}] + \lambda_1 \cdot \mathrm{E}[\text{out - of - control time} \mid \mathrm{S3}]) \\
+ A_0 \cdot \alpha \cdot \lambda_0 \cdot \mathrm{E}[\text{in - control time} \mid \mathrm{S3}] + C_A
\end{aligned} \tag{4.19}
$$

The probability for the occurrence of scenario 3 is:

$$
\begin{aligned}
P3 &= P(0 < T_a < T_p < T_f) \cdot P(\text{not signal} \mid \text{out - of - control}, T_a < T_p < T_f) \\
&+ P(0 < T_a < T_f < T_p) \cdot P(\text{not signal} \mid \text{out - of - control}, T_a < T_f < T_p) \\
&= \int_{T_p}^{\infty} \lambda^v v t_f^{\,v-1} e^{-(\lambda t_f)^v} dt_f \cdot \int_0^{T_p} \lambda_a^{\,va} \cdot va \cdot t_a^{(va-1)} \cdot e^{-(\lambda_a t_a)^{va}} dt_a \cdot (1 - \beta^M) \\
&+ \int_0^{T_p} \int_{T_a}^{T_p} \lambda^v v t_f^{\,v-1} e^{-(\lambda t_f)^v} \cdot \lambda_a^{\,va} \cdot va \cdot T_a^{(va-1)} \cdot e^{-(\lambda_a T_a)^{va}} dt_f dT_a \cdot (1 - \beta^N
\end{aligned} \tag{4.20}
$$

Scenario 4: Preventive maintenance happens before the quality shifts and process failure.

Expected cycle time for scenario 4 consists of time until preventive maintenance, average time spent on investigating false alarms and preventive maintenance time. Since preventive maintenance happens before quality shifts, scenario 4 keeps in control all the time.

$$\mathrm{E}[\text{cycle time} \mid \mathrm{S4}] = T_p + \gamma_1 \cdot T_F \cdot \alpha \cdot \lambda_0 \cdot T_p + T_{PM} \tag{4.21}$$

Expected cycle cost includes: cost of quality loss while production is in-control, cost of observing defects, cost of investigating false alarms and cost of preventive maintenance.

$$\mathrm{E}[\text{cycle cost} \mid \mathrm{S4}] = D_0 \cdot T_p + C \cdot \lambda_0 \cdot T_p + A_0 \cdot \alpha \cdot \lambda_0 \cdot T_p + C_p \tag{4.22}$$

The probability for the occurrence of scenario 4 is:

$$P4 = P(T_a > T_p, T_f > T_p) = (1 - \int_0^{T_p} {\lambda_a}^{va} \cdot va \cdot t^{(va-1)} \cdot e^{-(\lambda_a t)^{va}} dt) \cdot (1 - \int_0^{T_p} \lambda^v v t^{v-1} e^{-(\lambda t)^v} dt) \tag{4.23}$$

3.5 Scenario 5: Preventive maintenance happens between quality shifts and process failures but the TBE chart doesn't signal the shift.

Expected cycle time for scenario 5 consists of time until preventive maintenance, average time spent on investigating false alarms and preventive maintenance time. Since quality

shift happens before preventive maintenance, time until preventive maintenance includes in-control time and out-of-control time. First let's calculate the expected in-control time:

$$\mathrm{E}[\text{in - control time}\,|\,\mathrm{S5}] = \int t_a \cdot f(t_a \,|\, T_a < T_p < T_f)dt_a = \int_0^{T_p} \frac{\lambda_a{}^{va} \cdot va \cdot t^{va} \cdot e^{-(\lambda_a t)^{va}}}{1 - e^{-(\lambda_a T_p)^{va}}} dt \qquad (4.24)$$

So:

$$\mathrm{E}[\text{out - of - control time}\,|\,\mathrm{S5}] = T_p - E[\text{in - control time}\,|\,\mathrm{S5}] = T_p - \int_0^{T_p} \frac{\lambda_a{}^{va} \cdot va \cdot t^{va} \cdot e^{-(\lambda_a t)^{va}}}{1 - e^{-(\lambda_a T_p)^{va}}} dt \quad (4.25)$$

Then the expression for the expected cycle time is:

$$\mathrm{E}[\text{cycle time}\,|\,\mathrm{S5}] = T_p + \gamma_1 \cdot T_F \cdot \alpha \cdot \lambda_0 \cdot \mathrm{E}[\text{in - control time}\,|\,\mathrm{S5}] + T_A \qquad (4.26)$$

Expected cycle cost includes: cost of quality loss while production is in-control, cost of quality loss while production is out-of-control, cost of observing defects, cost of investigating false alarms and cost of reactive maintenance for quality shift.

$$\begin{aligned} \mathrm{E}[\text{cycle cost}\,|\,\mathrm{S5}] = {} & D_0 \cdot \mathrm{E}[\text{in - control time}\,|\,\mathrm{S5}] + D_1 \cdot \mathrm{E}[\text{out - of - control time}\,|\,\mathrm{S5}] \\ & + C \cdot (\lambda_0 \cdot \mathrm{E}[\text{in - control time}\,|\,\mathrm{S5}] + \lambda_1 \cdot \mathrm{E}[\text{out - of - control time}\,|\,\mathrm{S5}]) \\ & + A_0 \cdot \alpha \cdot \lambda_0 \cdot \mathrm{E}[\text{in - control time}\,|\,\mathrm{S5}] + C_A \end{aligned} \qquad (4.27)$$

The probability for the occurrence of scenario 5 is:

$$\begin{aligned} P5 &= P(T_a < T_p < T_f) \cdot P(\text{not signal}\,|\,\text{out - of - control}) \\ &= \int_0^{T_p} \lambda_a{}^{va} \cdot va \cdot t^{(va-1)} \cdot e^{-(\lambda_a t)^{va}} dt \cdot (1 - \int_0^{T_p} \lambda^v v t^{v-1} e^{-(\lambda t)^v} dt) \cdot \beta^{\lfloor \lambda_1 \mathrm{E}[\text{out-of-control time}\,|\,\mathrm{S5}] \rfloor} \end{aligned} \qquad (4.28)$$

Summing up the above 5 scenarios, the expected cycle time and cost for the integrated model of TBE chart and preventive maintenance are as follows:

$$E[\text{cycle time}] = P1 * E[\text{cycle time} \mid \text{S1}] + P2 * E[\text{cycle time} \mid \text{S2}] + P3 * E[\text{cycle time} \mid \text{S3}] + P4 * E[\text{cycle time} \mid \text{S4}] + P5 * E[\text{cycle time} \mid \text{S5}] \quad (4.29)$$

$$E[\text{cycle cost}] = P1 * E[\text{cycle cost} \mid \text{S1}] + \text{P2} * \text{E}[\text{cycle cost} \mid \text{S2}] + \text{P3} * \text{E}[\text{cycle cost} \mid \text{S3}] + \text{P4} * \text{E}[\text{cycle cost} \mid \text{S4}] + \text{P5} * \text{E}[\text{cycle cost} \mid \text{S5}] \quad (4.30)$$

Since this is a renewal-reward process, the expected cost per unit time O for the integrated model is:

$$O = \frac{E[\text{cycle cost}]}{E[\text{cycle time}]} \quad (4.31)$$

The objective function and decision variables for the integrated model are listed below:

$$\text{Objective function: minimize } O = \frac{E[\text{cycle cost}]}{E[\text{cycle time}]}$$

$$\text{Decision variables: } \alpha \text{ and } T_p \text{ , } \alpha \geq 0 \text{ , } T_p \geq 0$$

4.4 Sensitivity analysis

Sensitivity analysis in this section aims at analyzing the influence of input parameters on the integrated model, comparing the integrated model with two alternative models and analyzing the influence of shift and failure distributions on the expected cost per unit time. Results from sensitivity analysis not only promote our understanding of the model but

also help to develop some insights into the situation when the integrated model should be used.

4.4.1 Analysis approach

Design of Experiment (DOE) method is used to analyze the sensitivity of the integrated model's parameters on the expected cost per unit time (O) and decision variables T_p and α. There are 17 input parameters, but two of them γ_1 and C are kept constant with values $\gamma_1 = 0$ and $C = 5$. Low and high values for the remaining 15 input parameters are listed in Table 4.1.

Table 4.1 Low and High values for input parameters

Factor	A	B	C	D	E	F	G	H	J	K	L	M	N	O	P
Variable	θ_a	va	θ	v	λ_0	λ_1	V_0	V_1	T_R	T_A	T_{PM}	C_R	C_A	C_P	A_0
Low	100	1	200	2	0.01	0.1	100	300	2	1	1	10000	5000	2400	200
High	300	2	600	4	0.05	0.5	200	600	4	2	2	20000	10000	4800	500

Since the number of input parameters is quite large, a fractional factorial design 2_{IV}^{15-10} is applied to do the sensitivity analysis, which results in 32 experimental runs. Main effects can be separated with resolution IV, but two and above interactions are aliased. The

generators for this design are F=ABC, G=ABD, H=ABE, J=ACD, K=ACE, L=ADE, M=BCD, N=BCE, O=BDE and P=CDE.

Normal probability plot suggested by Neter et al. (1990) is used to identify important input variables. Since there is no replication, we cannot estimate experimental error. Furthermore, high order interactions are aliased with main effects, so we cannot estimate experimental error by high order interactions either. The significance of each input variable can only be estimated by its contribution to the total sum of squares. Variables lie close to the line are negligible while variables deviating from the line have significant effect on the response.

The simplex method (Murray 1972) is used to search for the optimal solution. In order to show the effectiveness of the integrated model in reducing the expected cost per unit time, two alternative models: preventive maintenance model and TBE-chart model are provided for comparison. For preventive maintenance model, only preventive maintenance with no TBE-chart, is used. The production process will stop either because of failure or time for preventive maintenance. Actually preventive maintenance model is a special case of the integrated model. When $\alpha = 0$, the integrated model reduces to preventive maintenance model with only one decision variable T_p. For TBE-chart model,

only TBE-chart with no preventive maintenance is used. The production process will stop either because of failure or true signal from TBE-chart. When $T_p \to \infty$, the integrated model tends to TBE-chart model with only one decision variable α. The optimal decision variables and cost for the integrated model, preventive maintenance model and TBE-chart model are recorded for each of the 32 runs.

4.4.2 Results for the analysis of input parameters on the integrated model

T_p^*, α^* and $Cost^*$ represent the optimal decision variables and cost for the integrated model. Results for the influence of the 15 input parameters on T_p^*, α^* and $Cost^*$ are summarized in Figures 4.1,4.2 and 4.3.

Figure 4.1 shows that three parameters have significant effects on α^*. F (λ_1) and B (va) have negative effects on α^*, which means increasing of F and B will result in decreasing of α^*. H (V_1) has positive effect on α^*, which means increasing of H results in increasing of α^*. Similarly, Figure 4.2 shows that F (λ_1), C (θ), O (C_P) have positive effect on T_p^* while B (va) has negative effect on T_p^*. Figure 4.3 tells us that N (C_A) and G (V_0) have positive effect on $Cost^*$ while A (θ_a), B (va), C (θ) and F (λ_1) have negative effect on $Cost^*$. Interestingly, B (va), shape parameter of the assignable cause, has a negative effect on all T_p^*, α^* and $Cost^*$. This is because as B (va) increases, it becomes easier to

predict the occurrence of assignable cause. This result is consistent with the result of Linderman *et al*. (2005).

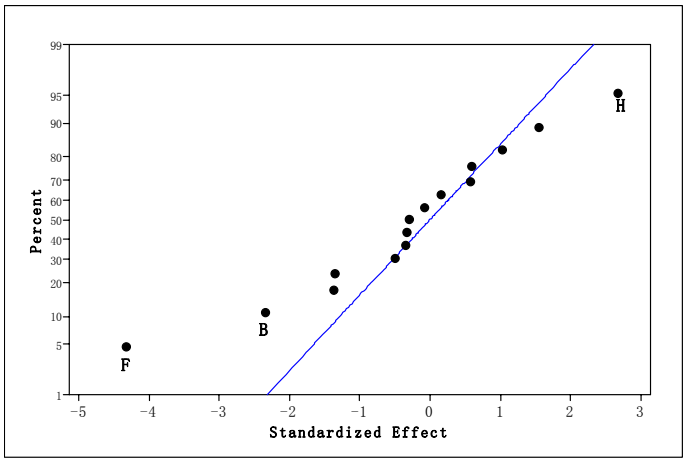

Figure 4.1 Normal Probability Plot for Alpha

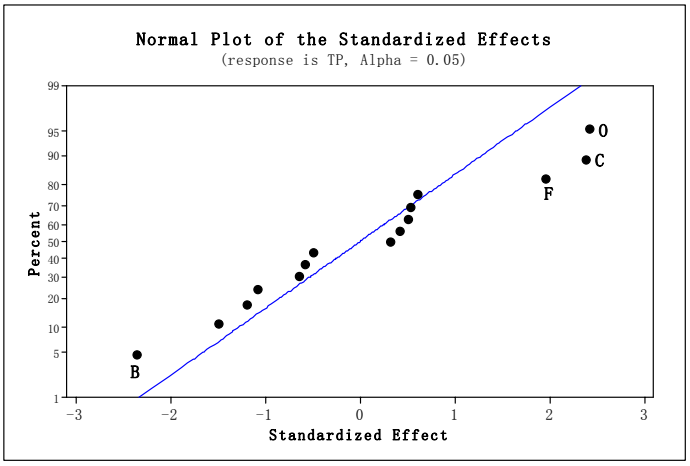

Figure 4.2 Normal Probability Plot for Tp

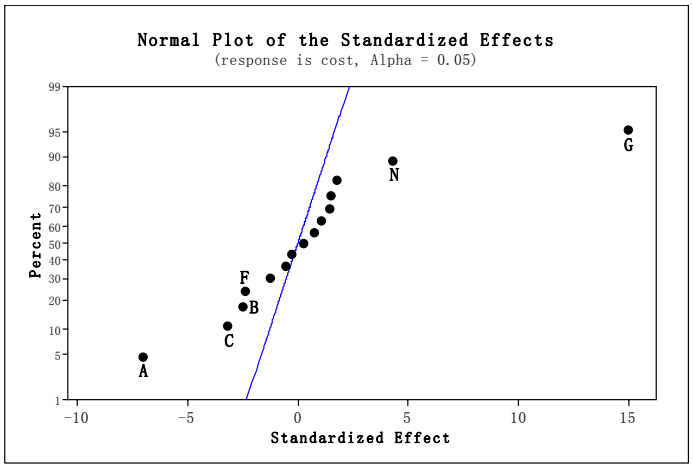

Figure 4.3 Normal Probability for Cost

4.4.3 Results for the comparison of models

Comparison of optimal cost between integrated model, preventive maintenance model and TBE-chart model can help to develop some insights into the situation when the integrated model should be used. Let $Cost_1^*$ and $Cost_2^*$ represent optimal cost for preventive maintenance model and TBE-chart model respectively. Optimal cost of integrated model $Cost^*$ is compared with $\min(Cost_1^*, Cost_2^*)$. If $Cost^* < \min(Cost_1^*, Cost_2^*)$, it is necessary to use integrated model. Otherwise, there is no need to use integrated model. The percentage of decrease in cost is calculated for each of the 32 runs.

$$\text{percentage of decrease in cost} = \frac{\min(Cost_1^*, Cost_2^*) - Cost^*}{Cost^*} \cdot 100\%$$

Among these 32 runs, 14 runs show that there is decrease in cost by using the integrated model. The percentage of decrease in cost ranges from 1.19% to 18.74%. For the remaining 18 runs, either preventive maintenance model or TBE-chart model is a better option. Two results can be drawn by examining values of 15 input parameters for 14 runs:

- When reactive maintenance cost after failure is very high compared with preventive maintenance cost and reactive maintenance cost after signal, it is better to use integrated model.
- When production in the out-of-control condition is very costly compared with production in the in-control condition, it is better to use integrated model.

The above two results are very intuitive. In practice, many processes satisfy the above conditions, and so the integrated model can be used widely.

4.4.4 Results for the analysis of shift and failure distribution

Throughout this chapter, Weibull distribution is used to model time to the occurrence of assignable cause and failure. The reason why Weibull distribution is chosen is that it is so versatile that it can not only represent Weibull distribution but also can represent exponential distribution by adjusting the value of shape parameter (McWilliams, 1989

and Dodson, 1994). In this part, the effect of shift and failure distributions' shape parameters on the expected cost per unit time for integrated model, TBE-chart model and preventive maintenance model is analyzed.

Table 4.2 Values for constant parameters

θ_a	va	θ	v	λ_0	λ_1	D_0	D_1	T_R	T_A	T_{PM}	C_R	C_A	C_P	A_0	γ_1	C
100		300		0.01	0.1	100	600	2	2	2	20000	5000	2400	200	0	5

Values for constant parameters are provided in Table 4.2. Results for the effect of shift and failure distributions' shape parameters on the expected cost per unit time for all models are summarized in Table 4.3 to Table 4.5 and Figure 4.4 to Figure 4.6.

Table 4.3 Effect of failure distribution's shape parameter on cost when va=1

va	v	integrated-cost	TBE-cost	PM-cost	Percentage of decrease
1	1.5	221.5052	222.5176	268.5301	0.46%
1	2	209.587	212.7549	257.9707	1.51%
1	2.5	203.43	207.7831	254.9335	2.14%
1	3	199.8887	204.9055	254.0131	2.51%
1	3.5	197.659	203.0937	253.728	2.75%
1	4	196.1549	201.88	253.6388	2.92%
1	4.5	195.0852	201.0289	253.6107	3.05%
1	5	194.2923	200.4096	253.6018	3.15%
1	5.5	193.6848	199.9457	253.599	3.23%
1	6	193.2081	199.5886	253.5981	3.30%

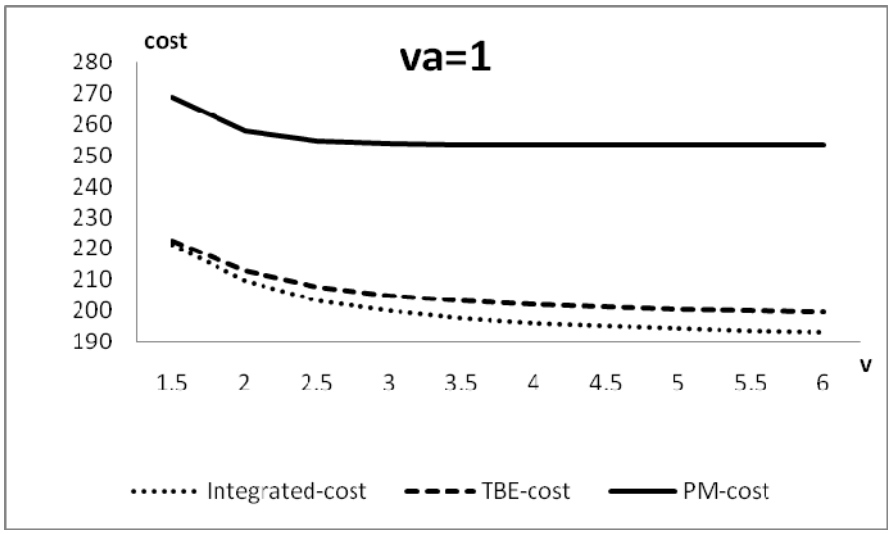

Figure 4.4: Effect of failure distribution's shape parameter on cost when va=1

Table 4.4 Effect of failure distribution's shape parameter on cost when va=2

va	v	integrated-cost	TBE-cost	PM-cost	Percentage of decrease
2	1.5	189.6231	213.3972	196.7537	3.76%
2	2	177.3112	202.9926	184.895	4.28%
2	2.5	172.7097	197.7069	180.9877	4.79%
2	3	170.8348	194.7081	179.6265	5.15%
2	3.5	170.0574	192.88	179.1401	5.34%
2	4	169.7345	191.7044	178.9643	5.44%
2	4.5	169.5988	190.9161	178.9003	5.48%
2	5	169.5414	190.3707	178.87	5.50%
2	5.5	169.5202	189.9825	178.8684	5.51%
2	6	169.5077	189.6983	178.8652	5.52%

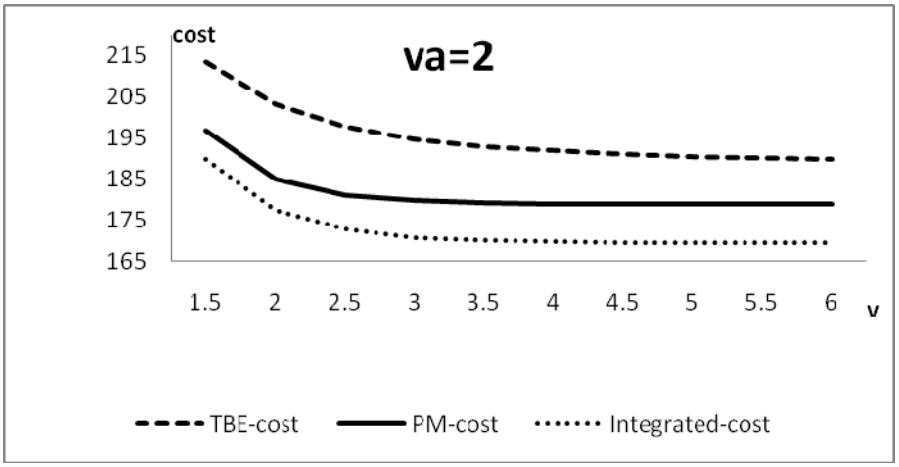

Figure 4.5: Effect of failure distribution's shape parameter on cost when va=2

Table 4.5 Effect of shift distribution's shape parameter on cost when v=2

va	v	integrated-cost	TBE-cost	PM-cost	Percentage of decrease
1.5	2	191.4416	205.6384	207.894	7.42%
2	2	177.3112	202.9926	184.895	4.28%
2.5	2	167.7748	191.1398	172.253	2.67%
3	2	161.513	190.3341	164.4529	1.82%
3.5	2	157.1984	189.8571	159.2433	1.30%
4	2	154.0795	189.5488	155.5584	0.96%
4.5	2	151.8237	189.3365	152.8364	0.67%
5	2	149.9845	189.184	150.7562	0.51%
5.5	2	149.1225	189.0702	149.1225	0%
6	2	147.8106	188.9826	147.8106	0%

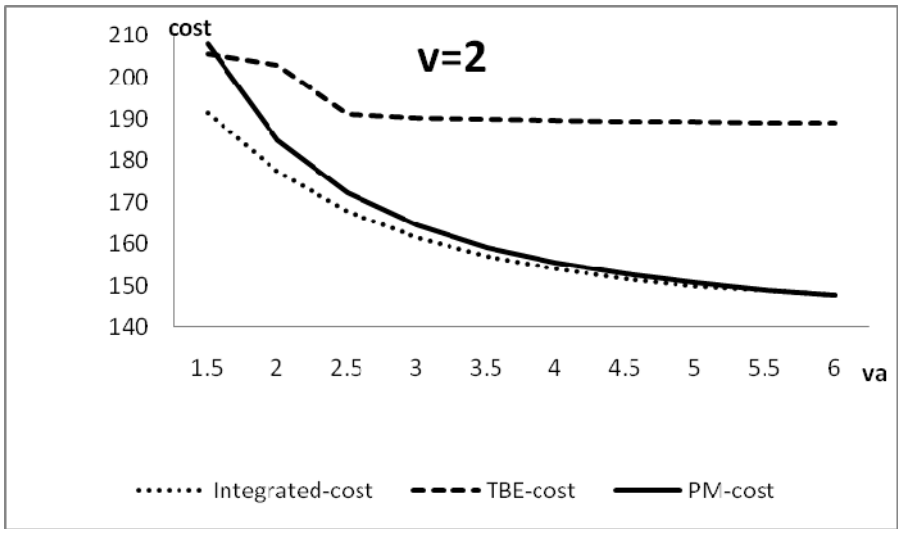

Figure 4.6 Effect of shift distribution's shape parameter on cost when v=2

Looking at Tables 4.3 to 4.5 and Figures 4.4 to 4.6, three conclusions can be drawn. Firstly, the failure distribution's shape parameter (v) and assignable cause's shape parameter (va) have a negative effect on the expected cost per unit time for integrated model, TBE-chart model and preventive maintenance model, which means cost will decrease as either v or va increases. Secondly, the expected cost per unit time for integrated model is the lowest no matter how the parameters change. When va=1(Figure 4.4), the expected cost per unit time for TBE-model is always smaller than the expected cost for preventive maintenance model. But when va=2(Figure 4.5), the result is opposite. When v=2 (Figure 4.6), the expected cost line for TBE-model intersects the expected cost line for preventive maintenance model at a point in the region of $1.5<va<2$. After the point of intersection, the expected cost per unit time for preventive maintenance model is smaller than the expected cost for TBE-model. Thirdly, the amount of decrease in cost (the last column in Tables 4.3, 4.4 and 4.5) by using integrated model increases as failure distribution's shape parameter (v) increases for both va=1 and va=2. This is because as v increases, the occurrence of failure becomes more and more predictable. But the amount of decrease in cost by using integrated model decreases as the shift distribution's shape

parameter (va) increases. This is because as va increases, more and more problems for the process are resulted from the assignable cause.

4.4.5 Numerical example

Suppose a quality engineer is considering what kind of monitoring actions should be used for a process with the parameters shown in Table 4.6. Now there are three options: pure preventive maintenance, pure TBE-chart and a combination of preventive maintenance and TBE-chart.

Table 4.6 Values for process parameters

θ_a	va	θ	v	λ_0	λ_1	D_0	D_1	T_R	T_A	T_{PM}	C_R	C_A	C_P	A_0	γ_1	C
100	2	600	4	0.01	0.1	100	600	2	2	2	20000	5000	2400	200	0	5

For each of the three options, optimal decision variables and corresponding cost can be calculated according to Sections 4.3 and 4.4.1. Results are summarized in Table 4.7.

Table 4.7 Summary of results

	Pure Preventive Maintenance	Pure TBE-Chart	Combination
T_p	41.7156		62.9375
α		0.447	0.3964
Cost	178.8697	188.6986	169.5831

Table 4.7 shows a combination of preventive maintenance and TBE-chart gives the lowest cost. The percentage of decrease in cost is 5.48%, which is significant. As a result, the engineer should use a combination of preventive maintenance and TBE-chart for this process.

4.5 Summary

In this chapter, an integrated model of TBE-chart and preventive maintenance is proposed. The implementing cost of control chart and preventive maintenance is considered and the cost minimization criterion is used to find the optimal values for decision variables. Both assignable cause and failure are considered, the occurrences of which are modeled by the versatile Weibull distribution. In the sensitivity analysis part, Design of Experiment (DOE) method is used to analyze the sensitivity of the integrated model's parameters on the expected cost per unit time and decision variables. Two alternative models, preventive maintenance model and TBE-chart model are provided for the purpose of comparison with the integrated model. The influence of shift and failure distributions on the expected cost per unit time is studied. Results of the sensitivity analysis help us to find the significant parameters for the expected cost per unit time and decision variables, identify the situations where integrated model is justifiable and know the effects of shift

and failure distributions' shape parameters on the expected cost per unit time for integrated model, TBE-chart model and preventive maintenance model. Finally, a numerical example is given to show the application of the integrated model.

Chapter 5 Statistical Design of Time-between-Events Control Chart System

Chapter 3 and chapter 4 work on improving the effectiveness of time-between-events chart. But both chapters focus on optimizing a single time-between-events chart. In this chapter, the scope is extended to time-between-events control chart system which consists of several time-between-events charts.

5.1 Introduction of time-between-events control chart system

The fabrication of a product usually goes through several process stages in series. The integration of all these stages constitutes a *multistage manufacturing system*. For example, in the manufacturing of a mechanical part, each stage usually pertains to the machining of a dimension. Some of the dimensions are critical to the overall quality of the product and the corresponding process stages have to be monitored by control charts. A *TBE control chart system* is the combination of all the TBE charts that are used to monitor the time between successive events at different process stages of a manufacturing system. Due to

the difference between production rates and other factors, some of the process stages may have more than one parallel stream or machine. In some applications, a single chart or a group chart is used to monitor the outputs from all the streams of a stage. However, in this chapter, a separate chart will be applied to the output of each individual stream. This scenario helps to detect and diagnose the out-of-control stream (Montgomery, 2005). Typically, the quality characteristics in parallel streams in a single stage have the same mean, standard deviation and target (Runger *et al*. 1996). Therefore, in this chapter, without loss of generality, a group of identical TBE charts (with the same rate of occurrences of the events) are used to monitor the quality characteristics of the parallel streams in a stage.

Even though many manufacturing systems consist of a series of process stages, the literature on the design of control chart systems that monitor multistage manufacturing systems is still limited. Many authors developed the group control chart for monitoring the output from multiple streams of a single stage (Runger *et al*. 1996; Nelson, 1986; Mortell and Runger, 1995). Peters and Williams (1987) developed a control scheme for a three-stage manufacturing system based on a lost-cost model. Williams and Peters (1989) presented an np-control scheme for a multistage production process. Several papers have

been published studying the multistage processes and the diagnosis problems (Ding *et al*. 2002; Zantek *et al*. 2002, 2006; Zhou *et al*. 2004). However, none of these approaches considered the multistage manufacturing processes as a whole and designed the charting parameters in an integrative and optimal manner.

Since the processes in different stages in a manufacturing system have different precision and other characteristics (e.g. rate of occurrences of the events, magnitudes of shifts), the importance of each stage is different. Currently the design of control chart assigns equal power to each stage without considering the quality dependence and importance of each stage. If all charts in a chart system are designed in an integrative and optimal manner, which means design the charts according to their importance and quality dependence with other charts, the performance of the chart system as a whole will be improved significantly. Wu *et al*. (2004b), Lam *et al*. (2005), Shamsuzzaman *et al*. (2005), Wu and Shamsuzzaman (2005) and Wu *et al*. (2007) developed integrated $\bar{x}$ and $\bar{x}\&S$ control chart systems for monitoring multistage manufacturing systems. Results show that the performance of charts has been improved significantly by designing them in an integrative and optimal manner. Although the good results achieved for designing charts in an integrative and optimal manner, to the best of the author's knowledge, the

integrated control chart system based on TBE data has not been reported in the literature yet. As it is introduced in Chapter 1, control chart based on TBE data which is called TBE chart is very effective for monitoring high-yield processes and is now widely used in practical. Since the manufacturing system usually consists of a series of process stages with quality dependence between each other, it would be very useful and necessary to develop the integrated control chart system based on TBE data.

This chapter presents statistical design of the control chart system for monitoring multistage manufacturing processes based on TBE data. It designs control limits of all the TBE charts in the system in an integrative and optimal manner. The false alarm rate is used as the constraint.

It is convenient to evaluate the performance of a control chart in terms of out-of-control Average Time to Signal, *ATS* (Montgomery, 2005). Following Woodall and Ncube (1985), the *ATS* value of the TBE control chart system is defined as the average time that one of the control charts in the chart system gives an out-of-control signal subsequent to any process in the manufacturing system going out of control. When any process is out of control, the control chart system should signal quickly (i.e. minimum out-of-control *ATS*).

But when the whole manufacturing system is in control, the chart system should produce large in-control Average Time to Signal, ATS_0 (i.e. minimum false alarms).

5.2 Optimization design of the TBE control chart system

5.2.1 Assumptions

A few assumptions are adopted in this chapter.

(1) Since the processes will often operate in the in-control condition for most of the time or relatively long periods (Montgomery, 2005), it is assumed that only one process is out of control at any moment in a manufacturing system. It is a conservative assumption, because, if more than one process are out of control simultaneously (e.g., due to some common mode failures), the out-of-control *ATS* will be even smaller compared with the *ATS* under this assumption (Wu *et al*. 2004b).

(2) The underlying probability distribution of the quality characteristic T_i (i.e. the mean time between successive events) in each process follows exponential distribution with known in-control rate of occurrence of the event $\lambda_{0,i}$ and out-of-control rate of occurrence of the event $\lambda_{\delta,i}$.

(3) The g_i parallel streams in the ith stage are assumed to have the same mean, standard deviation and target (Runger *et al*. 1996). Each of the g_i streams is monitored by a separate but identical control chart (with the same in-control and out-of-control parameters).

5.2.2 Input parameters

The design of the TBE chart system requires some additional input parameters as below.

s number of process stages in the control chart system

g_i number of streams or machines in the ith stage

$\lambda_{0,i}$ rate of occurrence of the event in the ith stage when the process is in-control

$\lambda_{\delta,i}$ rate of occurrence of the event in the ith stage when the process is out-of-control ($\lambda_{0,i} < \lambda_{\delta,i}$)

p_i probability of out-of-control occurrence in the ith stage

τ minimum allowable in-control ATS_0 of the chart system

V_i a vector $[v_1, v_2, \ldots]^T$ indicating the cause stage (upstream influencing stage) numbers. The rate of occurrence of the event in the *i*th stage is directly dependent on the rate of occurrences of the events in all of these cause stages.

Δ_i induced rate of occurrence of the event. It is the rate of occurrence of the event undergone by the *i*th stage due to the shifts in the rate of occurrence of the event (from its in-control value to the out-of-control value) of the cause stages. Δ_i is expressed as a function $f_i(\lambda_{v1}, \lambda_{v2}, \cdots)$ in terms of the output rate of occurrence of events of all cause stages.

Most of above parameters can be obtained from manufacturing records or can be estimated. The numbers s and g_i can be determined from the corresponding process planning.

The value of the parameter $\lambda_{0,i}$ at different stages can be estimated using the method of maximum likelihood. As an example, let $\tau_1, \tau_2, \ldots, \tau_r$ be the r observed values of time-between-events T_1 when the process in stage 1 is in-control. Then the maximum likelihood estimate of $\lambda_{0,1}$ in stage 1 is given by (Zhang *et al*. 2005),

$$\hat{\lambda}_{0,1} = r / \sum_{k=1}^{r} \tau_k \tag{5.1}$$

Similarly, the value of parameter $\lambda_{\delta,i}$ at different stages can be estimated from the data on the time-between-events T_i when the corresponding process is out-of-control.

The probability p_i that an out-of-control case occurs in the ith stage can be estimated from the historical data of the out-of-control cases. If such historical data are not available, p_i may be reasonably estimated by the following formula (Wu *et al*. 2004b).

$$p_i = g_i / \sum_{j=1}^{s} g_j \tag{5.2}$$

This means that the estimated probability that the out-of-control case happens in the ith stage is proportional to the number of parallel streams in this stage.

The specification τ is decided based on the trade-off between the false alarm rate and the detection power. If the cost of handling the false alarms is high, a larger τ should be used in order to reduce the false alarm frequency. However, a large τ may impair the effectiveness of the control chart at the same time. The actual in-control ATS_0 must be greater than or equal to τ. Finally, the vectors V_i and the formulae for Δ_i can be determined based on the information of design dimensioning and process planning (Wu *et al*. 2004b). The determination of V_i and Δ_i are explained in the section of example.

5.2.3 Optimization model

Based on the above parameters, the optimization design of the TBE control chart system can be conducted by using the following nonlinear optimization model.

$$\text{Objective function: } ATS = \text{minimum} \tag{5.3}$$

$$\text{Constraint function: } ATS_0 \geq \tau \tag{5.4}$$

$$\text{Design variables: } LCL_i, UCL_i \ (i = 1, 2, \ldots, s)$$

where, ATS is the average time to signal of the control chart system when any process in the manufacturing system is out of control (more specifically, when the rate of occurrence of the event in any process is shifted from its in-control value $\lambda_{0,i}$ to the out-of-control value $\lambda_{\delta,i}$). ATS_0 is the average time to signal when the whole system is in-control (or the rate of occurrences of the events of all processes remain in $\lambda_{0,i}$). The detailed formulae are derived in the next part.

The optimization algorithm optimizes the Lower and Upper Control Limits, LCL_i and UCL_i in order to minimize the out-of-control ATS of the chart system. These LCL_i and UCL_i are utilized to monitor the time-between-events T_i (or the rate of occurrence of the

event) at different stages in the manufacturing system. Upon each occurrence of the event, the observed value of T_i is plotted on the corresponding chart. If the plotted point falls between the LCL_i and UCL_i, it indicates that the process is in the state of statistical control and no action is warranted. If the plotted point falls below the LCL_i, it indicates that a possible decrease in the mean of T_i, or, equivalently, a possible increase in the rate of occurrence of the event. This means that the process may have deteriorated due to assignable cause and thus action should be taken to identify and remove it. If the point falls above the UCL_i, it indicates that a possible increase in the mean of T_i, or, equivalently, a possible decrease in the rate of occurrence of the event. This is an important indication of possible process improvement. If this happens, the management should look for possible causes for the improvement. If the causes for this are discovered, then action should be taken to maintain them.

5.2.4 Derivation of *ATS*

Calculation of the in-control ATS_0

In a single time unit, the probability that a control chart in the *i*th stage produces a false alarm is approximately equal to $\alpha_i\lambda_{0,i}$, where, α_i is the type I error probability and $\lambda_{0,i}$ is

the in-control rate of occurrence of the event (i.e. the in-control mean time between two successive events is equal to $1/\lambda_{0,i}$). The type I error probability α_i is given by

$$\alpha_i = 1 - \exp(-\lambda_{0,i} LCL_i) + \exp(-\lambda_{0,i} UCL_i) \tag{5.5}$$

Now, the probability that a control chart in the *i*th stage does not produce a false alarm is equal to $(1-\alpha_i\lambda_{0,i})$. Since each of the g_i streams in the *i*th stage runs a duplicate of the *i*th control chart, therefore, the probability P_0 that the whole control chart system generates a false alarm in a unit time is

$$P_0 = 1 - \prod_{i=1}^{s}\left(\prod_{j=1}^{g_i}\left(1-\alpha_i\lambda_{0,i}\right)\right) = 1 - \prod_{i=1}^{s}(1-\alpha_i\lambda_{0,i})^{g_i} \tag{5.6}$$

Finally,

$$ATS_0 = 1/P_0 \tag{5.7}$$

Calculation of the out-of-control *ATS*

Suppose that one of the g_j streams in the *j*th stage ($1 \le j \le s$) is out of control (i.e. the rate of occurrence of the event in this stage has been shifted from its in-control value $\lambda_{0,j}$ to

the out-of-control value $\lambda_{\delta j}$). Now, the probability w_i that control charts in the ith stage do not give a signal in a unit time is calculated differently for the following three cases.

Case 1 ($i = j$, the out-of-control stage)

The probability β_j that the control chart monitoring the out-of-control stream j fails to give a signal in a unit time is

$$\beta_j = 1 - \lambda_{\delta,j}(1 - \exp(-\lambda_{\delta,j} LCL_j) + \exp(-\lambda_{\delta,j} UCL_j)) \tag{5.8}$$

Thus, the probability that none of the charts in the jth stage gives a signal in a unit time on the condition that exactly one of the g_j streams is out-of-control and all other streams are in-control is

$$w_j = (1 - \alpha_j \lambda_{0,j})^{g_j - 1} \beta_j \tag{5.9}$$

Case 2 ($i \neq j$, and stage i is independent of stage j)

The probability (in a unit time) that a duplicate of the ith chart gives a signal due to the type I error can be approximated by $\alpha_i \lambda_{0,i}$. Thus, the probability that none of the charts in the ith stage gives a signal in a unit time is

$$w_i = (1 - \alpha_i \lambda_{0,i})^{g_i} \tag{5.10}$$

Case 3 ($i \neq j$, but stage i depends directly or indirectly on stage j)

Each of the g_i streams of stage i will undergo an induced rate of occurrence of the event as

$$\lambda_i = \Delta_i = f_i(\lambda_{v1}, \lambda_{v2}, ...) \tag{5.11}$$

where $(\lambda_{v1}, \lambda_{v2}, \cdots)$ are the output rate of occurrences of the events of the cause stages (or the immediate upstream stages having impact on the ith stage). The cause stages can be found from the dependent relationship vector V_i. Sometimes, a cause stage of the ith stage is, by itself, influenced by another stage. Consequently, λ_i has to be determined by a recursive procedure. Moreover, if a cause stage is the out-of-control stage j, the output rate of occurrence of the event from this cause stage (or in other words, the induced rate of occurrence of the event received by stage i from the out-of-control stage j) is,

$$\lambda_i = \frac{\lambda_{\delta,j} + \lambda_{0,j}(g_j - 1)}{g_j} \tag{5.12}$$

This is because that one, and only one, of the g_j streams in the jth stage goes out-of-control (having in-control rate of occurrence of the event $\lambda_{0,j}$ and out-of-control rate of occurrence of the event $\lambda_{\delta j}$). Then, the resultant rate of occurrence of the events of stage i is

$$\lambda_i' = \lambda_i + \lambda_{0,i} \tag{5.13}$$

Thus, the probability that none of the charts in the *i*th stage gives a signal in a unit time can be evaluated by

$$w_i = (\beta_i)^{g_i} = (1 - \lambda_i'(1 - \exp(-\lambda_i' LCL_i) + \exp(-\lambda_i' UCL_i)))^{g_i} \tag{5.14}$$

Combining all of the three cases, the probability that an out-of-control signal is produced in a unit time in stage *j* is calculated as follows.

$$q_j = 1 - \prod_{i=1}^{s} (w_i \mid \text{stage } j \text{ is out-of-control}) \tag{5.15}$$

Therefore, given that one process in the *j*th stage goes out-of-control, the value of the out-of-control *ATS* is

$$ats_j = 1/q_j \tag{5.16}$$

Since an out-of-control case may occur in any of the *s* stages, the final *ATS* for the control chart system is

$$ATS = \sum_{j=1}^{s} (ats_j \cdot p_j) \tag{5.17}$$

where, p_j is the probability that the out-of-control case takes place in the *j*th stage.

In the control chart system, a chart monitoring a process that is currently in control may produce an out-of-control signal (a misleading signal). It is mainly because of the induced rate of occurrence of the event discussed in case 3. Therefore, whenever a control chart produces an out-of-control signal, not only must the process being monitored by this chart, but also all upstream processes having direct or indirect impacts on this process be investigated. More advanced diagnostic methods can be found in many references (Ding *et al*. 2002; Zantek *et al*. 2002). The type I error may also generate misleading signal, but it is negligible.

5.2.5 Optimization search

In the actual optimization search, design variables LCL_i and UCL_i are replaced by the corresponding type I error probabilities $\alpha_1, \alpha_2, \ldots, \alpha_s$ associated with the s control charts. The variable α_i is the probability that the ith control chart produces an out-of-control signal when the ith process is in fact in control.

$$LCL_i = -\ln(1-0.5\alpha_i)/\lambda_{0,i} \qquad UCL_i = -\ln(0.5\alpha_i)/\lambda_{0,i} \tag{5.18}$$

Optimizing α_i is equivalent to optimizing LCL_i and UCL_i, as there is a one-to-one relationship between them. The parameter α_i is easier to handle during the optimization search, because it has finite lower bound (0) and upper bound (1) for the search and that a

simple equation among α_1, α_2, …, α_s (Eq. 5.19) can be established easily (Wu *et al*. 2004b).

$$\alpha_i = \frac{1}{\lambda_{0,i}}\left[1-\left(\frac{1-1/\tau}{\prod_{j=1, j\neq i}^{s}(1-\alpha_j\lambda_{0,j})^{g_j}}\right)^{1/g_i}\right] \tag{5.19}$$

This equation is used to determine the range of possible α_i value in the ith level search.

The optimization design can be carried out by using any software for constrained nonlinear programming. In our implementation, a dynamic search algorithm proposed by Wu *et al*. (2004b) is employed. In this algorithm, the optimal values of α_i of the first (s –1) control charts are searched step by step in (s –1) levels, using the same step size $d\alpha$. The last α_s is finally determined so that the resultant ATS_0 is exactly equal to the specified τ (i.e. satisfies constraint (Eq.5.4)). The overall optimization search is depicted in Fig. 5.1.

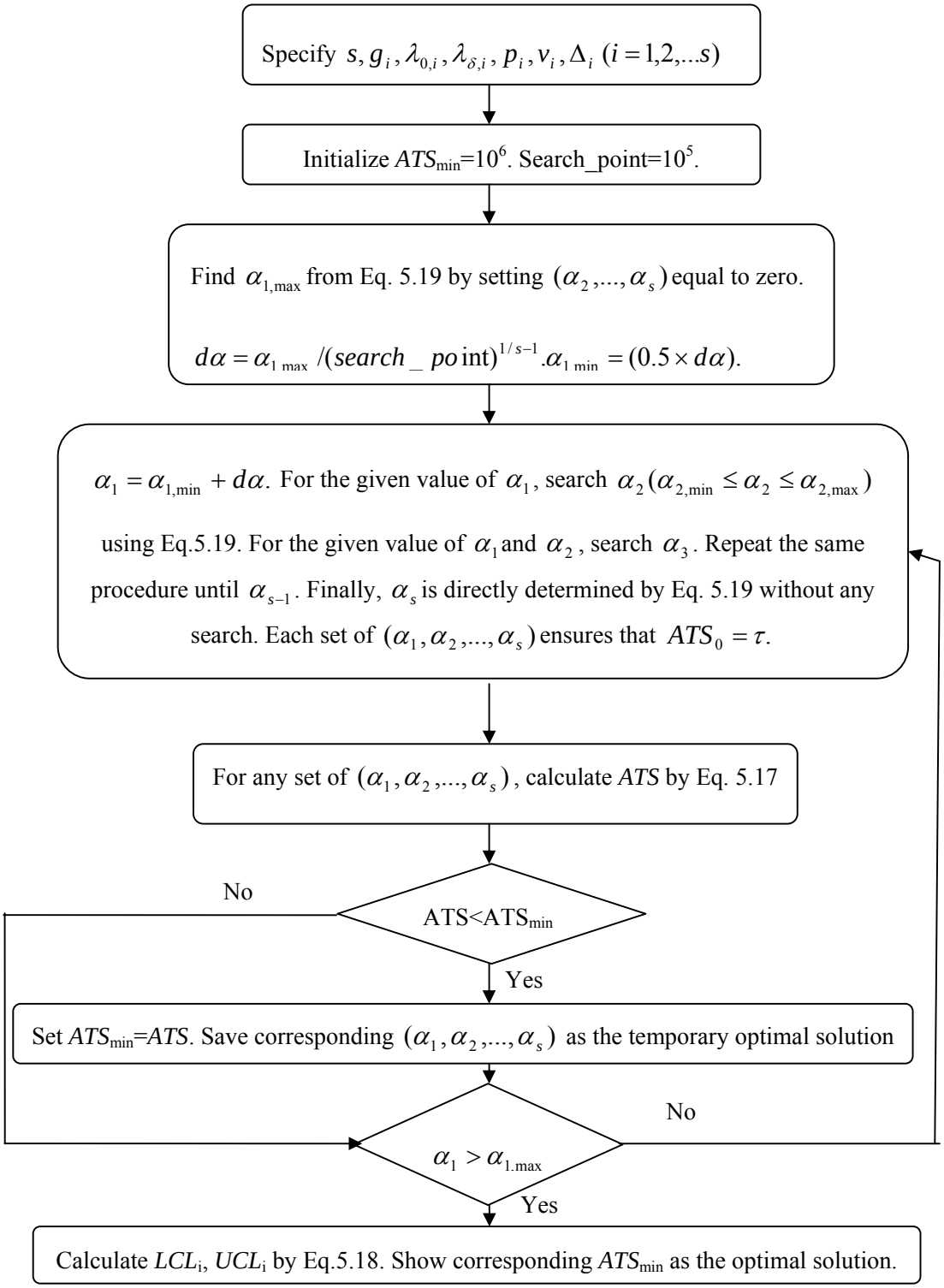

Fig. 5.1 Optimization algorithm

A computer program in C language has been developed to carry out the optimization design. The value of the step size $d\alpha$ is decided so that the total number of search points is always limited to 10^5 regardless of the number of α_i. Usually an optimal solution is obtained in less than one CPU second using a personal computer.

5.3 Performance analysis

This section compares the performance (measured by the out-of-control ATS) of the following two control chart systems.

1. Traditional chart system. In this system, the αi values of the control charts are made equal and set at 0.0027 in each stage of the chart system.

2. Integrated chart system. In this system, the α_i values (or equivalently the control limits) of the control charts are determined by the optimization design proposed in this chapter.

This section also investigates the effects of different input parameters on the performance of the chart systems through sensitivity study. In both studies, the in-control ATS_0 of the traditional chart systems is calculated by Eq. 5.7 and set as constraint in the optimization process, that is, both of the chart systems (integrated chart system and traditional chart

system) produce the same in-control ATS_0 (= τ) in each of the studies. Finally, the design of the integrated chart system is illustrated through an example.

5.3.1 Comparative study

The performance of the control chart systems is examined over one thousand cases. For each of the thousand cases, the value of the input parameter *s* (i.e. the number of stages in the manufacturing system) is first decided randomly. Then the values of the other four parameters at each of the *s* stages are generated, also randomly, within the following ranges.

s [2, 10]

g_i [1, 3]

$\lambda_{0,i}$ [0.001, 0.009]

$\lambda_{\delta,i}$ [0.01, 0.09]

p_i [0.1, 0.9]

The dependence between the stages (i.e. the vectors V_i and the induced failure rate functions Δ_i) is also randomly decided. Each stage may have up to two dependent stages and Δ_i is equal to either ($+\lambda\nu i$) or ($-\lambda\nu i$).

For each of the thousand cases, the traditional chart system and the integrated chart system are designed. The following response is investigated for each case.

$$R = ATS_{\text{integrated}} / ATS_{\text{traditional}} \tag{5.20}$$

Obviously, if the value of R is less than one, the integrated chart system will outperform the traditional system in a particular case in terms of the out-of-control ATS, and vice versa.

The execution of the comparative study in each of the thousand cases is summarized in the following steps.

1. Decide the input parameters (s, g_i, $\lambda_{0,i}$, $\lambda_{\delta,i}$, p_i, V_i, Δ_i) values randomly within the ranges prescribed above.

2. Design the traditional chart system.

    2.1 Calculate in-control ATS_0 of the chart system by Eq. 5.7.

    2.2 Calculate out-of-control ATS of the chart system by Eq. 5.17.

3. Design the integrated chart system.

    3.1 Set $\tau = ATS_0$.

3.2 Identify the optimal set of (α_1, α_2, …, α_s) and corresponding LCL_i, UCL_i (i = 1, 2, …, s) and out-of-control ATS following the optimization search presented in Fig.5.1.

4. Calculate ratio *R* by Eq. 5.20.

Table 5.1 displays the *R* (under column (5)) values of the two schemes of the chart systems in the first 4 cases. It is observed that in each of the 4 cases, the out-of-control ATS is considerably reduced by the integrated chart system compared to the traditional chart system.

The grand average $\overline{R}$ of the response *R* over the thousand runs is 0.81882. The value of $\overline{R}$ indicates that, from an overall viewpoint (considering different combinations of s, g_i, $\lambda_{0,i}$, $\lambda_{\delta,i}$ and p_i), the integrated chart system reduces the out-of-control ATS by about 18% compared to the traditional chart system. This improvement is achieved by the optimization of the charting parameters LCL_i and UCL_i, suggesting that the integrated design algorithm is an effective method to achieve better results in SPC.

Table 5.1 Comparative study

(1) Case No.		(2) Input parameters				(3) $ATS_{integrated}$	(4) $ATS_{traditional}$	(5) Ratio R
	s	$\lambda_{0,i}$	$\lambda_{\delta,i}$	p_i	g_i			
1	7	0.0080	0.051	0.21	1	269.9	404.6	0.6670
		0.0031	0.054	0.01	1			
		0.0079	0.067	0.28	1			
		0.0073	0.071	0.22	1			
		0.0042	0.038	0.03	2			
		0.0021	0.066	0.09	1			
		0.0048	0.077	0.16	1			
2	3	0.0048	0.019	0.31	2	1821.6	2191.1	0.8313
		0.0079	0.089	0.29	2			
		0.0035	0.087	0.40	1			
3	9	0.0048	0.023	0.15	3	1613.6	1798.3	0.8973
		0.0040	0.082	0.23	1			
		0.0015	0.067	0.03	2			
		0.0028	0.088	0.12	1			
		0.0044	0.030	0.07	1			
		0.0024	0.028	0.06	1			
		0.0089	0.067	0.02	1			
		0.0053	0.032	0.22	1			
		0.0014	0.021	0.10	2			
4	5	0.0059	0.074	0.35	2	851.9	938.3	0.9079
		0.0057	0.088	0.33	2			
		0.0050	0.022	0.08	1			
		0.0054	0.066	0.12	1			
		0.0066	0.071	0.12	3			

5.3.2 Sensitivity study

The effects of four input parameters (g_i, $\lambda_{0,i}$, $\lambda_{\delta,i}$ and p_i) on the performance of the control chart systems are investigated in this section. Each of these parameters has a low value, a nominal value and a high value, as shown below.

Parameter	Low	Nominal	High
g_i	1	3	5
$\lambda_{0,i}$	0.01	0.03	0.05
$\lambda_{\delta,i}$	0.03	0.06	0.09
p_i	0.1	0.3	0.6

The nominal value of the probability of out-of-control cases p_i is rounded down to ensure that the sum of the pi values for all stages is equal to 1.

The performance of a three-stage manufacturing system is studied for four different cases. It is assumed that stage 2 is dependent on stage 1, and stage 3 is dependent on stage 2. Therefore, if any out-of-control case occurs in stage 1, stage 2 will be affected directly and stage 3 will be influenced indirectly through the change in stage 2. On the other hand,

if stage 2 goes out-of-control, only stage 3 will be affected. In each case, all the parameters take their nominal values in both stages, except that one selected parameter (called the active parameter) takes its low value in stage 1, nominal value in stage 2, and high value in stage 3. For example, in case one, the first parameter g_i is designated as the active parameter. Therefore,

$g_1 = 1, g_2 = 3, g_3 = 5$

$\lambda_{0,1} = \lambda_{0,2} = \lambda_{0,3} = 0.03, \lambda_{\delta,1} = \lambda_{\delta,2} = \lambda_{\delta,3} = 0.06, p_1 = p_2 = p_3 = 0.3$

In each of the four cases, the values of the input parameters (s, g_i, $\lambda_{0,i}$, $\lambda_{\delta,i}$, p_i, V_i, Δ_i) values are first decided according to the above mentioned descriptions. Then the two control chart systems, i.e. the integrated chart system and the traditional chart system are designed (following the steps 2 to 4 in the comparative study).

The R values for all four cases are listed in Table 5.2 under column (6). It can be observed that in all of the four cases, the integrated chart system achieves obvious improvement in effectiveness compared to the traditional system. It is especially the case if any of the three parameters (g_i, $\lambda_{0,i}$ or p_i) has different values in the three stages, the integrated control chart system will have a substantially smaller ATS than that of the traditional system. The performance of the integrated chart system is relatively less

sensitive to the parameter $\lambda_{\delta,i}$. From Table 5.2, some general guidelines about how to allocate the power of the SPC system to different stages can be given. First, more power should be given to the stage which has the highest probability to be out of control. Second, more power should be given to the stage which has larger process shift. Third, more power should be given to the stage which has more streams.

The actual *R* value would differ for different systems and circumstances. However, it is believed that the integrated control chart system would be effective in general and beneficial to many real systems. The reason is that, in any manufacturing system, the influential parameters would be in general different among several stages.

Table 5.2 Sensitivity study

(1) Case No.	(2) Active parameter			(3) Optimal α_i			(4) $ATS_{integrated}$	(5) $ATS_{traditional}$	(6) Ratio *R*
				α_1	α_2	α_3			
1	g_1 = 1	g_2 = 3	g_3 = 5	0.00003841	0.00003841	0.00482912	587.654	667.638	0.8802
2	$\lambda_{\delta,1}$ = 0.03	$\lambda_{\delta,2}$ = 0.06	$\lambda_{\delta,3}$ = 0.09	0.00000776	0.00000776	0.00489042	906.335	911.668	0.9942
3	$\lambda_{0,1}$ = 0.01	$\lambda_{0,2}$ = 0.03	$\lambda_{0,3}$ = 0.05	0.01498123	0.00089036	0.00136648	853.457	1092.642	0.7811
4	p_1 = 0.1	p_2 = 0.3	p_3 = 0.6	0.00002725	0.00002725	0.01718253	387.357	587.472	0.6594

5.3.3 An example

A part is machined in a four-stage manufacturing system. Stage 1 and stage 2 of the manufacturing system turn surface 1 and surface 2 (datum: surface zero) of the part, respectively; stage 3 drills the hole (datum: surface 2); and stage 4 mills the slot (datum: surface 2). Since the process in stage 4 is much more time consuming, two machines are used in parallel. The four dimensions that are formed at the four stages are monitored by TBE charts. The specifications of the system are summarized below.

Number of stages in the system: $s = 4$

Number of streams: $g_1 = g_2 = g_3 = 1$, $g_4 = 2$

In-control rate of occurrence of the event:

$\lambda_{0,1} = 0.01$, $\lambda_{0,2} = 0.03$, $\lambda_{0,3} = 0.02$, $\lambda_{0,4} = 0.04$

Out-of-control rate of occurrence of the event:

$\lambda_{\delta,1} = 0.05$, $\lambda_{\delta,2} = 0.06$, $\lambda_{\delta,3} = 0.04$, $\lambda_{\delta,4} = 0.06$

The probabilities p_i of the out-of-control occurrences are estimated from historical records, which show that the numbers of out-of-control cases occurring in each of the four stages are 2, 3, 5 and 4, respectively. Therefore,

$$p_1 = 2/(2+3+5+4) = 0.143$$
$$p_2 = 3/(2+3+5+4) = 0.214$$
$$p_3 = 5/(2+3+5+4) = 0.357$$
$$p_4 = 4/(2+3+5+4) = 0.286$$

From the description of the production planning it is revealed that stage 3 and stage 4 are directly dependent on stage 2. Therefore, the dependent relationship vectors V_i and the formulae for Δ_i are determined as follows (Wu *et al*. 2004b).

$V_3 = [2]^T, \quad V_4 = [2]^T$

$\Delta_3 = \lambda_2, \quad \Delta_4 = \lambda_2$

So, if stage 2 goes out of control (i.e. the rate of occurrence of the event in this stage is shifted from its in-control value $\lambda_{0,2}$ (= 0.03) to the out-of-control value $\lambda_{\delta,2}$ (= 0.06)), stages 3 and 4 will be affected directly (i.e. the rate of occurrences of the events in these stages will be changed). According to Eq. 5.12, the induced rate of occurrences of the events received by stages 3 and 4 are,

$$\Delta_3 = \lambda_3 = (\lambda_{\delta,2} + \lambda_{0,2}(g_2 - 1))/g_2 = (0.06 + 0.03(1-1))/1 = 0.06$$

$$\Delta_4 = \lambda_4 = (\lambda_{\delta,2} + \lambda_{0,2}(g_2 - 1))/g_2 = (0.06 + 0.03(1-1))/1 = 0.06$$

Originally, a traditional TBE chart system that adopts the same type I error probability of 0.0027 for all TBE charts is used to monitor the manufacturing processes. As a result, the in-control ATS_0 of the chart system is equal to 2645.86 (Eq. 5.7).

In order to improve the effectiveness of the chart system, an integrated chart system is designed (following the optimization algorithm presented in Fig. 5.1). The QA (Quality Assurance) manager requires that the false alarm rate of the integrated chart system be maintained at the same level as for the traditional system. Thus, τ is specified as 2645.86. The computer program works out the integrated chart system for this example in 0.031 CPU second in a personal computer (Pentium IV, CPU 2.40 GHz). The results are listed below (the Center Line CL_i is computed by $CL_i = \ln(2)/\lambda_{0,i}$).

Stage 1: LCL = 0.38752, CL = 69.31472, UCL = 555.50880 (α = 0.0077355)

Stage 2: LCL = 0.00679, CL = 23.10491, UCL = 283.31757 (α = 0.0004071)

Stage 3: LCL = 0.35751, CL = 34.65736, UCL = 247.20895 (α = 0.0142495)

Stage 4: LCL = 0.00053, CL = 17.32868, UCL = 268.87495 (α = 0.0000427)

ATS_0 = 2645.86, ATS = 1501.52

It can be observed that, while both the integrated chart system and the traditional chart system have the same ATS_0 (= τ = 2645.86) value, the out-of-control ATS of the integrated system is 1501.52 and that of the traditional system is 1936.17. It means that the out-of-control ATS of the integrated system has been reduced by about 22% compared to the traditional system. This is a significant improvement in effectiveness.

In the optimal solution, majority of the type I error probability (or the power) is allocated to stage 3. The reason is that, this stage has relatively small allowable shift in the rate of occurrence of the event and high probability of out-of-control occurrences.

5.4 Summary

This chapter develops the integrated TBE control chart system for monitoring multistage manufacturing processes. It is found that, by properly allocating the power among the individual charts based on the values of the influential parameters, the effectiveness of the system as a whole can be significantly improved. Therefore, the product quality is further guaranteed.

Few input parameters that can be obtained from manufacturing information and records are required for the optimization design of the integrated TBE control chart system.

Furthermore, the use of the integrated control chart system will not in any sense increase the difficulties for the shop floor operators to run and understand the control charts, because the control charts in the integrated system are almost the same as that in the traditional system, except that the positions of the control limits have been adjusted.

The design algorithm of the integrated control chart system can be easily computerized. The design of a chart system has to be conducted only once, and the resultant system can be used continuously until the process parameters have changed. It is also noted that the actual model, layout, scenario and interactions between stages of a particular system may be somewhat different from the model discussed here, but the proposed algorithm will be generally applicable. The procedures and formulae can be easily modified to cope with different models.

Chapter 6 Economic Design of Time-between-Events Control Chart System

In Chapter 5 the integrated TBE control chart system for monitoring multistage manufacturing processes is developed. Results show that by properly allocating the power among the individual charts based on the values of the influential parameters, the effectiveness of the system as a whole can be significantly improved. But in Chapter 5 only the statistical properties of the control chart system are considered, such as *ATS*. However, the implementation of the TBE chart system has significant economic impact as it involves various costs, such as the cost incurred by the occurrence of events, cost of false alarms, cost of locating and removing the assignable cause and cost of allowing the system to operate in an out-of-control state. Therefore, it is quite reasonable to take the economic issues into account when designing the TBE chart system.

This chapter presents an economic design of the integrated control chart system for monitoring multistage manufacturing processes based on TBE data. It designs control

limits of all the TBE charts in the system in an integrative and optimal manner in order to maximize the profit associated with the implementation of the SPC system. The false alarm rate is used as the constraint.

6.1 Economic design of the TBE control chart system

6.1.1. Assumptions

Other than the three assumptions listed in Chapter 5, section 5.2.1, two more assumptions are needed for this chapter.

(1) There is a single assignable cause shifting the system from an in-control state to the out-of-control state. The occurrence rate of the assignable cause, $\lambda_{a,i}$ in each stage is independent and known (Zhang *et al.*, 2005).

(2) The system continues operating during searching for possible assignable cause and the expected time to locate and remove the assignable cause in each stage is known.

6.1.2. Input parameters

The input parameters for this chapter can be divided into two parts: process parameters and cost parameters. Process parameters are just the input parameters in Chapter 5. The estimation method for process parameters is the same as that introduced in Chapter 5.

Cost parameters are listed in the nomenclature part at the beginning of this thesis. Cost parameters B_0, B_1, A_0, A_i and C can be estimated from the data on the in-control and out-of-control cases and the information obtained from financial department. Admittedly, there are some difficulties in estimating the cost parameters. However, a higher degree of accuracy in estimating the cost parameters may not be essential as the errors associated with the estimation of the cost parameters are negligible; results from Sensitivity Study II will show this.

6.1.3. Optimization model

Based on the above parameters, economic design of the TBE control chart system can be conducted by using the following nonlinear optimization model.

$$\text{Objective function: } O = \text{maximum} \tag{6.1}$$

$$\text{Constraint function: } ATS_0 \geq \tau \tag{6.2}$$

$$\text{Design variables: } LCL_i \ (i = 1, 2, \ldots, s)$$

Control charts are most often used to detect deterioration in process quality (Reynolds and Glosh, 1981). Therefore, for simplicity, only the lower control limit LCL_i is

considered in this chapter. However, the requirement for both lower and upper control limits (LCL_i and UCL_i) can easily be fulfilled by a simple modification to the proposed model. The proposed TBE chart system is utilized to monitor the time-between-events T_i (or the rate of occurrence of the event) at different stages in the manufacturing system. Upon each occurrence of the event, the observed value of T_i is plotted on the corresponding chart. If the plotted point falls below the LCL_i, it indicates a possible decrease in the mean of T_i, or, equivalently, a possible increase in the rate of occurrence of the event. This means that the process may have deteriorated due to the assignable cause and thus action should be taken to identify and remove it. If the plotted point falls above the LCL_i, it indicates that the process is in the state of statistical control and no action is needed. The larger value of T_i, the better it is. The reason is that the larger value of T_i indicates a possible increase in the mean of T_i, or, equivalently, a possible decrease in the rate of occurrence of the event. This means that the process may have improved.

The design algorithm optimizes LCL_i in order to maximize the expected profit per unit time, O in an operational cycle. The calculation of the profit O will be described shortly. The calculation of the in-control ATS_0 and the out-of-control Average Time to Signal ATS is the same as in Chapter 5, section 5.2.4, so there is no need to repeat it here.

6.1.4. Calculation of expected profit per unit time, *O* in an operational cycle

An operational cycle is defined as the time period from the startup or re-instatement of the system until the location and removal of the assignable cause (Zhang *et al*., 2005). That means, the operational cycle consists of the expected in-control time, t_1 (the expected time from the startup of the cycle to the occurrence of the assignable cause), the expected out-of-control time, t_2 (the expected time from the occurrence of the assignable cause to the detection of the lack of control), and the expected assignable cause location and removal time, t_3 (the time from the detection of the lack of control to the location and removal of the assignable cause).

Expected length of an operational cycle, L

The system is assumed to be in-control if all the stages are in-control. The time of occurrence of the assignable cause for the *i*th stage is assumed to follow an exponential distribution with parameter $\lambda_{a,i}$. The random variable X denotes the in-control time of the whole system. Then the probability that the variable X takes on a value larger than or equal to y is,

$$\begin{aligned}\Pr(X \geq y) &= \Pr(X_1 \geq y, X_2 \geq y, \ldots X_s \geq y) \\ &= \prod_{i=1}^{s} \Pr(X_i \geq y) = \prod_{i=1}^{s} \exp(-\lambda_{a,i} \cdot y) = \exp\left(-\sum_{i=1}^{s} \lambda_{a,i} \cdot y\right)\end{aligned} \tag{6.3}$$

Therefore,

$$t_1 = 1/\sum_{i=1}^{s} \lambda_{a,i} \tag{6.4}$$

The system is assumed to be out-of-control if any of the process stage is out-of-control, and the state of out-of-control will continue until a chart gives a signal. Thus, the expected out-of-control time for the whole system is equal to the out-of-control *ATS* of the system.

$$t_2 = ATS \tag{6.5}$$

Since the expected time to locate and remove an assignable cause for the *i*th stage is d_i and the probability that this stage is out of control is p_i, then, the expected time to locate and remove an assignable cause for the whole system in an operational cycle is,

$$t_3 = \sum_{i=1}^{s} d_i p_i \tag{6.6}$$

Thus, the expected length of an operational cycle, *L* is,

$$L = t_1 + t_2 + t_3 = 1/\sum_{i=1}^{s} \lambda_{a,i} + ATS + \sum_{i=1}^{s} d_i p_i \tag{6.7}$$

Expected profit in an operational cycle, P

The expected number of false alarms, M can be estimated from the in-control ATS_0 and the expected in-control time t_1 of the system.

$$M = t_1 / ATS_0 \tag{6.8}$$

When the system is in-control, the expected time to the occurrence of an event for the ith stage is $1/\lambda_{0,i}$. Thus the expected number of events, m_i can be calculated by

$$m_i = \frac{t_1}{1/\lambda_{0,i}} \cdot g_i = \frac{\lambda_{0,i} \cdot g_i}{\sum_{i=1}^{s} \lambda_{a,i}} \tag{6.9}$$

When the system is out-of-control, the expected time to the occurrence of an event would be different for different stages depending on which stage goes out-of-control and the interdependency between the process stages. Suppose the ith stage goes out-of-control (detailed descriptions are given in the calculation of the out-of-control ATS in Chapter 5, section 5.2.4), then the expected number of events, n_i observed during the occurrence of the assignable cause to the detection of the out of control condition can be calculated by

$$n_i = p_i \left\{ \frac{t_2}{1/\lambda_{\delta,i}} + \frac{t_2}{1/\lambda_{0,i}} (g_i - 1) \right\} + \sum_{j=1, j\neq i}^{s} p_j \frac{t_2}{1/\lambda'_j} g_j \tag{6.10}$$

$$\lambda'_j = \begin{cases} \lambda_{0,j} + \lambda_j & \text{if stage } j \text{ depends on the out - of - control stage } i \\ \lambda_{0,j} & \text{if stage } j \text{ does not depend on the out - of - control stage } i \end{cases}$$

where, λ_j is the induced rate of occurrence of the event received by stage *j* from the out-of-control stage *i* and can be approximated by Eq.5.12 in Chapter 5. Eq. 6.10 can be rewritten as,

$$n_i = p_i \cdot ATS \cdot \lambda_{\delta,i} + p_i \cdot ATS \cdot \lambda_{0,i}(g_i - 1) + \sum_{j=1, j\neq i}^{s} p_j \cdot ATS \cdot \lambda_j' \cdot g_j \qquad (6.11)$$

Now, the expected profit in an operational cycle, *P* can be calculated by (Duncan, 1956),

$$P = B_0 \cdot 1/\sum_{i=1}^{s} \lambda_{a,i} + B_1 \cdot \left(ATS + \sum_{i=1}^{s} d_i p_i \right) - A_0 \cdot M - \sum_{i=1}^{s} p_i A_i - C \cdot \left(\sum_{i=1}^{s} m_i + \sum_{i=1}^{s} n_i \right) \qquad (6.12)$$

Since a renewal reward process is considered (Ross, 1970), the average profit per unit time in an operational cycle, *O* can be calculated by,

$$O = P \div L = \left[B_0 \cdot 1/\sum_{i=1}^{s} \lambda_{a,i} + B_1 \cdot \left(ATS + \sum_{i=1}^{s} d_i p_i \right) - A_0 \cdot M - \sum_{i=1}^{s} p_i A_i - C \cdot \left(\sum_{i=1}^{s} m_i + \sum_{i=1}^{s} n_i \right) \right] \div \left[1/\sum_{i=1}^{s} \lambda_{a,i} + ATS + \sum_{i=1}^{s} d_i p_i \right] \qquad (6.13)$$

6.1.5. Optimization algorithm

The optimization algorithm is similar to the algorithm in Chapter 5. But as the current optimization model has changed, the optimization algorithm is repeated here with some modifications.

A dynamic search algorithm (Wu *et al*., 2004b) is employed to find the optimum value of the design variable LCL_i (i = 1, 2,…, s). In the actual optimization process, the variable

LCL_i is replaced by the corresponding type I error probabilities α_1, α_2, …, α_s associated with s control charts. The variable α_i is the probability that the ith control chart produces an out-of-control signal when the ith process is in fact in control.

$$LCL_i = -\ln(1-\alpha_i)/\lambda_{0,i} \tag{6.14}$$

Optimizing α_i is equivalent to optimizing LCL_i, but the former is easier to handle during the optimization search. It is because that α_i has finite lower bound (0) and upper bound (1) for the search and that a simple equation among α_1, α_2, …, α_s (Eq. 6.15) can be established easily (Wu *et al*., 2004b).

$$\alpha_i = \frac{1}{\lambda_{0,i}}\left[1-\left(\frac{1-1/\tau}{\prod_{j=1,j\neq i}^{s}(1-\alpha_j\lambda_{0,j})^{g_j}}\right)^{1/g_i}\right] \tag{6.15}$$

This equation is used to determine the range of possible α_i values in the ith level search. The objective of the optimization search is to identify the optimal values for (α_1, α_2, …, α_s) that will jointly maximize the profit O and ensure ATS_0 (the false alarm rate) equals to the specification (i.e. $ATS_0 = \tau$).

The overall optimization search is outlined as follows.

(1) Specify s, g_i, $\lambda_{a,i}$, $\lambda_{0,i}$, $\lambda_{\delta,i}$, p_i, d_i, V_i, Δ_i, τ, B_0, B_1, A_0, A_i, and C

(2) Initialize O_{max} as a small number, say 10^{-5}. O_{max} is used to record the maximum O.

(3) Carry out the searches in $(s-1)$ levels.

(3.1) Each design point $(\alpha_1, \alpha_2, \ldots, \alpha_s)$ will automatically make ATS_0 equal to τ.

(3.2) Calculate O by Eq. 6.13.

(3.3) If this O value is larger than the current O_{max}, replace O_{max} by O and record the current design point $(\alpha_1, \alpha_2, \ldots, \alpha_s)$ as the temporary optimal solution.

(4) When the whole search is completed, the optimal design point $(\alpha_1, \alpha_2, \ldots, \alpha_s)$ is finalized.

(5) Calculate the control limits of the s control charts by Eq. 6.14.

A computer program in C language has been developed to carry out the optimization design. The value of the step size $d\alpha$ is decided so that the total number of search points is always limited to 100000 regardless of the number of α_i. Usually, an optimal solution is obtained in less than one CPU second using a personal computer.

6.2 Performance analysis

This part studies the effects of different input parameters on the performance of the control chart system. Firstly, the effects of the process parameters ($\lambda_{a,i}$, $\lambda_{0,i}$, $\lambda_{\delta,i}$, g_i, p_i, d_i) on the profit O are investigated. Then, errors associated with the estimation of the cost parameters (B_0, B_1, A_0, A_i, C) are analyzed. Two different control chart systems, i.e., a traditional chart system and an integrated chart system are designed. For the traditional chart system, the α_i values of the control charts are made equal and set at 0.0027 in each stage of the chart system, and for the integrated chart system, the α_i values (or equivalently the control limits) of the control charts are determined by the optimization design proposed earlier. In both of the sensitivity studies, the in-control ATS_0 of the traditional system is calculated and set as a constraint in the optimization process, that is, both of the chart systems (integrated chart system and traditional chart system) produce the same in-control ATS_0 ($= \tau$) in each of the studies. Finally, the economic design of the integrated chart system is illustrated through an example.

6.2.1. Sensitivity study I

This section studies the effects of six process parameters ($\lambda_{a,i}$, $\lambda_{0,i}$, $\lambda_{\delta,i}$, g_i, p_i, d_i) on the performance (measured by the profit O) of the control chart system. Each of these six parameters has a low value, a nominal value and a high value, as shown below.

Parameter	Low	Nominal	High
$\lambda_{a,i}$	0.0001	0.0005	0.0009
$\lambda_{0,i}$	0.001	0.005	0.009
$\lambda_{\delta,i}$	0.01	0.05	0.09
g_i	1	1	4
p_i	0.1	0.5	0.9
d_i	0.1	0.5	0.9

The nominal value denotes the value under normal circumstances. The nominal value of g_i is equal to its low value, because it is assumed that there is usually only one stream in a stage, unless the production rate in this stage is much lower than that in other stages. It is noted that the values of $\lambda_{a,i}$, $\lambda_{0,i}$ and $\lambda_{\delta,i}$ are decided in order of ($\lambda_{a,i} < \lambda_{0,i} < \lambda_{\delta,i}$). The

occurrence of nonconforming items is a very common phenomenon in many kinds of industries, and the occurrence rate $\lambda_{\delta,i}$ of nonconforming items increases when process shifts from in control to out of control, so $\lambda_{0,i} < \lambda_{\delta,i}$. Comparing with the occurrence of nonconforming items, the occurrence of assignable causes is not so often, so it is assumed that $\lambda_{a,i} < \lambda_{0,i}$.

The performance of a two-stage manufacturing system, where stage 2 is influenced by stage 1, is studied for six different cases. In each case, all the parameters take their nominal values in both stages, except that one selected parameter (called the *active parameter*) takes its low value in stage 1 and high value in stage 2. For example, in case one, the first parameter $\lambda_{a,i}$ is designated as the active parameter. Therefore,

$$\lambda_{a,1} = 0.0001,\ \lambda_{a,2} = 0.0009$$

$$\lambda_{0,1} = \lambda_{0,2} = 0.005,\ \lambda_{\delta,1} = \lambda_{\delta,2} = 0.05,\ g_1 = g_2 = 1,\ p_1 = p_2 = 0.5,\ d_1 = d_2 = 0.5$$

For each of the six cases, a traditional chart system and an integrated chart system are designed. The cost parameters' values ($B_0 = 150.0$, $B_1 = 50.0$, $A_0 = 10.0$, $A_1 = A_2 = 20$, $C = 0.5$) are kept constant for both systems. The ratio R between O values resulting from each chart system is calculated as follows.

$$R = O_{\text{integrated}} / O_{\text{traditional}} \tag{6.16}$$

Obviously, if the value of R is greater than one, the integrated system will outperform the traditional system in a particular case in terms of the profit O, and *vice versa*.

The R values for all six cases are listed in Table 6.1 under column (6). It can be observed that in all of the six cases, the integrated system achieves an obvious improvement in effectiveness compared to the traditional system. It is especially the cases when each of the five parameters $\lambda_{a,i}$, $\lambda_{\delta,i}$, g_i, p_i or d_i has different values in the two stages, that the integrated system considerably improves the profit compared to the traditional system. The performance of the integrated chart system is relatively less sensitive to the parameter $\lambda_{0,i}$. The actual R value would differ for different systems and circumstances. However, it is believed that the integrated chart system would be effective in general and beneficial to many real systems. The reason is that, in any manufacturing system, the influential parameters would be in general different among several stages.

Table 6.1 Sensitivity study I

(1) Case No.	(2) Active parameter		(3) Optimal α_i		(4) $O_{\text{integrated}}$	(5) $O_{\text{traditional}}$	(6) Ratio R
			α_1	α_2			
1	$\lambda_{a,1} = 0.0001$	$\lambda_{a,2} = 0.0009$	0.000000027	0.005399937	124.157	114.819	1.08133
2	$\lambda_{0,1} = 0.001$	$\lambda_{0,2} = 0.009$	0.002324019	0.002741775	107.570	107.527	1.00040
3	$\lambda_{\delta,1} = 0.01$	$\lambda_{\delta,2} = 0.09$	0.000000027	0.005399937	81.924	75.140	1.09029
4	$g_1 = 1$	$g_2 = 3$	0.000000054	0.003599974	123.718	119.109	1.03870
5	$p_1 = 0.1$	$p_2 = 0.9$	0.000000027	0.005399937	122.750	108.683	1.12943
6	$d_1 = 0.1$	$d_2 = 0.9$	0.000000027	0.005399937	124.157	114.819	1.08133

6.2.2. Sensitivity study II

In practice, there may be some errors in estimating different cost parameters (B_0, B_1, A_0, A_i, *and* C). The deviation of the ratio R (Eq.6.16) (or in other words, the deviation of improvement in profit obtained by the integrated system compared to that obtained by the traditional system) incurred by the error associated with the estimation of the cost parameters is evaluated and analyzed in this section.

Similar to the previous study, a two stage manufacturing system is considered where stage 2 is influenced by stage 1. The process parameters at both stages are assumed to be equal and set at their nominal values.

$\lambda_{a,1} = \lambda_{a,2} = 0.0005$, $\lambda_{0,1} = \lambda_{0,2} = 0.005$, $\lambda_{\delta,1} = \lambda_{\delta,2} = 0.05$, $g_1 = g_2 = 1$, $p_1 = p_2 = 0.5$,

$d_1 = d_2 = 0.5$

The reference values of the cost parameters are decided as follows.

$B_0 = 100$, $B_1 = 30$, $A_0 = 6$, $A_1 = 15$, $A_2 = 25$, $C = 0.4$

The investigation is carried out by one-factor-at-a-time basis (Xie *et al*. 2001, Zhang *et al*. 2005), i.e., each time one (the active parameter), of the six cost parameters is picked out to vary from its reference value, while all others are kept constant at their reference values. The traditional and integrated chart systems are designed and the ratio R_r is calculated (Eq. 6.16). The subscript "*r*" denotes "real". For example, in the first case, B_0 is the active parameter. Therefore,

$B_{0,r} = 100$, $B_{1,r} = 30$, $A_{0,r} = 6$, $A_{1,r} = 15$, $A_{2,r} = 25$, $C_r = 0.4$, $R_r = 1.086769292$

Now, suppose B_0 has been underestimated by 30%, that is, $\hat{B}_0 = 0.7B_{0,r}$. If this $\hat{B}_0$ is used in the optimization process, the ratio $R_{0.7}$ is found to be 1.066843297. The relative error in $R_{0.7}$ due to the underestimated $\hat{B}_0$ can be calculated as follows.

$$e_{0.7} = \frac{|R_{0.7} - R_r|}{R_r} = \frac{|1.066843297 - 1.086769292|}{1.086769292} = 0.018335074 \quad (6.17)$$

Following this procedure similarly, it is found that the relative error in $R_{1.3}$ due to overestimating B_0 by 30% is 0.010810639.

If the real value of B_0 is different from 100, the relative errors will differ correspondingly. All of these individual errors (e) and the average errors ($\bar{e}$) are calculated and listed in Table 6.2. Similarly, the average errors associated with all other active parameters (B_1, A_0, A_1, A_2, *and* C) are calculated and listed in Table 6.3. It is found that the average errors incurred by under estimating or overestimating different cost parameters are not quite notable (< 3%). It may be concluded that the improvement in profit obtained by the integrated design compared to that obtained by the traditional design is not significantly affected by slight or moderate error in the estimation of the cost parameters.

Table 6.2 Relative and average errors in R when B_0 is the active parameter

Active parameter	Parameters values constant at their reference values					Relative error, e	
B_0	B_1	A_0	A_1	A_2	C	$e_{0.7}$	$e_{1.3}$
100	30	6	15	25	0.4	0.018335074	0.010810639
110	30	6	15	25	0.4	0.017104371	0.010013553
120	30	6	15	25	0.4	0.016024738	0.009324665
130	30	6	15	25	0.4	0.015070752	0.008723605
140	30	6	15	25	0.4	0.014222182	0.008194747
150	30	6	15	25	0.4	0.013462796	0.007725925
160	30	6	15	25	0.4	0.012779455	0.007307536
170	30	6	15	25	0.4	0.012161434	0.006931906
180	30	6	15	25	0.4	0.011599900	0.006592834
190	30	6	15	25	0.4	0.011087526	0.006285256
200	30	6	15	25	0.4	0.010618182	0.006004995
210	30	6	15	25	0.4	0.010186709	0.005748582
220	30	6	15	25	0.4	0.009788733	0.005513106
230	30	6	15	25	0.4	0.009420523	0.005296111
240	30	6	15	25	0.4	0.009078879	0.005095510
Average error, $\bar{e}$						0.012729417	0.007304598

Table 6.3 Average error in *R* for different active parameters

Active parameter	Average error, $\bar{e}$	
	$\bar{e}_{0.7}$	$\bar{e}_{1.3}$
B_0	0.012729417	0.007304598
B_1	0.020816521	0.018223566
A_0	0.000000037	0.000000037
A_1	0.000001734	0.000001734
A_2	0.000002891	0.000002829
C	0.000023767	0.000023772

6.2.3. An example

A part is machined in a four-stage manufacturing system. Stage 1 turns the upper surface 1 (datum: surface 0); stage 2 turns surface 2 (datum: surface 1); stage 3 drills the hole (datum: surface 2); and stage 4 mills the slot (datum: surface 2). Since the process in stage 4 is much more time consuming, two machines are used in parallel. The four dimensions that are formed at the four stages are monitored by TBE charts. The specifications of the system are summarized below.

Average profit per unit time when the system is in-control: $B_0 = 250$

Average profit per unit time when the system is out-of-control: $B_1 = 60$

Average cost associated with one false alarm: $A_0 = 15$

Average costs for locating and removing the assignable causes: $A_1 = 15$, $A_2 = 25$, $A_3 = 30$, $A_4 = 20$

Average cost for observing and plotting a sample: $C = 0.5$

Number of stages in the manufacturing system: $s = 4$

Number of streams: $g_1 = g_2 = g_3 = 1$, $g_4 = 2$

Out-of-control rate of occurrence of the event:

$\lambda_{\delta,1} = 0.04$, $\lambda_{\delta,2} = 0.06$, $\lambda_{\delta,3} = 0.03$, $\lambda_{\delta,4} = 0.05$

In-control rate of occurrence of the event:

$\lambda_{0,1} = 0.002$, $\lambda_{0,2} = 0.003$, $\lambda_{0,3} = 0.002$, $\lambda_{0,4} = 0.003$

Rate of occurrence of the assignable cause:

$\lambda_{a,1} = 0.0001$, $\lambda_{a,2} = 0.0002$, $\lambda_{a,3} = 0.0002$, $\lambda_{a,4} = 0.00015$

The probabilities p_i of the out-of-control occurrences are estimated from historical records, which show that the numbers of out-of-control cases occurring in each of the four stages are 2, 3, 5 and 4, respectively. Therefore,

$$p_1 = 2/(2+3+5+4) = 0.143$$
$$p_2 = 3/(2+3+5+4) = 0.214$$
$$p_3 = 5/(2+3+5+4) = 0.357$$
$$p_4 = 4/(2+3+5+4) = 0.286$$

From the description of the production planning it is revealed that stage 2 is directly dependent on stage 1, and stages 3 and 4 are directly dependent on stage 2. Therefore, the dependent relationship vectors V_i and the formulae for Δ_i are determined as follows (Lam *et al.*, 2005).

$V_2 = [1]^T$, $V_3 = [2]^T$, $V_4 = [2]^T$

$\Delta_2 = \lambda_1$, $\Delta_3 = \lambda_2$, $\Delta_4 = \lambda_2$

So, if stage 1 goes out of control (i.e. rate of occurrence of the event in this stage is shifted from its in-control value $\lambda_{0,1}$ (= 0.002) to the out-of-control value $\lambda_{\delta,1}$ (= 0.04)), stage 2 will be affected directly. According to Eq.5.12 in Chapter 5, the induced rate of occurrence of the event received by stage 2 is,

$$\lambda_2 = \Delta_2 = (\lambda_{\delta,1} + \lambda_{0,1}(g_1 - 1))/g_1 = (0.04 + 0.002(1-1))/1 = 0.04$$

Meanwhile, stages 3 and 4 will be influenced indirectly through the changes in stage 2 (Eq.5.11 in Chapter 5), and the induced rate of occurrence of the event received by stages 3 and 4 are,

$\lambda_3 = \Delta_3 = \lambda_2 = 0.04$, $\lambda_4 = \Delta_4 = \lambda_2 = 0.04$

On the other hand, if stage 2 is out of control, only stages 3 and 4 will be affected, and the induced rate of occurrences of the events received by stages 3 and 4 are,

$$\lambda_3 = \Delta_3 = (\lambda_{\delta,2} + \lambda_{0,2}(g_2 - 1))/g_2 = (0.06 + 0.003(1-1))/1 = 0.06$$

$$\lambda_4 = \Delta_4 = (\lambda_{\delta,2} + \lambda_{0,2}(g_2 - 1))/g_2 = (0.06 + 0.003(1-1))/1 = 0.06$$

Originally, a traditional TBE chart system that adopts the same type I error probability of 0.0027 for all TBE charts is used to monitor the manufacturing processes. As a result, the in-control ATS_0 of the chart system is equal to 28490 (Eq.5.7 in Chapter 5).

Now, the QA (Quality Assurance) manager decides to design an integrated chart system in order to improve the expected profit O. He requires that the false alarm rate of the integrated chart system be maintained at the same level as for the traditional system. Thus, τ is specified as 28490. The computer program works out the integrated chart system for

this example in 0.156 CPU second in a personal computer (Pentium IV, CPU 2.40 GHz). The results are listed below.

Stage 1: $LCL = 0.09453$ ($\alpha = 0.0001890$)

Stage 2: $LCL = 0.06302$ ($\alpha = 0.0001890$)

Stage 3: $LCL = 4.08116$ ($\alpha = 0.0081291$)

Stage 4: $LCL = 0.99573$ ($\alpha = 0.0029827$)

$ATS_0 = 28490$, $O = 224.067$

It can be observed that, while both the integrated chart system and the traditional system have the same ATS_0 value ($= \tau = 28490$), the profit O resulting from the integrated system and the traditional system are 224.047 and 206.939, respectively. It indicates that the integrated system improves the profit by about 8.3%, on average, compared to the traditional system.

6.3 Summary

This chapter proposes the economic design of the control chart system based on time-between-events (TBE) data. The design algorithm optimizes the control limits of each chart in the chart system in order to maximize the profit associated with the monitoring of

a multistage manufacturing system. It is found that, by properly allocating the power among the individual charts based on the values of the influential parameters, the profit of the SPC system can be significantly improved.

Chapter 7 Conclusions and Future Research

7.1 Conclusions

Time-between-events chart has shown to be very useful in manufacturing systems, in reliability and maintenance monitoring, and also in service-related applications in general. Examining the existing time-between-events chart, it is found that the existing time-between-events chart can be improved in many aspects. This thesis focuses on improving the existing time-between-events chart by making it more practical, enhancing the effectiveness of the time-between-events chart by integrating it with other techniques and at the same time increasing the average profit per unit time or reducing the average cost per unit time.

Chapter 3 and chapter 4 focus on improving a single time-between-events chart. Process shift size is always assumed fixed for the existing time-between-events chart and shift size is always determined subjectively. The time-between-events chart designed under this assumption may not reflect real situation and can only achieve optimal performance

for the particular shift size while work unsatisfactorily for other shift sizes. In order to make the time-between-events chart more practical and more effective for a range of process shifts, chapter 3 develops the model of time-between-events chart under the random process shift which follows Rayleigh distribution. Economic aspects of the process have been considered. Two comparisons have been conducted. The first comparison is between the statistical design and economic design of time-between-events chart under random process shift. The results show that there is significant improvement in average profit per unit time by using economic design but the improvement decreases as λ_1 / λ_0 increases. The second comparison is between the random process shift and fixed process shift of time-between-events chart. The results show that the time-between-events chart under random process shift is more realistic than the chart under fixed process shift. Finally, the sensitivity of input parameters on the average profit per unit time is evaluated.

Tagaras (1988) pointed out that in most cases, it is advisable to integrate control chart and preventive maintenance. Following this suggestion, there are a lot of papers which integrate control chart and preventive maintenance. But these papers either do not consider process failure or only consider exponentially distributed process failure. Until now, no one has developed a general model which considers both assignable cause and

process failure and both of them are Weibull distributed. Furthermore, no one has integrated time-between-events chart and preventive maintenance. Chapter 4 fills this gap. In chapter 4, an integrated model of time-between-events chart and preventive maintenance is developed. Both assignable cause and failure are considered, and their occurrences are modeled with Weibull distribution. The implementing cost of the control chart and preventive maintenance is considered and the cost minimization criterion is used to find the optimal values of decision variables. Design of Experiment technique is used to study the parameter sensitivity of the integrated model with respect to the expected cost per unit time and the decision variables. Two alternative models, preventive maintenance model and TBE-chart model are used for the purpose of comparison with the integrated model. The results of comparison show that by adopting the integrated model, the average cost per unit time can be decreased in about half of the time. Suggestions for when to use the integrated model have also been provided. Finally the influence of shift and failure distributions on the expected cost per unit time is studied.

Chapters 5 and 6 develop a time-between-events chart system consisting of several individual time-between-events charts, each of which is used to monitor the time between successive events at different process stages in the manufacturing of a product in a

multistage manufacturing system. Previously each of the time-between-events charts in the system is designed individually. This design does not take the quality linkage between each stage into consideration. Furthermore, the false alarm rate for the entire system is increased. Chapters 5 and 6 propose a new design algorithm which considers all the time-between-events charts within a system in an integrative and optimal manner so that the quality linkage can be considered. Chapter 5 focuses on studying the statistical properties of the system while chapter 6 focuses on the economical properties. Results from Chapter 5 and 6 show that by designing all the time-between-events charts in the system in an integrative manner, the out of control *ATS* (in chapter 5) and average profit per unit time (in Chapter 6) can be significantly improved.

Results from each chapter show that the methods used in this thesis improve the effectiveness of the existing time-between-events chart and make it more practical. However, this thesis also has its limitations. The limitations of this thesis and future research directions are discussed in the next section.

7.2 Future Research

This part discusses the limitations of this thesis and proposes some possible future research directions.

The first limitation is that the random process shift in Chapter 3 is restricted to modeling by Rayleigh distribution only. Although the Rayleigh distribution is easier to estimate because there is only one parameter involved, several commonly used distributions should also be taken into consideration and compared with the Rayleigh distribution, which can make the model more robust and widely applicable. This is a possible future research direction.

The second limitation is that in Chapter 4, it is assumed that preventive maintenance and reactive maintenance can restore the system to an as good as new condition. The reason for making this assumption is to simplify the model. However, this assumption is seldom satisfied in reality. As possible future work, the integration of time-between-events chart and preventive maintenance model can be extended to imperfect maintenance situation, and the Markov chain method may be used to solve the problem.

The third limitation is related to Chapters 5 and 6. In Chapters 5 and 6, one time-between-events chart is assigned to each stage. Although all the time-between-events charts are designed in an integrative manner, the number of time-between-events chart can be quite large if there are many stages. For the time-between-events chart, two decision variables (upper control limit and lower control limit) are required before

implementing the chart, and so the total number of decision variables is 2^n (n is the number of stages in the system). Since the manufacturing system is always very complex, the number of stages n is always very large, resulting in many decision variables. It would thus be very complex to design this kind of control chart system. How to reduce the number of charts to monitor the whole system would be a useful and interesting topic. One possible solution for this problem is to treat it as a multivariate problem, with each variable denoting the quality characteristic at each stage. But new problems arise for such a multivariate problem, which are the number of stages cannot be too large because otherwise the size of the covariance matrix would be very large and how to identify which stage is out of control. These problems are worth researching in the future.

The fourth limitation is that Chapters 3, 5, 6 assume the time between events follows exponential distribution. Although it is a common assumption in many research works, it is actually not practical. In reality, most of the time between events actually follows Weibull distribution. Although in Chapter 4, both of the occurrences of assignable cause and failure are modeled by Weibull distribution, the time between the occurrences of events is still modeled by exponential distribution. As possible future work, the time between events should be modeled by Weibull distribution, and both the scale parameter

and shape parameter can be changed when the assignable cause happens, instead of keeping one variable fixed as in the case of some of the existing research work.

The fifth limitation is that it is assumed that 100% inspection is done for the time-between-events chart here. But in the reality, this assumption is seldom satisfied. In the future, sampling frequency and sampling size should be taken into consideration when designing time-between-events chart.

The sixth limitation is that the improving techniques, such as random process shift, preventive maintenance and multistage system, are applied one at a time in this thesis. The results of this thesis show that introducing random process shift, integrating time-between-events chart with preventive maintenance and designing the time-between-events charts in the system in an integrative manner can significantly improve the effectiveness of the monitoring system, but only one method at a time has been taken in this thesis. In reality, the monitoring techniques usually include both control chart and maintenance, and the manufacturing system always consists of multi-stage processes. As a result, designing a monitoring system which considers control chart, preventive maintenance and multi-stage problems all at the same time can be quite useful. How to

combine all the improving techniques proposed in this thesis and apply them at the same time would be worth exploring in the future.

Reference

1. Alemi, L. and Neuhauser, D. (2004). Time-between control chart for monitoring asthma attacks. *Joint Commission Journal of Quality and Patient Safety*, 30(2), 95-102.

2. Aparisi, F. and Garcia-Diaz, J.C. (2007). Design and optimization of EWMA control charts for in-control, indifference, and out-of-control regions, *Computers & Operations Research*, 34(7), 2096-2108.

3. Bai, D.S. and Lee, K.T. (2002). Variable sampling interval X-bar control charts with an improved switching rule, *International Journal of Production Economics*, 54, 57-64.

4. Barlow, R. E. and Hunter, L.C. (1960). Optimum preventive maintenance policies, *Operations Research*, 8, 90-100.

5. Barlow, R. E., Hunter, L. C. and Proschan, F. (1963). Optimum checking procedures, *Journal of the Society for Industrial and Applied Mathematics*, 4, 1078-1095.

6. Batson, R.G., Jeong, Y., Fonseca, D.J. and Ray, P.S. (2006). Control charts for monitoring field failure data, *Quality and Reliability Engineering International*, 22, 733-755.

7. Beichelt, F. (1981). Minimax Inspection Strategies for Single Unit System, *Naval Research Logistics Quarterly*, 28, 375-381.

8. Ben-Daya, M. and Rahim, M. A. (2000). Effect of maintenance on the economic design of X-bar control chart, *European Journal of Operational Research*, 120, 131-143.

9. Benneyan, J.C. (2001a). Number –between g-type statistical quality control charts for monitoring adverse events, *Health Care Management Science*, 4,305-318.

10. Benneyan, J.C. (2001b). Performance of number –between g-type statistical control charts for monitoring adverse events, *Health Care Management Science*, 4,319-336.

11. Biswas, P. and Kalbfleisch J. D. (2008). A risk-adjusted CUSUM in continuous time based on the Cox model, *Statistics in Medicine*, 27(17), 3382-3406.

12. Borror, C.M., Keats, J.B. and Montgomery, D.C. (2003). Robustness of the time between events CUSUM, *International Journal of Production Research*, 41(15), 3435-3444.

13. Bourke, P. (1991). Detecting a shift in fraction nonconforming using run-length control charts with 100% inspection, *Journal of Quality Technology*, 23, 225-238.

14. Bourke, P. (2001a). The geometric CUSUM chart with sampling inspection for monitoring fraction defective, *Journal of Applied Statistics*, 28(8), 951-972.

15. Bourke, P. (2001b). Sample size and the Binomial CUSUM control chart: the case of 100% inspection, *Metrika*, 53, 51-70.

16. Bourke, P. (2008). Performance comparisons for the synthetic control chart for detecting increases in fraction nonconforming, *Journal of Quality Technology*, 40(4), 461-475.

17. Broadbent, S.R. (1958). The inspection of a Markov process, *Journal of the Royal Statistical Society*, B, 20, 111-119.

18. Bucchianico, A.D., Mooiweer, G.D. and Moonen, E.J.G. (2005). Monitoring infrequent failures of high-volume production processes, *Quality and Reliability Engineering International*, 21, 521-528.

19. Calvin, T.W. (1983). Quality control techniques for 'zero-defects'. *IEEE Transactions on Components, Hybrids, and Manufacturing Technology*, 6, 323-328.

20. Carot, V., Jabaloyes, J.M. and Carot, T. (2002). Combined double sampling and variable sampling interval X-bar chart, *International Journal of Production Research*, 40(9), 2175-2186.

21. Cassady, C.R., Bowden, R.O., Liew, L. and Pohl, E.A. (2000), Combining preventive maintenance and statistical process control: a preliminary investigation, *IIE Transactions*, 32,471-478.

22. Chan, L.Y., Lai, C.D., Xie, M. and Goh, T.N. (2000).A two-stage decision procedure for monitoring processes with low fraction nonconforming, *European Journal of Operational Research*, 150,420-436.

23. Chan, L.Y., Lai, C.D., Xie, M. and Goh, T.N. (2003). A two-stage decision procedure for monitoring processes with low fraction nonconforming, *European Journal of Operational Research*, 150, 420-436.

24. Chan, L.Y., Lin, D.K.J., Xie, M. and Goh, T.N. (2002). Cumulative probability control charts for geometric and exponential process characteristics, *International Journal of Production Research*, 40(1), 133-150.

25. Chan, L.Y., Ouyang, J.T. and Lau, H.Y.K. (2007). A two-stage cumulative quantity control chart for monitoring poisson processes, *Journal of Quality Technology*, 39(3), 203-223.

26. Chan, L.Y., Xie, M. and Goh, T.N. (2000). Cumulative quantity control charts for monitoring production processes, *International Journal of Production Research*, 38(2), 397-408.

27. Chang, T.C. and Gan, F.F. (2001). Cumulative sum charts for high yield processes, *Statistica Sinica*, 11, 791-805.

28. Chen, H.F. and Cheng, Y.Y. (2007). Non-normality effects on the economic-statistical design of X-bar charts with Weibull in-control time, *European Journal of Operational Research*, 176(2), 986-998.

29. Chen, J.T. (2009). A new approach to setting control limits of cumulative count of conforming charts for high-yield processes, *Quality and Reliability Engineering International*, published online, DOI: 10.1002/qre.1015.

30. Chen, P.W. and Cheng, C.S. (2007). Cumulative count of conforming chart with variable sampling intervals for markov dependent production processes, *Proceedings of the Second International Conference on Innovative Computing, Information and Control*, 2007.

31. Chen, Y.K. (2004). Economic design of X-bar control charts for non-normal data using variable sampling policy, *International Journal of Production Economics*, 92(1), 61-74.

32. Chou, C.Y., Liu, H.R., Huang, X.R. and Chen, C.H. (2002). Economic-statistical design of multivariate control charts using quality loss function, *The International Journal of Advanced Manufacturing Technology*, 20(12), 916-924.

33. Chung, K.J. (1991). A simplified procedure for the economic design of control charts: A unified approach, *Engineering Optimization*, 17, 81-87.

34. Ciriaco, V. F. and Richard, M. F. (1989). A survey of preventive maintenance models for stochastically deteriorating single-unit system, *Naval Research Logistics*, 36(4), 419-446.

35. Coory, M., Duckett, S. and Sketcher-Baker, K. (2008). Using control charts to monitor quality of hospital care with administrative data, *International Journal for Quality in Health Care*, 20(1), 31-39.

36. Costa, A.F.B. and Machado, M.A.G. (2008). Bivariate control charts with double sampling, *Journal of Applied Statistics*, 35(7), 809-822.

37. De Magalhaes, M.S. and Moura Neto, F.D. (2005). Joint economic model for totally adaptive X-bar and R charts, *European Journal of Operational Research*, 161(1), 148-161.

38. De Magalhaes, M.S., Costa, A.F.B. and Moura Neto, F.D. (2006). Adaptive control charts: A Markovian approach for processes subject to independent disturbances, *International Journal of Production Economics*, 99(1-2), 236-246.

39. Ding, Y., Ceglarek, D. and Shi, J. (2002). Fault diagnosis of multistage manufacturing processes by using state space approach. ASME Transactions, *Journal of Manufacturing Science and Engineering*, 124, 313-322.

40. Dodson, B. (1994), Weibull Analysis, Quality Press, Milwaukee, WI.

41. Duncan, A.J. (1956). The economic design of X-bar charts used to maintain current control of a process, *Journal of the American Statistical Association*, 51, 228-242.

42. Duncan, A.J. (1986). *Quality Control and Industrial Statistics*, 5th edition, Irwin, Homewood, IL.

43. Gan, F.F. (1992). Exact run length distributions for one-sided exponential CUSUM schemes, *Statistica Sinica*, 2, 297-312.

44. Gan, F.F. (1993). An optimal design of CUSUM control charts for binomial counts, *Journal of Applied Statistics*, 20(4), 445-460.

45. Gan, F.F. (1998). Design of one- and two-sided exponential EWMA charts, *Journal of Quality Technology*, 30(1), 55-69.

46. Gan, F.F. and Chang, T.C. (2000). Computing average run lengths of exponential EWMA charts, *Journal of Quality Technology*, 32(2), 183-187.

47. Girshick, M.A., Mosteller, F. and Savage, L.J. (1946). Unbiased estimates for certain binomial sampling problems with applications, *The Annals of Mathematical Statistic*s, 17, 13-23.

48. Goh, T.N. (1987). A control chart for very high yield processes, *Quality Assurance*, 13, 18-22.

49. Grigg, O.A., Farewell, V.T. and Spiegelhalter, D.J. (2003). Use of risk-adjusted CUSUM and RSPRT charts for monitoring in medical contexts, *Statistical Methods in Medical Research*, 12(2), 147-170.

50. Haldane, J.B.S. (1945). A labor-saving method of sampling, *Nature*, 155(3924), 49-50.

51. Herbert, D., Curry, A. and Angel, L. (2003). Use of Quality Tools and Techniques in Services, *Service Industries Journal*, 23(4), 61-80.

52. Hunter, J.S. (1986). The exponentially weighted moving average schemes, *Journal of Quality Technology*, 18, 203-210.

53. Jiao, J.X.R. and Helo, P.T. (2008). Optimization design of a CUSUM control chart based on taguchi's loss function, *International Journal of Advanced Manufacturing Technology*, 35, 1234-1243.

54. Jones, L.A. and Champ, C.W. (2002). Phase I control charts for times between events, *Quality and Reliability Engineering International*, 18, 479-488.

55. Juang, M. and Anderson, G. (2004). A bayesian method on adaptive preventive maintenance problem, *European Journal of Operational Research*, 155(2), 453-473.

56. Kaminsky, F.C., Benneyan, R.D., Davis, R.D. and Burke, R.J. (1992). Statistical control charts based on a geometric distribution, *Journal of Quality Technology*, 24(2), 63-69.

57. Kao, S.C., Ho, C.C. and Ho, Y.C. (2006). Transforming the exponential by minimizing the sum of the absolute differences, *Journal of Applied Statistics*, 33(7), 691-702.

58. Kao, S.C. and Ho, C.C. (2007). Monitoring a process of exponentially distributed characteristics through minimizing the sum of the squared differences, *Quality & Quantity*, 41, 137-149.

59. Khoo, M.B.C. and Xie, M. (2008). A study of time-between-events control chart for the monitoring of regularly maintained systems, *Quality and Reliability Engineering International*, published online DOI: 10.1002/qre.977.

60. Kittlitz, JR.R. G. (1999). Transforming the exponential for SPC applications, *Journal of Quality Technology*, 31(3), 301-308.

61. Kotani, T., Kusukawa, E. and Ohta, H. (2005). Exponentially weighted moving average chart for high-yield processes, *Industrial Engineering and Management System*, 4(1), 75-81.

62. Kuralmani, V., Xie, M., Goh, T.N. and Gan, F.F. (2002). A conditional decision procedure for high yield processes, *IIE Transactions*, 34, 1021-1030.

63. Lai, C.D., Chan, L.Y. and Xie, M. (2001). Distribution of runs in a two-stage process monitoring model, *Communications in Statistics: Simulation and Computation*, 30(3), 547-557.

64. Lai, C.D., Govindaraju, K. and Xie, M. (1998). Effects of correlation on fraction non-conforming statistical process control procedures, *Journal of Applied Statistics*, 25(4), 535-543.

65. Lai, C.D., Xie, M. and Govindaraju, K. (2000). Study of a Markov model for a high-quality dependent process, *Journal of Applied Statistics*, 27(4), 461-473.

66. Lam, Y.C., Shamsuzzaman, M., Zhang, S. and *Wu*, Z. (2005). Integrated control chart system- optimization of sample sizes, sampling intervals and control Limits. *International Journal of Production Research*, 43(3), 563-582.

67. Lee, K.T. and Bai, D.S. (2000). Variable sampling interval X-bar control charts with runs rules, *International Journal of Industrial Engineering –Theory, Application and Practice*, 7(2), 147-158.

68. Linderman, K., McKone-Sweet, K.E. and Anderson, J.C. (2005), An integrated systems approach to process control and maintenance, *European Journal of Operational Research*, 164,324-340.

69. Lin, Y.C. and Chou, C.Y. (2005). On the design of variable sample size and sampling intervals X-bar charts under non-normality, *International Journal of Production Economics*, 26(2), 249-261.

70. Lin, Y.C. and Chou, C.Y. (2007). Non-normality and the variable parameters X-bar control charts, *European Journal of Operational Research*, 176(1), 361-373.

71. Liu, J.Y., Xie, M. and Goh, T.N. (2006a). CUSUM chart with transformed exponential data, *Communications in Statistics: Theory and Methods*, 35, 1829-1843.

72. Liu, J.Y., Xie, M., Goh, T.N. and Chan, L.Y. (2007). A study of EWMA chart with transformed exponential data, *International Journal of Production Research*, Vol. 45, 3(1), 743-763.

73. Liu, J.Y., Xie, M., Goh, T.N., Liu, Q.H. and Yang, Z.H. (2006b). Cumulative count of conforming chart with variable sampling intervals, *International Journal of Production Economics*, 101, 286-297.

74. Liu, Y.F., He, Z., Shu, L.J. and Wu, Z. (2009). Statistical computation and analyses for attribute events, *Computational Statistics and Data Analysis*, doi: 10.1016/j.csda.2009.02.010.

75. Lorenzen, T.J. and Vance, L.C. (1986). The economic design of control charts: A unified approach, *Technometrics*, 28, 3-10.

76. Lucas, J.M. (1985). Counted Data CUSUM's, *Technometrics*, 27(2), 129-144.

77. Lu, W.B. and Tsai, T.R. (2008). Exponentially weighed moving average control chart for gamma distribution with type I censoring, *Proceedings of The 3rd International Conference on Innovative Computing Information and Control.*

78. Luss, H. (1976). Maintenance policies when deterioration can be observed by inspection, *Operations Research*, 24, 359-366.

79. Madsen, R.W. (1993). Generalized binomial distributions, *Communications in Statistics: Theory and Method*, 22, 3065-3086.

80. Makis, V. and Fung, J. (1995), Optimal preventive replacement, lot sizing and inspection policy for a deteriorating production system, *Journal of Quality in Maintenance Engineering* 1(4), 41-55.

81. Makis, V. and Fung, J. (1998), An EMQ model with inspections and random machine failures, *Journal of the Operational Research Society* 49 (1), 66-76.

82. Marcellus, R.L. (2008). Bayesian monitoring to detect a shift in process mean, *Quality and Reliability Engineering International*, 24(3), 303-313.

83. McCool, J. and Joyner-Motley, T. (1998). Control charts applicable when the fraction nonconforming is small, *Journal of Quality Technology*, 30(3), 240-247.

84. McShane, L.M. and Turnbull, B.W. (1991). Probability limits on outgoing quality for continuous sampling plans, *Technometrics*, 33(4), 393-404.

85. McWilliams, T.P. (1989), Economic control chart designs and the in-control time distributions: a sensitivity study, *Journal of Quality Technology*, 21, 103-151.

86. Montgomery, D.C. (2005). *Introduction to Statistical Quality Control*, 5th edition, John Wiley & Sons, Inc..

87. Mortell, R.R. and Runger, G.C. (1995). Statistical process control of multiple stream processes. *Journal of Quality Technology*, 27, 1-12.

88. Murray, W. (1972), Numerical methods for unconstrained optimization, London and New York, Academic Press, 1972.

89. Nelson, L.S. (1986). Control chart for multiple stream processes. *Journal of Quality and Technology*, 18, 255-256.

90. Neter, J., Kutner, M.H., Nachtsheim, C.J. and Wasserman, W. (1990), Applied Linear Statistical Models, Irwin, Chicago, IL.

91. Noorossana, R., Saghaei, A., Paynabar, K. and Samini, Y. (2007). On the conditional decision procedure for high yield processes, *Computers & Industrial Engineering*, 53, 469-477.

92. Ohta, H., Kusukawa, E. and Rahim, A. (2001). A CCC-r chart for high-yield processes, *Quality and Reliability Engineering International*, 17, 439-446.

93. Page, E.S. (1954). Continuous inspection schemes, *Biometrika*, 41, 100-114.

94. Panagiotidou, S. and Nenes, G. (2008), An economically designed, integrated quality and maintenance model using an adaptive Shewhart chart, *Reliability Engineering and System Safety*, doi: 10.1016/j.ress.2008.07.003.

95. Peters, M.R. and Williams, W.W. (1987). Economic design of quality monitoring efforts for multistage production systems. *IIE Transactions*, 19, 81-87.

96. Pettersson, M. (2004). SPC with applications to Churn Management, *Quality and Reliability Engineering International*, 20(5), 397-406.

97. Qian, C. H., Kodo, I. and Toshio, N. (2005). Optimal preventive maintenance policies for a shock model with given damage level, *Journal of Quality in Maintenance Engineering*, 11(3), 216-227.

98. Reynolds, M. R. and Glosh, B. (1981). Designing control charts for means and variances. *ASQ Quality Congress Transaction*, American Society for Quality Control, San Francisco, 400-407.

99. Reynolds, M.R.JR. and Stoumbos, Z.G. (1998). The SPRT chart for monitoring a proportion, *IIE Transactions on Quality and Reliability*, 30, 545-561.

100. Reynolds, M.R.JR. and Stoumbos, Z.G. (1999). A CUSUM chart for monitoring a proportion when inspecting continuously, *Journal of Quality Technology*, 31, 87-108.

101. Roberts, S.W. (1959). Control charts tests based on geometric moving averages, *Technometrics*, 1,239-250.

102. Ross, S.M. (1970). Applied Probability Models with Optimization Applications, *(Holden Day: San Francisco, CA).*

103. Ross, S. (1996). Stochastic Processes, second edition, John Wiley & Sons, New York.

104. Runger, G.C., Alt, F.B. and Montgomery, D.C. (1996). Controlling multiple Stream processes with principal components. *International Journal of Production Research*, 34(11), 2991-2999.

105. Sampath Kumar, V.S. and Rajarshi, M.B. (1987). Continuous sampling plans for markov-dependent production process, *Naval Research Logistics*, 34, 629-644.

106. Saniga, E.M., (1984). Isodynes for X-bar and R control charts. *Frontiers in Statistical Quality Control*, H.J. Lertz, G.B. Wetherill and P.T. Wilrich. Physica, 2, Vienna, 268-273.

107. Schwertman, N.C. (2005). Designing accurate control charts based on the geometric and negative binomial distributions. *Quality and Reliability Engineering International*, 21, 743-756.

108. Shamsuzzaman, M, Lam, Y.C. and Wu, Z. (2005). Control chart systems with independent quality characteristics. *International Journal of Advanced Manufacturing Technology*, 26, 1298-1305.

109. Sheu, S., Yeh, R., Lin, Y. and Juang, M. (2001). A Bayesian approach to an adaptive preventive maintenance model, *Reliability Engineering and System Safety*, 71(1), 33-44.

110. Shin, H.W. and Sohn, S.Y. (2007). Application of an EWMA combining technique to the prediction of currency exchange rates, *IIE Transactions*, 39, 639-644.

111. Steiner, S.H. and Mackay, R.J. (2000). Monitoring processes with highly censored data, *Journal of Quality Technology*, 32, 199-208.

112. Steiner, S.H. and Mackay, R.J. (2001). Detecting changes in the mean from censored lifetime data, *Frontiers in Statistical Quality Control 6*, H.J.Lenz and P.T. Wilrich, editors, Physica-Verlag, 275-289.

113. Sun, J. and Zhang, G.X. (2000). Control charts based on the number of consecutive conforming items between two successive nonconforming items for the near zero-nonconformity processes, *Total Quality Management*, 11(2), 235-250.

114. Surucu, B. and Sazak, H.S. (2009). Monitoring reliability for a three-parameter Weibull distribution. *Reliability Engineering and System Safety*, 94, 503-508.

115. Tagaras, G. (1988). An integrated cost model for the joint optimization of process control and maintenance, *Journal of Operational Research Society*, 39(8), 757-766.

116. Tang, L.C. and Cheong, W.T. (2004). Cumulative conformance count chart with sequentially updated parameters, *IIE Transactions*, 36, 841-853.

117. Tang, L.C. and Cheong, W.T. (2006). A control scheme for high-yield correlated production under group inspection, *Journal of Quality Technology*, 38(1), 45-55.

118. Taylor, H.M. (1975). Optimal replacement under additive damage and other failure models, *Naval Research Logistics Quarterly*, 22, 1-18.

119. Vardeman, S. and Ray, D. (1985). Average run lengths for CUSUM schemes when observations are exponentially distributed, *Technometrics*, 27(2), 145-150.

120. Villalobos, J.R., Munoz, L. and Gutierrez, M.A. (2005). Using fixed and adaptive multivariate SPC charts for online SMD assembly monitoring, *International Journal of Production Economics*, 95(1), 109-121.

121. Williams, W.W. and Peters, M.R. (1989). Economic design of an attributes control system for a multistage serial production process. *International Journal of Production Research*, 27, 1269-1286.

122. Woodall, W.H. (1997). Control charts based on attribute data: bibliography and review, *Journal of Quality Technology*, 29(2), 172-183.

123. Woodall, W.H. (2006). The use of control charts in health-care and public-health surveillance, *Journal of Quality Technology*, 38(2), 89-104.

124. Woodall, W.H. and Adams, B.M. (1993). The statistical design of CUSUM charts, *Quality Engineering*, 5(4), 559-570.

125. Woodall, W. H. and Montgomery, D.C. (1999). Research issues and ideas in statistical process control, *Journal of Quality Technology*, 31(4), 376-386.

126. Woodall, W.H. and Ncube, M.M. (1985). Multivariate CUSUM quality control procedures. *Technometrics*, 27(3), 285-292.

127. Wu, J. and Makis, V. (2008), Economic and economic-statistical design of a chi-square chart for CBM, *European Journal of Operational Research*, 188(2), 516-529.

128. Wu, Z., Jiao, J.X. and He, Z. (2009). A control scheme for monitoring the frequency and magnitude of an event, *International Journal of Production Research*, 47(11), 2887-2902.

129. Wu, Z., Lam, Y.C., Zhang, S. and Shamsuzzaman, M. (2004b). Optimization designs of control chart systems. *IIE Transactions*, 36(5), 447-455.

130. Wu, Z. and Luo, H. (2004). Optimal design of the adaptive sample size and sampling interval np control chart, *Quality and Reliability Engineering International*, 20(6), 553-570.

131. Wu, Z., Shamsuzzaman, M. and Pan, E.S. (2004a). Optimization design of control charts based on Taguchi's loss function and random process shifts, *International Journal of Production Research*, 42(2), 379-390.

132. Wu, Z. and Shamsuzzaman, M. (2005). The design and application of the integrated control charts for monitoring process mean and variance. *Journal of Manufacturing Systems*, 24(4), 302-314.

133. Wu, Z., Shamsuzzaman, M. and Wang, Q. (2007). The cost minimization and manpower deployment to SPC in a multistage manufacturing system. *International Journal of Production Economics*, 106, 275-287.

134. Wu, Z. and Spedding, T.A. (1999). Evaluation of ATS for CRL control chart, *Process Control and Quality*, 11(3), 183-191.

135. Wu, Z. and Tian, Y. (2005). Weighted-loss-function CUSUM chart for monitoring mean and variance of a production process, *International Journal of Production Research*, 43(15), 3027-3044.

136. Wu, Z. and Wang, Q.N. (2007). A single CUSUM chart using a single observation to monitor a variable, *International Journal of Production Research*, 45(3), 719-741.

137. Wu, Z., Xie, M. and Tian, Y. (2002). Optimization design of the X-bar & S charts for monitoring process capability, *Journal of Manufacturing Systems*, 21(2), 83-92.

138. Wu, Z., Yeo, S.H. and Fan, H.T. (2000). A comparative study of the CRL-type control charts, *Quality and Reliability Engineering International*, 16, 269-279.

139. Wu, Z., Yeo, S.H. and Spedding, T. (2001). A synthetic control chart for detecting fraction nonconforming increases, *Journal of Quality Technology*, 33(1), 104-111.

140. Wu, Z., Zhang, X.L. and Yeo, S.H. (2001). Design of the sum-of-conforming-run-length control charts, *European Journal of Operational Research*, 132, 187-196.

141. Xie, M. and Goh, T.N. (1997). The use of probability limits for process control based on geometric distribution, *International Journal of Quality & Reliability Management*, 14(1), 64-73.

142. Xie, M., Goh, T.N. and Kuralmani, V. (2000). On optimal setting of control limits for geometric chart, *International Journal of Reliability, Quality and Safety Engineering*, 7(1), 17-25.

143. Xie, M., Goh, T.N. and Kuralmani, V. (2002a). *Statistical Models and Control charts for High-quality Processes*, Boston, Kluwer Academic Publisher.

144. Xie, M., Goh, T.N. and Ranjan, P. (2002b). Some effective control chart procedures for reliability monitoring, *Reliability Engineering and System Safety*, 77, 143-150.

145. Xie, M., Tang, X.Y. and Goh, T.N. (2001). On economic design of cumulative count of conforming chart, *International Journal of Production Economics*, 72, 89-97.

146. Xie, W., Xie, M. and Goh, T.N. (1995). A Shewhart-like charting techniques for high yield processes, *Quality and Reliability Engineering International*, 11, 189-196.

147. Yang, Z.L., Xie, M. and Kuralmani, V. (2002). On the performance of geometric charts with estimated control limits, *Journal of Quality Technology*, 34(4), 448-458.

148. Yeung, T.G., Cassady, C.R. and Schneider, K. (2008), Simultaneous optimization of X-bar control chart and age-based preventive maintenance policies under an economic objective, *IIE Transactions*, 40, 147-159.

149. Zantek, P.F. (2006). Design of cumulative sum schemes for start-up processes and short runs, *Journal of Quality Technology*, 38(4), 365-375.

150. Zantek, P., Li, S. and Chen, Y. (2007). Detecting multiple special causes from multivariate data with applications to fault detection in manufacturing, *IIE Transactions*, 39, 771-782.

151. Zantek, P. F., Wright, G. P. and Plante, R. D. (2002). Process and product improvement in manufacturing systems with correlated Stages. *Management Science*, 48(5), 591-606.

152. Zeifman, M.I. and Ingman, D. (2005). Modeling of unexpected shift in SPC, *Journal of Applied Statistics*, 32(4), 375-386.

153. Zhang, C.W., Xie, M. and Goh, T.N. (2005). Economic design of exponential charts for time between events monitoring, *International Journal of Production Research*, Vol. 43, 23(1), 5019-5032.

154. Zhang, C.W., Xie, M. and Goh, T.N. (2006). Design of exponential control charts using a sequential sampling scheme, *IIE Transactions*, 38, 1105-1116.

155. Zhang, C.W., Xie, M. and Goh, T.N. (2008). Economic design of cumulative count of conforming charts under inspection by samples, *International Journal of Production Economics*, 111, 93-104.

156. Zhang, C.W., Xie, M., Liu, J.Y. and Goh, T.N. (2007). A control chart for the Gamma distribution as a model of time between events, *International Journal of Production Research*, 45(23), 5649-5666.

157. Zhou, S. Y., Chen, Y. and Shi, J. J. (2004). Statistical estimation and testing for variation root-cause identification of multistage manufacturing processes. *IEEE Transactions on Automation Science and Engineering*, 1(1), 73-83.

158. Zuckerman, D. (1977). Replacement models under additive damage, *Naval Research Logistics Quarterly*, 24, 549-558.